



Politechnika Krakowska
Wydział Inżynierii Lądowej



WHZ Westsächsische
Hochschule Zwickau
University of Applied Sciences

Parametrizing macroscopic road network model of traffic-calmed zones

Parametryzacja sieci drogowej w modelach makrosymulacyjnych z uwzględnieniem stref ruchu uspokojonego

Author: Jan Paszkowski

Supervisors:

Prof. dr hab. inż. Andrzej Szarata

Dr. rer. nat. Matthias Richter, prof. WHZ

Zwickau, Kraków 2023

Parametrizing macroscopic road network model of traffic-calmed zones.

Scientific consultations:

dr hab. inż. Vitalii Naumov, prof. PK

dr hab. inż. Jacek Chmielewski

Layout correction:

Marta Buczyńska

Language correction:

Krystofer Mackie

Abstract

Traffic assignment of the macroscopic transportation model has a significant role in the transportation modelling and planning. It is significant, that it reproduces a real situation with the highest similarity possible. Therefore, it is crucial, that the entry data are the best reproduction of the users' behaviours possible.

In this thesis, Author investigates an important factor of the supply model – link's volume delay function (VDF). Those type of functions presents a travel time as a function of the traffic volume and are present since the beginning of the modelling. However, there is still a gap in the VDF estimation for the traffic-calmed streets. This is caused by a lack of methodology able to estimate VDFs for the streets with the changing velocity. On parallel, the new methods of the video detection of the vehicles opens the new possibilities of the trajectory collecting.

This thesis shows the method of Volume-delay functions estimation suitable for the traffic-calmed links, but also applicable for the other link types. This is achieved through the precise development and calibration of the microscopic model. Later, its results are used to estimate VDFs through the density-travel time data.

The method shown in this thesis is shown in the practical application. Firstly, the influence on the toy network is shown to validate the influence of the traffic-calmed links on the traffic assignment. Finally, the method is shown in the Kraków model to see the changes of the traffic assignment in the city network.

Streszczenie

Rozkład ruchu w makroskopowym modelu transportowym ma znaczącą rolę w modelowaniu i planowaniu transportu. Istotnym jest, żeby model prezentował wyniki zgodne z rzeczywistością w jak największym stopniu. Z tego powodu konieczne jest, żeby dane wejściowe oraz zachowania użytkowników modelu były odtworzone najdokładniej, jak to możliwe.

W tej pracy doktorskiej autor bada ważny element modelu popytu – funkcję oporu odcinka (VDF). Tego typu funkcja, badana od początków modelowania transportu, wyraża czas przejazdu odcinka jako funkcję natężenia ruchu. Jednakże, ciągle brakuje badań obejmujących funkcje oporu dla odcinków o ruchu uspokojonym. Jest to spowodowane brakiem metod badań tego typu funkcji dla odcinków, w ciągu których zmienia się prędkość. Jednocześnie, powstały nowe metody, pozwalające badać trajektorie i ruch pojazdów używające wideo detekcji, które w prosty i tani sposób pozwalają uzyskać wiele danych o ruchu pojazdów.

Praca ta przedstawia metodę estymacji funkcji oporu odcinka, która jest użyteczna dla odcinków ruchu uspokojonego, lecz nie tylko dla nich. Metoda ta polega na dokładnej budowie i kalibracji modelu mikroskopowego oraz późniejszemu odwzorowaniu zachowań kierowców w różnych warunkach ruchu. Dzięki zastosowaniu modeli mikroskopowego, badane są później zależności między gęstością ruchu, a czasem przejazdu odcinka.

Praca ta również pokazuje zastosowanie praktyczne metody. Na sieci testowej pokazany jest wpływ zmiany funkcji oporu na rozkład ruchu, a w modelu Krakowa pokazane są zmiany są na realnym odcinku ulicy.

Contents

1.	Introduction.....	7
1.1.	The topic of the thesis	7
1.2.	Prerequisites for writing the thesis.....	7
1.3.	The aim of the thesis	8
1.4.	Challenges met in thesis	11
2.	Literature review	12
2.1.	Macroscopic model	12
2.2.	Trip-based and activity-based models	13
2.3.	Four step model	15
2.3.1.	Trip generation	16
2.3.2.	Trip distribution	18
2.3.3.	Modal split.....	19
2.3.4.	Traffic assignment.....	19
2.4.	Volume-Delay functions	24
2.4.1.	Existing types of VDFs	26
2.4.2.	Solving the problem of demand exceeding capacity	29
2.4.3.	Methods of VDFs estimation	31
2.5.	The Microsimulation model	34
2.5.1.	Microsimulation model calibration.....	37
2.6.	Vehicle movement surveying	39
2.6.1.	Measurements inside the vehicle	39
2.6.2.	Measurements outside the vehicle	40
2.6.3.	Video detection – vision-based vehicle speed estimation	43
2.6.4.	Unmanned aircraft	46
3.	Traffic calming	50
3.1.	Traffic calming definition and level of influence	50
3.1.1.	Link related measures.....	52
3.1.2.	Intersection related measures.....	53
3.1.3.	Traffic calming on main roads	54
3.1.4.	Area traffic calming	55
3.1.5.	Impact on the pollution.....	55
3.1.6.	Impact on the noise.....	57
3.1.7.	Impact on the driving behaviour and speed	59
3.2.	Conclusions from the literature review	63

Parametrizing macroscopic road network model of traffic-calmed zones.

4.	Research method	64
4.1.	Aerial video recording – quadcopter.....	67
4.2.	Video detection of the vehicles.....	68
4.3.	Trajectories and driving behaviour characteristics.....	69
4.4.	Developing the microscopic (Vissim) model	70
4.5.	Simulating traffic volumes	72
4.5.1.	Volume, density and travel time relation	73
4.6.	Volume-delay function	74
4.7.	Application in macroscopic (Visum) model	76
5.	Research method - example	77
5.1.1.	Video Data Collection.....	77
5.1.2.	Trajectory Analysis.....	78
5.1.3.	Microsimulation Model.....	81
5.2.	Sensitivity analysis	84
6.	Research application.....	94
6.1.	Influence on traffic assignment – Toy network	94
6.1.1.	Problem formulation	94
6.1.2.	Result.....	95
6.1.3.	Comparison with the Results of the current solutions	97
6.2.	Implementation of the model in real conditions – Krakow case.....	100
6.2.1.	Introduction	100
6.2.2.	Measurement.....	102
6.2.3.	Speed profiles calibration	103
6.2.4.	Volume-delay functions.....	106
6.2.5.	Impact on the Kraków model	108
7.	Summary and conclusions	112
7.1.	Research summary.....	112
7.2.	General conclusions.....	113
7.3.	Further research	114
7.3.1.	Applying unmanned aircrafts and video detection in transport modelling ..	114
7.3.2.	Volume-delay function database for the link types.....	114
7.3.3.	Volume – delay functions comparison – finding the VDF modification for traffic-calmed roads.....	115
8.	Literature	117
9.	List of figures.....	136
10.	List of Tables	139
11.	List of formulas	139

1. Introduction

1.1. The topic of the thesis

This thesis undertakes a topic of modelling the traffic calmed road areas in a macrosimulation model. Especially, modelling of traffic assignment changes will be taken into consideration.

1.2. Prerequisites for writing the thesis

This thesis faces the problem of discovering a volume-delay relation on various types of streets, with an emphasis on the traffic calming areas. After researching available methods for a complex discovery and estimating volume-delay functions for this type of streets, it turned out that there was a lack of methods for translating drivers' characteristic behaviour into a volume-delay relation.

At the same time, new possibilities for vehicle movement discovery arose. With the development of machine learning, new methods of vehicle detection emerged, allowing for the accurate observation of trajectories and movement characteristics of multiple vehicles simultaneously.

To sum up, a lack of research in volume-delay functions, along with these new measurement possibilities, enabling the creation of a new method of VDF discovery, was the prerequisite for writing this thesis.

1.3. The aim of the thesis

The aim of this thesis is to create a method for discovering drivers' behaviour and reproducing it in micro- and macrosimulation models. This modelling will be focused on the influence of the behaviour on the traffic assignment. In this thesis, behaviour will be studied using the example of the traffic-calmed streets. This should be achieved through:

1. Collecting and processing video data in order to obtain vehicle trajectories. Drivers' behaviour on a given street, especially a traffic-calmed street, is characterised by its trajectory (vehicle path), including speed, which, especially in the case of specific traffic calming measures, may change along the link. Because of that, the vehicle's movement has to be studied continuously and expressed as speed profiles, written in the form of velocity according to its position on the street ($V(x)$).
2. Developing and calibrating a microsimulation model. This can be achieved using velocity data from the previous point. Furthermore, it is possible to input acceleration or other car-following model parameters.
3. Simulating various traffic volumes using the microscopic model in order to identify suitable Volume-delay function parameters, as well as how they are influenced by the traffic calming. This can be done by estimating the relation between traffic volume (traffic flow) and the delay (expressed as the difference between travel time of the free and actual traffic flow). For analysis purposes, this relation can also be shown as the relation of the velocity (V) to the particular traffic volume (q) and presented as $V(q)$ relation. Volume-delay function estimation is based on the estimation of volume-delay function parameters, which gives a function shape compliant with the Volume-delay relation. For example, for BPR function, those parameters are: a , b , c and c' parameters.
4. Observing the effects of the change of traffic parameters, as caused by the change of the Volume-delay function in the macrosimulation model. The key observation is the change of the traffic assignment result, precisely, described as the traffic volumes (q) and the differences between them, as caused by implementing different volume-delay functions in the macroscopic model.

On Figure 1 the graphical version of the thesis research logic have been presented.

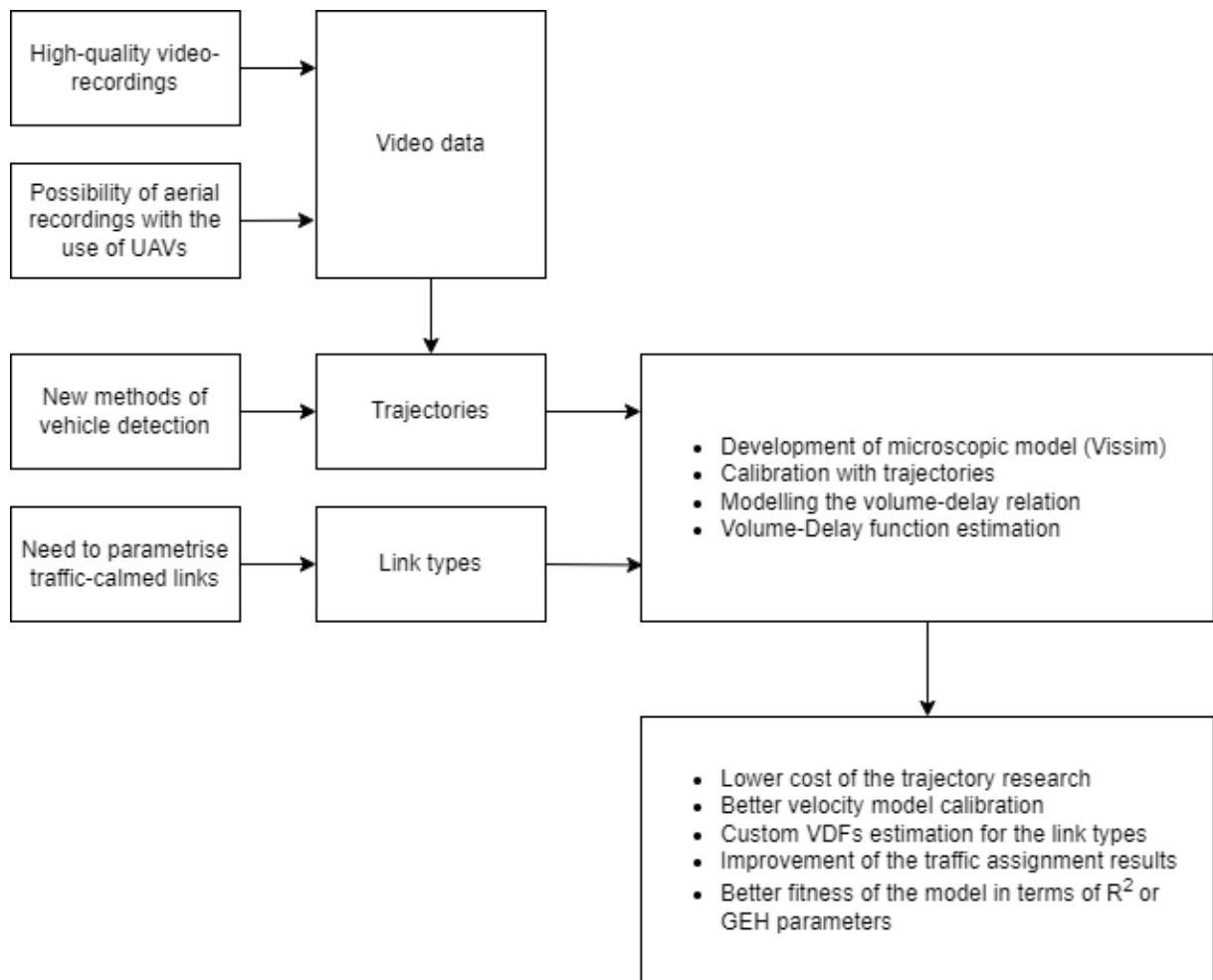


Figure 1: Thesis research logic diagram

As seen on the graphic from fig. x, technical developments have brought a new research possibilities to explore the driving behaviour more precisely and with a lower cost of measurements. This developments are high-quality video recordings, offering a good picture quality and high resolution within a small camera size and low equipment costs. Moreover, with the development of the unmanned aircrafts (drones) it is now possible to cover a great amount of the measured link at once, which also means gathering more trajectories at once. Secondly, with the development of the machine learning algorithms, it became possible to detect the vehicles without errors.

Those developments meet the growing need for the more accurate macroscopic traffic modelling. In this case, with the ongoing challenge how

and where to introduce the traffic measure need to have a proper tool to predict the impact of the traffic calming introduction.

Therefore, this thesis covers a method of the volume-delay function estimation, which is useful for the various link type, but especially traffic-calmed roads estimation. This type of link covers usually a streets outside the main corridor, which means, that the streets are usually lacking the measuring infrastructure, such as induction loops or on-street cameras. Moreover, this method is able to register a characteristic behaviour of the variable velocity on the traffic-calmed link, which enables to reproduce it in the modelling.

The impact of this thesis will be the method of estimating and example volume-delay functions and knowledge how the traffic assignment is influenced by traffic calming. Moreover, the impact in the matter of a novel method, will be a possibility to create an accurate microscopic model and the volume-delay functions with a lower cost of data gathering.

Progress in machine learning in the field of video detection lets now to measure movement characteristics of vehicles with high precision without installing inside them speed measuring or GPS devices. Development and technical progress in aerial recording using unmanned aircraft (drone), such as camera resolution, hover stabilisation and flight time enables to record a greater area. This makes calibration of microsimulation models to be very precise and enables to use them to research difficult or impossible before phenomena.

Reproducing the travel behaviour in microsimulation model will lead in this thesis to discover capacity and volume-delay functions for traffic-calmed roads, which was difficult or impossible before, due to lack of the proper methods and technology.

1.4. Challenges met in thesis

The first challenge of the thesis was a speed research. The thesis challenge in this topic was to find a method to acquire data about drivers' behaviour such as speed, acceleration, braking, using trajectories acquired through video detection on traffic-calmed road and to reproduce them in a microsimulation model.

Secondly, the challenge was to find a method of using the aforementioned trajectory and speed data to develop and calibrate the microscopic model. It was possible by acquiring data about drivers' behaviour such as speed, acceleration, braking, using trajectories acquired through video detection on traffic-calmed road and to reproduce them in a microsimulation model.

Third challenge was to parametrise the traffic calming influence on the traffic assignment through capacity and volume-delay function parameters.

Final challenge was to check the influence of the traffic-calmed-link volume-delay functions on the traffic assignment and calculate the difference to the initial traffic volume. It is expected, that traffic calming changes the traffic assignment in such a way, that it causes decrease of the speed (in one point or on the street), therefore lowers the capacity and increase travel time along with the increase of traffic flow, thus the shape of the function and the equilibrium assignment changes.

2. Literature review

2.1. Macroscopic model

Transportation modelling is a mathematical reproduction of the behaviour and the decision-making process of the users and the traffic state of the transport network. Modelling is based on the identification and description of the processes taking place in the transport network and the variables defining the traffic potentials of the analysed area. In general, the macroscopic model is the reproduction of the real transport system or its part based on the collected data in order to replace the analysed object in the planned experiments.

The majority of decision-making procedures include modelling as a critical step, making it an integral part of planning. This includes transportation planning, notably because the effects of transport investments are visible for decades, sometimes even for centuries. It is impossible to account for every factor and influence, despite the multitude of software and mathematical techniques at our disposal and current computing capacity. Transportation services need to identify the critical factors that determine the effects of activities undertaken on transport systems. In this light, models are supposed to reproduce the view and reaction of the individual system user, while also simplifying the factors that are critical in changing the model results.

Macroscopic model describes the behaviour of the users group in the whole process of the trip realisation, from the probability of the trip taking place, through the mean of transport to the choice of the path to the destination. The level of the influence between the users is limited to the general traffic flow conditions, such as saturation, traffic congestion, vehicle capacity, etc. [1].

The history of transportation modelling begins in the USA in the 1950s with the Detroit and Chicago transportation studies. In the early 1960s, modelling reaches London and spreads in America, Europe, and finally the whole world. In 1970, modelling is unified and evolves to be used together with the economic analysis of investment. During this time, the concept of supply and demand is implemented into transportation modelling as a means of researching the meeting of the supply and demand function [4].

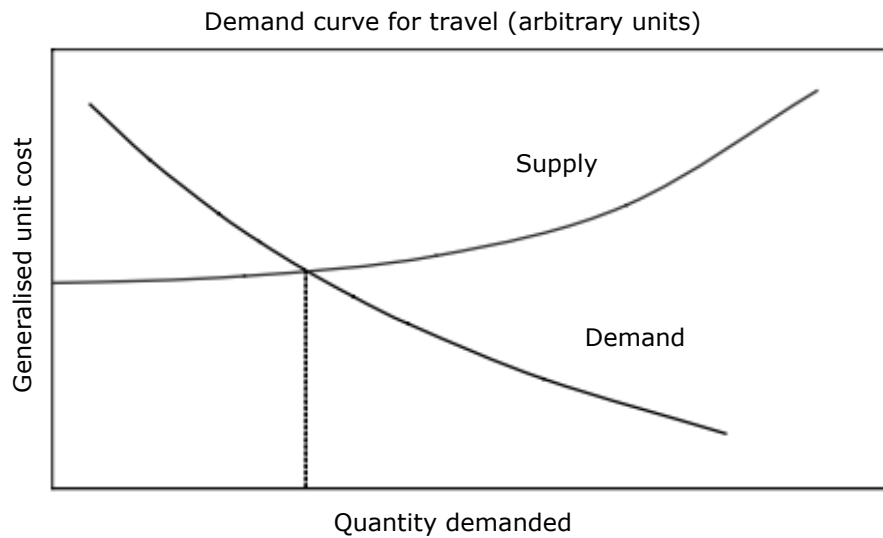


Figure 2: Demand – supply chart. Source: [3]

In the case of the transportation model, supply represents the transport network, including roads, public transport systems and all elements related to movement within the transport system. According to the supply model, the transport network is described using parameters corresponding to demand data, such as capacity and travel time depending on the traffic volume. These parameters determine the final results of the model.

Demand is recognised as a spatial distribution of trips for all of the transport subsystems. Precisely, demand represents each travel decision made by the system users (people), incorporating origin, destination and mode of transportation in the given period of time [3].

2.2. Trip-based and activity-based models

Trip-based models, for example the Four-step model, generate trips according to information about the spatial development of the analysed land area. These models then enable one to choose a proper mode of transportation to achieve an equilibrium. However, this approach is mostly disconnected from the behavioural conditions of the users. This means trip-based models can give proper results for most of the forecasting of the infrastructure project, but can be unusable when forecasting demand management policies results [4].

Activity-based models are closely connected to the users' travel behaviour. This approach assumes that the trips used in modelling demand are part of an activity, which can contain more than one trip. An example of such activity is shown in the Figure 3:

Parametrizing macroscopic road network model of traffic-calmed zones.

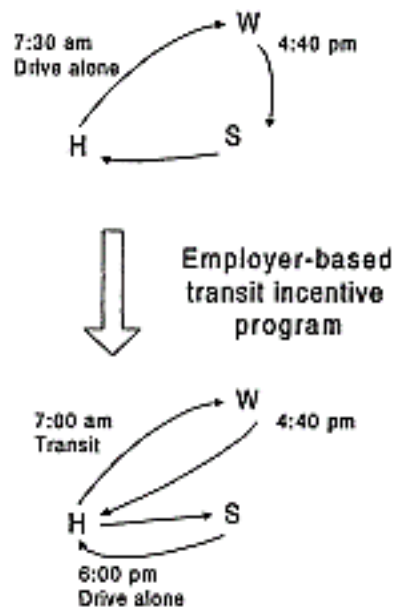


Figure 3: Example of trips within an activity. Source: [4]

In the Figure 3 we can see that the activity (going to and back from work) is split into different trips. This could describe a person driving to work (first trip), driving from work to a shop (second trip), and finally driving home from the shop (third trip). Alternately, a person can take public transport to and from work (first and second trip) and then drive from home to a shop and back (third and fourth trip). In that case, we can see that the demand management policy (program for using public transport to commute to work) has switched mode of transportation and, in consequence, trip setting [4].

To summarise, when comparing trip-based and activity-based approach models, we can see that the activity-based approach generates trips by taking into account the individual's decision-making process involved in travel behaviour, whereas the trip-based approach simplifies trip generation, omitting the decision-making process involved in the activities. As for the model result, trip-based models are acceptable for analysing changes in network and capacity, however, for policy changes, they deliver worse results than the activity-based model.

In this thesis, the trip-based approach, in particular the four-step model, will be analysed in further detail.

2.3. Four step model

Out of the different macrosimulation model building methods, we consider Four-step model. It consists of four steps: Trip generation, trip distribution, mode choice and traffic assignment.

The aim of the four step model is to determine equilibrium flows. Its working system is presented on Figure 4

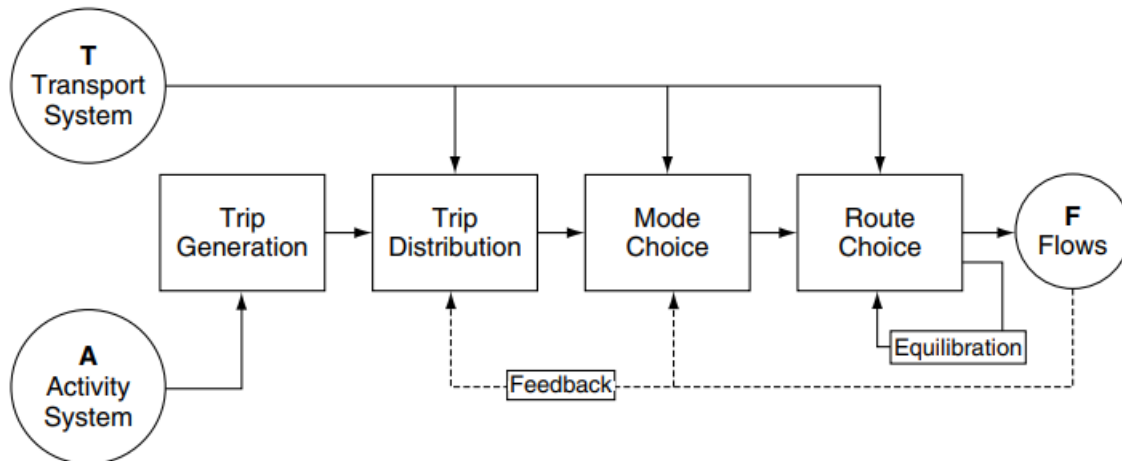


Figure 4: The four-step model. Source: [3]

Trip generation is a first stage in which spatial analysis are undertaken to determine the amount of trips going in and out (attraction and production) of each homogenous area during peak hour.

Trip distribution creates a matrix of trips between origin and destination areas based on gravity functions, which determines the probability of existing trips based on production and attraction together with distance or travel time.

Mode choice determines the amount of trips taken by every available means of transport, such as car, public transport and bike. It is determined by functions defining the probability of specific means of transport being chosen, according to distance, availability and motivation (home-work, home-school etc.)

Traffic assignment sets the path for every trip generated, distributed and assigned to transport mode in the previous stage. For traffic assignment, Wardrop's principle of user equilibrium algorithm is usually used. Its assumptions are, that every user chooses the path with the lowest cost (cost is represented by travel time) and, that transport systems aim to achieve equilibrium – the state in which no vehicle can switch from one path to another with a lower cost. The four-step model requires iteration of traffic

assignments, because travel time on the link, the main factor in assigning a trip to a path, depends on traffic flow, defined as the amount of trips through the link in the form of a volume-delay function. Iterations should be undertaken until the model reaches the equilibrium state.

In this study, only the final step of the four-step model will be taken into consideration, that is, the traffic assignment reaction on the volume-delay functions existing on traffic calmed roads. Each of the four steps will be further explained in the following chapters.

2.3.1. Trip generation

The first step translates the model from the activity-based to the trip-based model. It defines the travels in the transport systems, from home to work, school and other types of activities. Trip generation is based on zones, which are specific, bordered land areas with similar spatial development and homogenous travel behaviours. The result of this step is a trip quantification into production and attraction for each of the zones. To achieve this, trips are typically divided into four categories of motivation:

- Home-based work trips
- Home-based school trips
- Other home-based trips
- Non-home based trips.

Estimating the quantity of trips for these motivations can be achieved via a spatial, social and econometric analysis. This enables us to discover the number of trips in general produced from or attracted to the zone, based on the amount of users carrying out certain activities in each zone, such as living, working, learning, shopping and other.

The second part of trip generation is setting the trips within in a time period. During behaviour analysis, an hour share is estimated for every motivation. This enables us to estimate a morning and afternoon peak hour. Finally, the total production and attraction for every zone is generated for that specific time period [4].

Parametrizing macroscopic road network model of traffic-calmed zones.

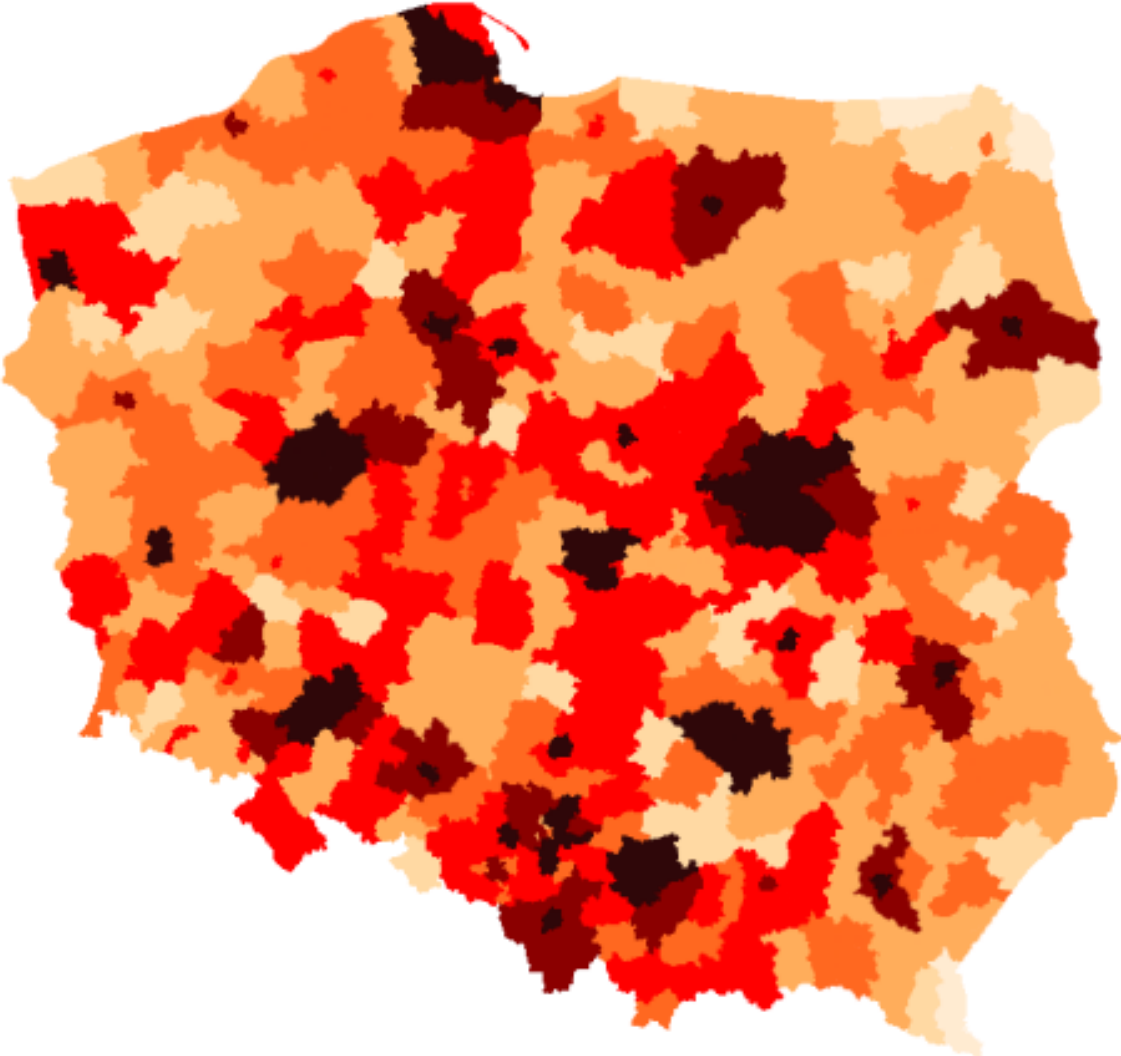


Figure 5: Trip generation (cars) – Intermodal National Traffic model. Source:[2]

2.3.2. Trip distribution

The aim of the second step is to combine the trips from production to attraction for the particular time period. This would result in the trip matrix showing the traffic flow between the zones.

The process of calculating the trip matrix can be divided into two stages. The first is based on the quantity of production and attraction trips, stating, according to the proportional model that the more trips are available, the more demand there is between zone origin-destination pairs.

The second stage is called the gravitational model and is based on the principle that, the greater the distance between origin and destination, the fewer trips take place. The relation between distance and decrease of trips is called an impedance function. This function is researched individually for the model according to a survey of the users' behaviour [3].

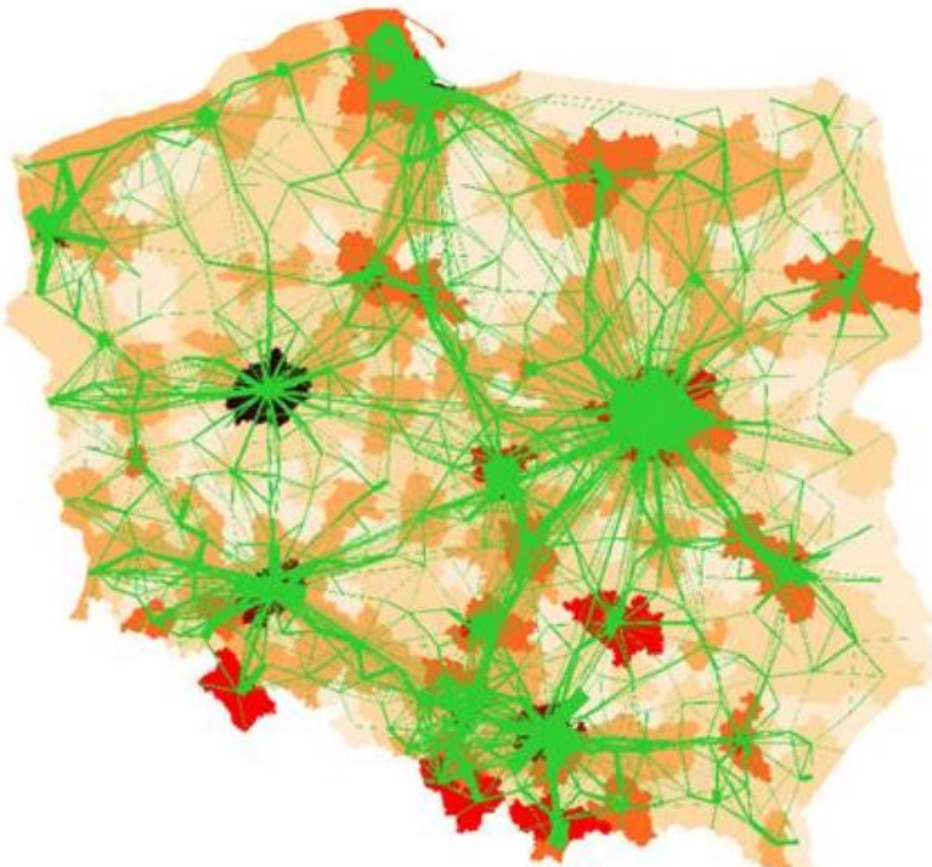


Figure 6: Trip distribution (cars) for the May weekend peak hour – Intermodal National Traffic model
Source: [2]

2.3.3. Modal split

Modal split, that is the mode choice model, indicates an amount of trips between zones taken with each mode of transportation. In a four-step model, the mode choice model determines the probability of the choice of a particular mode of transportation through mathematical functions. These functions are modelled based on the users' behaviour, taking into consideration both the cost and attractiveness of using a mode of transportation (travel time is also included in cost), and user preferences for a particular mode of transportation. Mode choice models are calculated based on traffic surveys.

Typically, mode choice modelling is divided into three or four transport modes, resulting in trip matrices for each of them. First, the trips are divided into pedestrian and non-pedestrian. Next, the trips are divided between individual (motorised) and public transport. Sometimes, there is also distinction made for a fourth mode of transportation – bicycle transport.

Modal split is a mathematical reproduction of a transport network user decision, i.e. which mode of transportation to choose. The basic factors influencing this decision are called trip cost, which, aside from the monetary costs, depends in great part on distance and travel time. Other factors influencing a mode choice can be less easily measurable, such as safety, reliability, punctuality, comfort, etc. [1,3]

2.3.4. Traffic assignment

The demand for travel is a spatial and temporal phenomenon, and in order to model it, one must formally represent the supply of infrastructure and services for transportation. The most popular method for accomplishing this is by using a network [3].

A transport network is an analytical tool that makes it easier to identify traveller routes and their associated "costs" in a broad sense. Formally, a network of links L and nodes N can be used to depict a network of travel. A node connects two links, and two or more links connect a node. When the direction of travel in links is regularly defined, they are known as directed links. A link that is not directed can be followed both ways. If two links connect the same pair of nodes in the same direction, they are said to be parallel (4). Moreover, a link may contain more parameters describing transportation networks:

- Link length, typically measured in meters, kilometres, or another appropriate unit.

Parametrizing macroscopic road network model of traffic-calmed zones.

- Link cost, related to travel time, distance and other factors.
- Link capacity, i.e. maximum traffic flow travelling through the link per unit of time
- Volume-delay (capacity restraint) function, indicating travel time according to traffic volume.

To transfer traffic flow from the Origin-Destination matrix to the network, artificial constructs called centroids and connectors are used. A centroid represents the zone and a connector indicates the nodes in which traffic flow emerges from the zone's centroid to the network [5].

Most network links can only handle a given amount of traffic before reaching their capacity. It can be assumed that the typical capacity for a lane is equal to 1800 passenger cars per hour, roughly one car every 2 seconds. Capacity, of course, depends on factors like width, gradient, curvature, surface, speed limit and vehicle composition [6].

In case of traffic volume, in which the need to use the link is greater than the capacity, queuing will occur. In reality, such a queue will spill back, blocking previous intersections. In the macroscopic models, simplification occurs when such queues are represented as delay [4].

Traffic assignment is the process of assigning trips from demand (trip matrices) to supply (network). It is undertaken by the principles and algorithms that reproduce realistic and desirable route choice behaviour.

The fundamental presumption in traffic assignment is that the traveller is rational, i.e., they choose the route with the lowest perceived (and predicted) individual costs. In most cases, cost is based on travel time or financial costs. In most cases, monetary cost is proportional to travel time or trip length, sometimes varying depending on the toll fees on some of the paths. Costs are also adjusted to represent drivers' perceptions, the end result of which is a generalised route choice compliant with drivers' behaviour.

The most basic and simple traffic assignment method is 'all-or-nothing' assignment. It doesn't account for congestion, meaning trip cost remains unchanged no matter how many other users choose a particular link.

The heterogeneity in drivers' perceptions of costs and the composite measure they want to minimize are highlighted by stochastic techniques of traffic assignment (distance, travel time and generalised costs). Stochastic approaches must take into account second-best routes in terms of engineering or projected costs; this causes extra issues because there may be several second-best alternatives between each OD pair. Several approaches have been put forward to include these factors, but only the

simulation-based and proportion-based approaches have received a comparatively high level of acceptability. The first introduces unpredictability in perceived costs by drawing inspiration from stochastic (Monte Carlo) simulation. Proportion-based approaches, on the other hand, divide flows into proportions and compute them using formulas that are similar to logit [5].

For the realistic functioning of traffic assignment, the capacity restraint has to be considered. This means that each link needs a function relating flow and travel costs. For this, the traffic assignment model needs to be able to find an equilibrium within path choices in the traffic flow. This equilibrium was originally described by Wardrop in 1952, stating: "Under equilibrium conditions traffic arranges itself in congested networks in such a way that no individual trip maker can reduce his/her path costs by switching routes." [7]

Wardrop adheres to two principles. The first one, referred to as user equilibrium, is mentioned above. It can also be explained thus: "Under equilibrium conditions traffic arranges itself in congested networks such that all routes between any OD pair have equal and minimum costs while all unused routes have greater or equal costs." If these conditions do not hold, at least some drivers would be able to reduce their costs by switching to other routes.

The second Wardrop principle, also known as "System optimum", states: "Under equilibrium conditions traffic should be arranged in congested networks in such a way that the total travel cost (all trips) is minimised.". This principle refers to design and traffic organisation, whereas the first one refers to the behaviour of individual drivers. The second principle receives attention in such areas as mobility management, congestion pricing, etc.

Mathematically, the first Wardrop principle, known as user equilibrium is described as a state when no driver can reduce unilaterally their travel costs by moving to another route [8]. It can be mathematically described as follows in formula 1 [9]:

Formula 1: Wardrop's first principle

$$(x-x^*)c(x^*)\geq 0 \quad (1)$$

where:

x is a vector of feasible link flows,

$c(x^*)$ is a vector of link costs,

x^* indicates equilibrium link flows

Parametrizing macroscopic road network model of traffic-calmed zones.

There is also a variant of the user equilibrium, where it is assumed, that during the route choice process an error can be made. In this case, the probability distribution of the paths is used. This variant is called a stochastic user equilibrium [10].

The second Wardrop principle, known also as the system optimum aims to minimise a total system time. This can be formulated mathematically as follows in Formula 2 [8]:

Formula 2: Wardrop's second principle

$$\text{Min } \sum_a x_a c_a \quad (2)$$

where:

x_a is the feasible link flow,
 c_a is the link cost,

However, for big networks, the user-equilibrium algorithm in itself is relatively slow. Therefore more time-efficient algorithms are used, based on user-equilibrium rule, for example the LUCE (Linear User Cost Equilibrium) algorithm, used in PTV Visum, which aims to be 10-100 times faster than other methods [11].

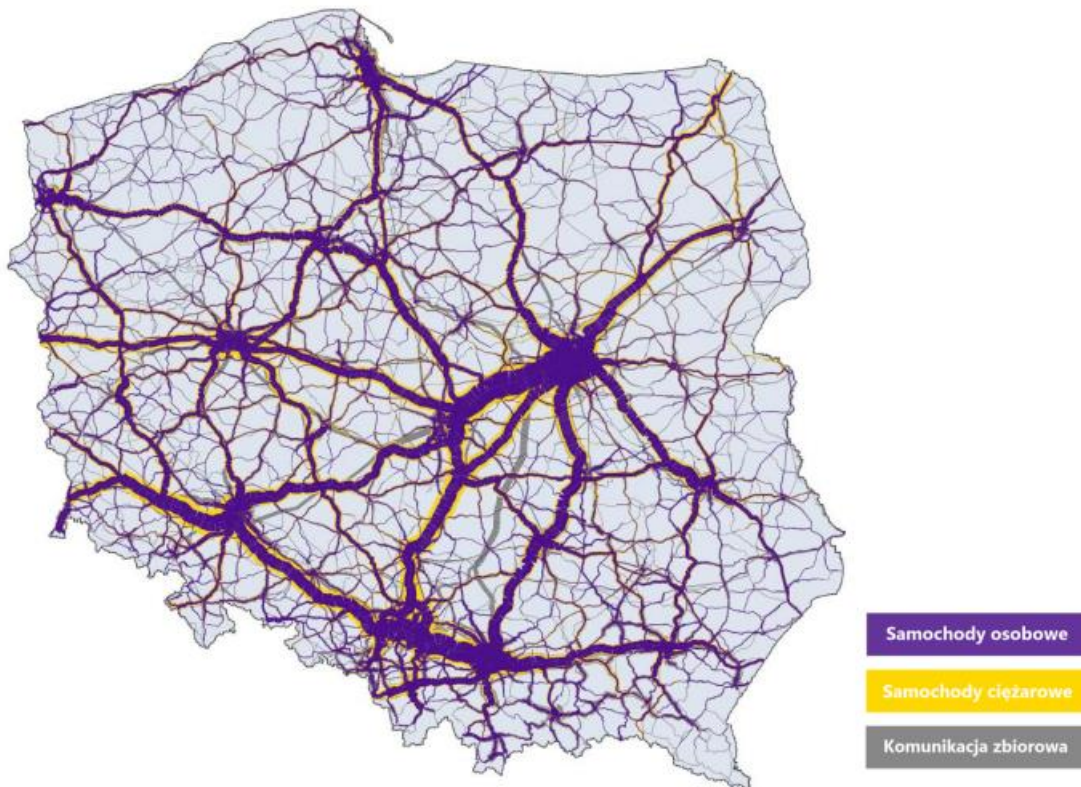


Figure 7 Traffic assignment for road transport in Poland in 2030. Source:[249]

Parametrizing macroscopic road network model of traffic-calmed zones.



Figure 8 Map of the emissions in the passenger road traffic, based on the traffic assignment. Source:[250]

2.4. Volume-Delay functions

Volume-delay functions are a common tool used by traffic engineers and planners to analyse and predict the flow of vehicles on a road network. These functions describe the relationship between the volume of vehicles on a road and the resulting delay experienced by those vehicles. Volume-delay functions can be used to compare the performance of different road networks. By comparing the volume-delay functions for two different road networks, it is possible to determine which network is more efficient in terms of traffic flow and delay. Primarily, fundamental diagrams of traffic flow are used in modelling highway traffic, helping to understand capacity effects, different traffic states, etc.

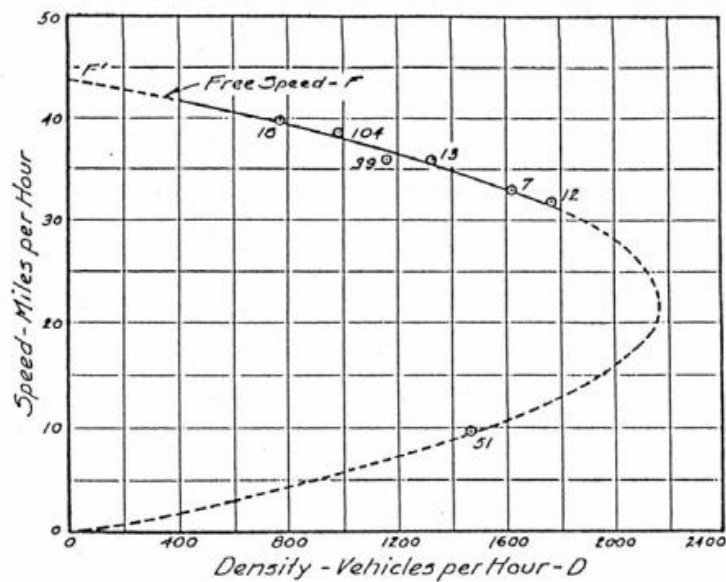


Figure 9: Greenshield's fundamental diagram of traffic flow, source: [12]

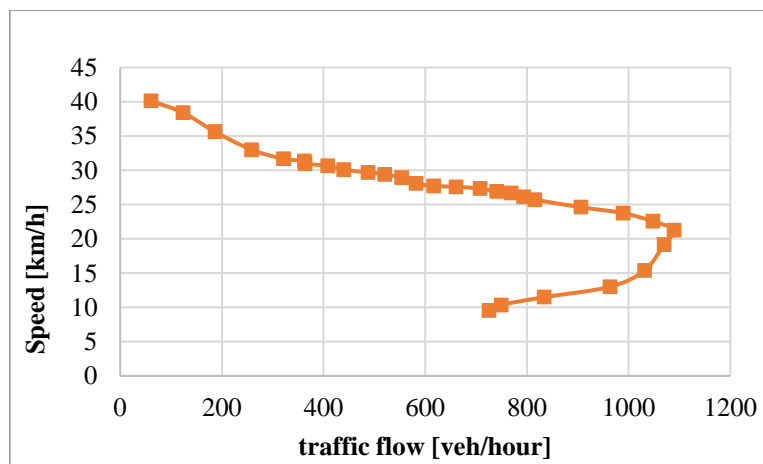


Figure 10 The example of the fundamental diagram of the Thesis research, source: own

Volume-delay function (also called VDFs) describes link travel time as a function of traffic flow (which is a result of traffic assignment), capacity and

free flow travel time (which are the constant link parameters). This function is widely used in static macroscopic traffic assignment to describe in-current link travel times in traffic flow resulting from traffic assignment. It reproduces congestion effects generating delay, allowing for the traffic assignment problem, where travel times are minimised to comply with traffic flows in the real network. A saturation grade is typically used to describe traffic volume in VDF, which is a ratio between traffic volume and capacity, allowing us to separate the function parameters from the capacity.

In macrosimulation models, the network is described as a graph, in which links (sometimes also nodes) create resistance. This resistance in the links is described as a relation between saturation grade and travel time, known as volume-delay function. Volume-delay function is a non-descending, continuous, differentiable function, usually calibrated based on assumptions or observations of the observed travel time and the corresponding volume data [13]. For minimal traffic flow, the result of the volume-delay function is equal to 1, meaning that travel time is equal to free flow travel time. With the growth of traffic flow expressed in vehicles per hour, the function is growing. When saturation grade is equal to 1, meaning that traffic flow has reached capacity, the function starts to grow dramatically.

Volume delay function is a macrosimulation approximation of fundamental traffic phenomena occurring in dynamic traffic models, such as gridlocks, spillbacks etc. [14]. VDFs are integrable and differentiable, increasing functions, and usually consist of two parts. The first represents results where the traffic flows are lower than the capacity. VDF, contrary to fundamental diagram, has a form of function, and contains both a hypocritical part (where the traffic volume is less than capacity) and hypercritical part. The hypercritical part represents the situation where traffic flow exceeds capacity, which is in contradiction with the traffic flow definition. The result is that the VDFs and macroscopic assignment are not strictly related to the flows measured in reality. Figure 8 shows the example of the BPR volume-delay function, using formula 3.

Formula 3: BPR volume-delay function

$$t_{cur} = t_0(1 + a \cdot sat^b) \quad (3)$$

Where:

t_{cur} : Travel time in the current traffic volume

t_0 : Free flow travel time

sat: Saturation grade (q/q_{max})

a,b: function coefficients

In the figure 8, a comparison of the function shapes for the coefficient $a=1$ and various coefficients b are shown.

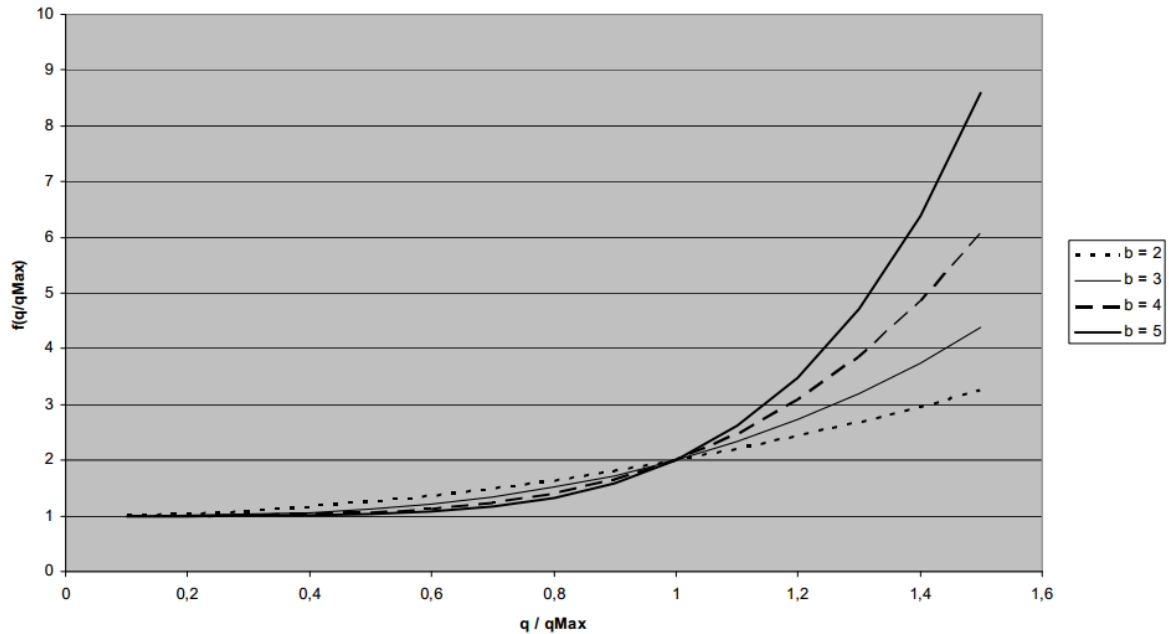


Figure 11: Example of Volume-delay functions source: [15]

2.4.1. Existing types of VDFs

The first VDFs, such as Webster, were created in the late 50s as an attempt to reproduce the queuing phenomena and speed/flow relation in 1958. In 1964, the Bureau of Public Roads published "Traffic assignment manual", which contained a simple VDF called BPR function [16], widely used up until now. Later functions would try to improve the accuracy (Spiess [17], Moses [18], Lazar [19]) in the field of queue arrival rates (Davidson [20], Huntsinger [21]), peak hour fluctuations (Small [6], Akcelik [22-24]), congestion definition (Kucharski[14]) and fluid dynamics compliance (Newell [25], Cheng [26], Zhou [27]). An overview of the most important VDFs is shown in Table 1.

Parametrizing macroscopic road network model of traffic-calmed zones.

Table 1: Overview of the most important VDFs, source: [28]

Author/s/Year	Paper title	Function	Remarks
Webster (1958)	Traffic signal settings	$d = \frac{c(1-\lambda)^2}{2(1-\lambda x)} + \frac{x^2}{2V(1-x)} - 0.65\left(\frac{c}{V^2}\right)^{\frac{1}{3}}x^{(2+5\lambda)}$	Queueing model-based, $\lambda = g/c$ ratio
CATS (1960)	Data projections	$tt = t_f \cdot 2^{\left(\frac{V}{C}\right)}$	
Smock (1962)	An iterative assignment approach to capacity restraint on arterial networks	$tt = t_f \cdot e^{\left(\frac{V}{C}-1\right)}$	
BPR (1964)	Traffic Assignment Manual	$tt = t_f \left[1 + \alpha \left(\frac{V}{C}\right)^{\beta} \right]$	
Davidson (1966)	A flow-travel time relationship for use in transportation planning	$tt = t_f \left[1 + j \cdot \frac{V}{C-V} \right]$	Single queueing with random arrival rates and exponentially distributed service rates
Davidson (1978)	The theoretical basis of a flow-travel time relationship for use in transportation planning	$tt = t_f \left[1 + J \cdot \frac{V}{C-V} \right], J = \frac{k+1}{2k}$	Queue system with random arrivals and an Erlang service distribution
Newell (1982)	Applications of queueing theory	$tt = t_f \left[1 + \frac{\gamma}{36\mu \cdot t_0} \cdot \left(\frac{D}{\mu}\right)^3 \right]$	Fluid based queue with quadratic arrival rates and fixed inflow curvature parameter

Parametrizing macroscopic road network model of traffic-calmed zones.

Small (1983)	The incidence of congestion tolls on urban highways	$tt = \begin{cases} t_f, & \text{if } V \leq C \\ t_f + \frac{1}{2}P \cdot \left(\frac{V}{C} - 1\right), & \text{if } V > C \end{cases}$	Peak hourbased
Spiess (1990)	Conical volume-delay functions	$tt = t_f \cdot \left[2 + \sqrt{\alpha^2 \left(1 - \frac{V}{C}\right)^2 + \beta^2} - \alpha \left(1 - \frac{V}{C}\right) - \beta \right]$	Well-defined VDF properties proposed
Akçelik (1991)	Travel time functions for transport planning purposes: Davidson's function, its timedependent form and an alternative travel time function	$tt = t_f + 0.25T \cdot \left[\left(\frac{V}{C} - 1\right) + \sqrt{\left(\frac{V}{C} - 1\right)^2 + \frac{8JV}{TC^2}} \right]$	Timedependent form, derived by using the coordinate transformation technique
Huntsinger and Roupail (2011)	Bottleneck and queuing analysis: calibrating volumedelay functions of travel demand models	$tt = \begin{cases} t_f \left[1 + \alpha \left(\frac{V}{C}\right)^\beta \right], & \text{if } V \leq C \\ t_f \left[1 + \alpha \left(\frac{D}{C}\right)^\beta \right], & \text{if } V > C \end{cases}$ <p>$D = \text{demand at capacity} + \text{queue}$</p>	Queued demand-based
Moses et al. (2013)	Development of speed models for improving travel forecasting and highway performance evaluation	$tt = \begin{cases} t_f \left[1 + \alpha \left(\frac{V}{C}\right)^\beta \right], & \text{if } V \leq C \\ t_f \left[1 + \alpha \left(\frac{D}{C}\right)^\beta \right], & \text{if } V > C \end{cases}$ <p>$D = C + (C - V)$</p>	
Kucharski and Drabicki (2017)	Estimating macroscopic volume delay functions with the traffic density derived from measured speeds and flows	$tt = t_f \left[1 + \alpha \left(\frac{k}{k_c}\right)^\beta \right]$	Density as proxy of V/C

Parametrizing macroscopic road network model of traffic-calmed zones.

Lazar et al. (2020)	Routing for traffic networks with mixed autonomy	$tt = t_f \left[1 + \alpha \left(\frac{V^H + V^A}{C} \right)^\beta \right]$	Mixed flowbased
Cheng et al. (2022)	Estimating key traffic state parameters through parsimonious spatial queue models	$tt = t_f \left[1 + \frac{\gamma \cdot g(m)}{\mu \cdot t_f} \cdot \left(\frac{D}{\mu} \right)^4 \right]$	Fluid based queue with cubic arrival rates and fixed inflow curvature parameter
Zhou et al. (2022)	A meso-to-macro cross-resolution performance approach for connecting polynomial arrival queue model to volume-delay function with inflow demand-to-capacity ratio	$tt = t_f \left[1 + \frac{\gamma \cdot g(m)}{\mu \cdot t_f} \cdot \left(\frac{D}{\mu} \right)^4 \right]$ $\mu = \frac{C}{f_d \cdot \left(\frac{D}{C} \right)^{n-1}}$ $\gamma = 64C \cdot \frac{L f_p}{v_{co}} \cdot \left(\frac{D}{C} \right)^{s-4}$	Fluid based queue with a family of inflow curvature parameter values, derived from two elasticity forms and D/C ratio

As mentioned above, in the various VDFs, different approaches can be seen when it comes to the entry variables, depending on the entry data available. In this thesis, thanks to the data from the microscopic model and the precise reproduction of traffic, the most suitable types of functions would be those considering traffic volume, precisely, density as an entry data. This allows for an uncomplicated VDF estimation, possible in numerous applications.

2.4.2. Solving the problem of demand exceeding capacity

In the macroscopic model, traffic flow is strictly connected with demand flow. The principles of traffic sets a capacity for each link, together with the behaviour according to the fundamental diagram of traffic flow. It represents capacity drop, spillbacks, gridlocks, etc. and can be handled

with dynamic traffic flow models. In static traffic flow models this situation is simplified, yet still applied in large scale traffic demand models. The first (hypocritical) part of the Volume-delay function complies with traffic flow definition and can be estimated according to empirical observation. Issues arise in the hypercritical part of the function, where empirical observation is impossible, and thus cannot be estimated that way. In practice, the hypocritical part is estimated, and for the hypercritical parts, arbitrary parameters are used. Table 2 shows the literature review of the existing solutions for congested conditions.

Table 2: Demand definition for congested conditions in literature [28]

Categories	Author/s/Year	Paper title	Detailed definition
Highest flow rates associated with traffic intensity	Kimber and Hollis (1979)	Traffic queues and delays at road junctions	Definition of traffic demand in a stream is q and the capacity available to it μ (both expressed in average vehicles per unit time) at a given stage, traffic intensity is defined as $\rho = q/\mu$
Peak-period inflow Volume D	Small (1983)	The incidence of congestion tolls on urban highways	Peak-period inflow Volume D, uniform rate and delay result from queuing behind a single bottleneck with a constant capacity
Approximated overflow rate	Moses et al. (2013)	Development of speed models for improving travel forecasting and highway performance evaluation	$D = capacity + (capacity - volume)$

Parametrizing macroscopic road network model of traffic-calmed zones.

Queued demand	Huntsinger and Roupail (2011)	Bottleneck and queuing analysis: calibrating volume-delay functions of travel demand models	$D = \text{demand at capacity} + \text{queue}$
Approximation through density	Kucharski and Drabicki (2017)	Estimating macroscopic volume delay functions with the traffic density derived from measured speeds and flows	$D = k \frac{k}{k_c} \cdot \text{capacity}$
Total volume during congested period	Wu et al. (2021); Cheng et al. (2022) based on Newell (1982)	Estimating key traffic state parameters through parsimonious spatial queue models	$D = \sum_{t_0}^{t_3} q(t), t \in [t_0, t_3]$

2.4.3. Methods of VDFs estimation

In different cities in Poland, for the purposes of urban or regional transport models, various methods of collecting data to estimate VDFs are used. In every Polish example of VDF estimation mentioned below, the BPR function was used.

In the Gdańsk metropolitan area model, for the streets covered by the local ITS, Tristar, data on velocity and traffic flow are collected by system elements placed at points of the network. This system contains ANPR

Parametrizing macroscopic road network model of traffic-calmed zones.

cameras recognising vehicles' registration plates, Wi-Fi and Bluetooth scanners, allowing us to register the time and address of the drivers' mobile devices. This allows us to register the time at which a particular vehicle reaches a measuring point and calculate its velocity. For places outside Tristar system's coverage, and for the purposes of building the transportation model, data from the GPS navigation application Targeo was used [29, 30]. The results of the VDF estimation have been shown below:

Table 3: Comparison of VDF estimation used in Gdańsk, source: [29, 30]

Parameter	α	β	γ	c	R	MSE
<i>Morska Section Cisowa</i>						
BPR	-0,31	1,52	–	–	0,63	16,7
CONICAL	2,34	1,42	-0,002	–	0,65	15,6
INRETS	-5,4	–	–	-0,03	0,61	16,9
<i>Morska Section Grabówek</i>						
BPR	-0,48	1,39	–	–	0,78	17,9
CONICAL	2,34	1,42	-0,002	–	0,79	17,6
INRETS	-3,4	–	–	-0,1	0,75	17,8
<i>Wielkopolska Section Mały Kack</i>						
BPR	-0,31	1,73	–	–	0,70	13,6
CONICAL	2,43	1,39	-0,001	–	0,76	16,1
INRETS	-9,59	–	–	-0,02	0,68	16,1
<i>Wielkopolska Section Karwiny</i>						
BPR	-0,35	1,23	–	–	0,83	8,02
CONICAL	1,68	1,71	-0,013	–	0,83	8,01
INRETS	-8,19	–	–	-0,03	0,82	8,56

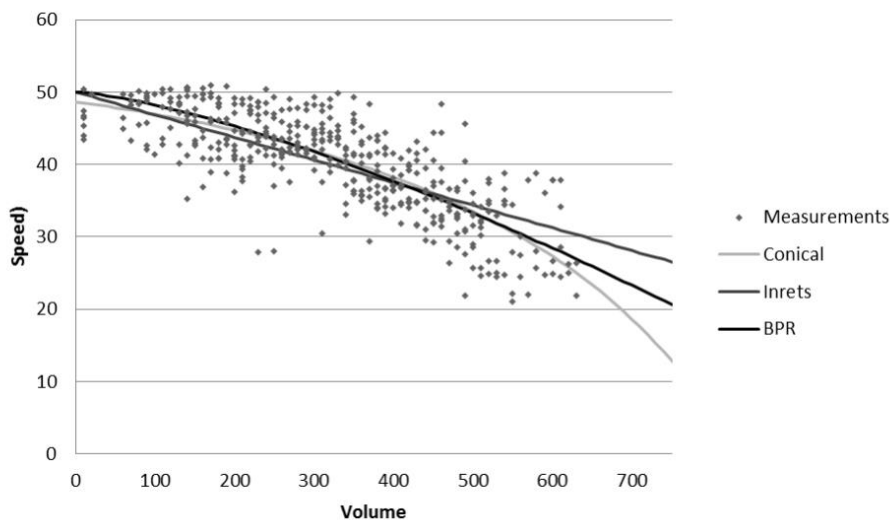


Figure 12: Graphical presentation of the VDF estimation used in Gdańsk, source: [29, 30]

In the Silesian Metropolitan area model, data was collected by measuring traffic volumes and velocities at set measuring points for the required road categories. For free flow velocity, 0,95 percentile of the velocity measurements were used. The capacity was defined accordingly. Traffic volumes and speeds for the volume-speed relation were collected in 5-minute intervals for the q/q_{max} from 0,1 to 1,2. During these

Parametrizing macroscopic road network model of traffic-calmed zones.

measurements, there was no congestion, so the parameters of the function were taken from the Highway authority (GDDKiA) model [31].

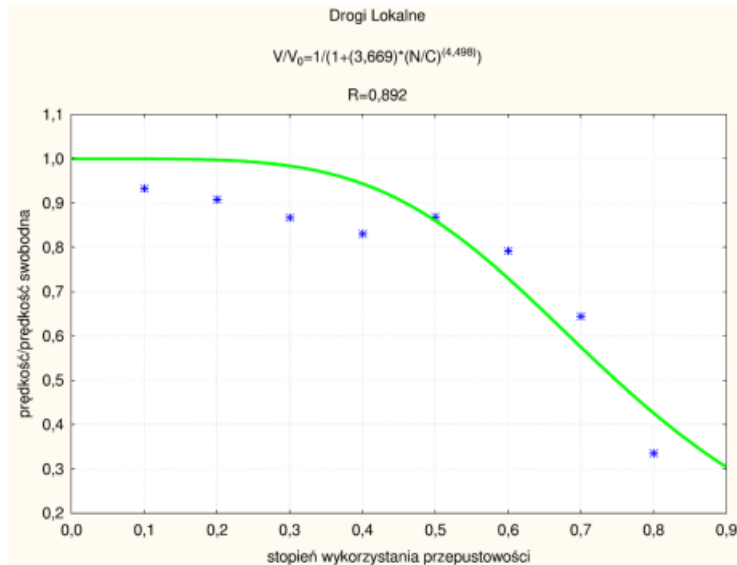


Figure 13: Example of the function used in Katowice model: Velocity multiplier as a function of saturation grade. Source: [31]

For many analyses in Poland, such as the Kielce transport model, there are no measurements taken under local conditions, but standard VDF parameters are used, taken from the literature, such as [32].

2.5. The Microsimulation model

In the microsimulation model, every vehicle is analysed separately according to its features, such as speed, acceleration, etc. and the driver's behaviour is represented according to current traffic situations in every frame (time stamp) of the simulation [15]. For correct functioning of the microsimulation model, it is essential that it be calibrated to reproduce a real situation (unimpeded speed, interactions, reactions). Based on these parameters, demand (traffic) moves along its path during the simulation. Path choice or traffic assignment usually takes place outside of the microsimulation model – the most important calculations of the microsimulation model are costs (travel times). Microscopic models are dynamic models – the result (state of the traffic on network) is a function of time. The result of the simulation depends on many parameters, so it is difficult to describe the influence of separate parameters on the model. Every vehicle can be described according to basic parameters: position, velocity, acceleration in time. Average simulation time is long (ex. 30 min) and discretised simulation time is dense (ex. 1s). Because of the above, microsimulation models require a lot of computing power, and precise network reproduction, requiring a great amount of information, which is very hard or impossible to achieve for bigger areas like cities. Each simulation run represents one stochastic situation taken from the whole set of every possible situation. The result of the simulation could be presented as, for example: animation, trajectories (spatial and movement data), average travel times or speeds, unimpeded traffic speed or delay as an effect of growing density.

An example of microsimulation traffic modelling is PTV Vissim software. Vissim's traffic flow model is a stochastic, time-step based, microscopic model that treats driver-vehicle units as basic entities. The car following model is based on the Wiedemann model.

A traffic flow model is used to move vehicles through the network. Vissim uses Wiedemann's psycho-physical perception model, as opposed to simpler models that provide a mainly constant speed and deterministic automobile following logic. The essential idea behind this model is that when a driver of a faster moving vehicle hits his individual perception threshold for a slower moving vehicle, he begins to decelerate. Because he cannot precisely determine the speed of that vehicle, his speed will drop until he begins to slightly accelerate again after reaching another perception threshold. There is a gradual and consistent acceleration and deceleration.

Parametrizing macroscopic road network model of traffic-calmed zones.

Different driver behaviours are taken into account using speed and distance distribution functions.

Wiedemann's traffic flow model is based on the notion that a driver has four distinct driving states:

- Free driving: There is no effect from preceding vehicles. The driver is in this state as he attempts to reach and maintain his desired speed. In practice, the speed will fluctuate in free driving due to non-ideal throttle control. It will constantly fluctuate around the desired speed.
- Approaching : The process by which a driver adjusts his velocity to match the slower speed of a previous vehicle. The driver decelerates as he approaches, so that there is no difference in speed once he reaches the desired safety distance.
- Following : The driver follows the car in front of them without intentionally decelerating or accelerating. He maintains a consistent safety distance. However, due to poor throttle control, the speed difference fluctuates around zero.
- Braking: If the distance to the preceding vehicle is less than the desired safety distance, the driver applies medium to high deceleration rates. This can occur if the preceding car's driver rapidly alters their speed or if the driver of a third vehicle changes lanes to squeeze between two vehicles.

Figure 9 shows driving behaviour reproduced in the model:

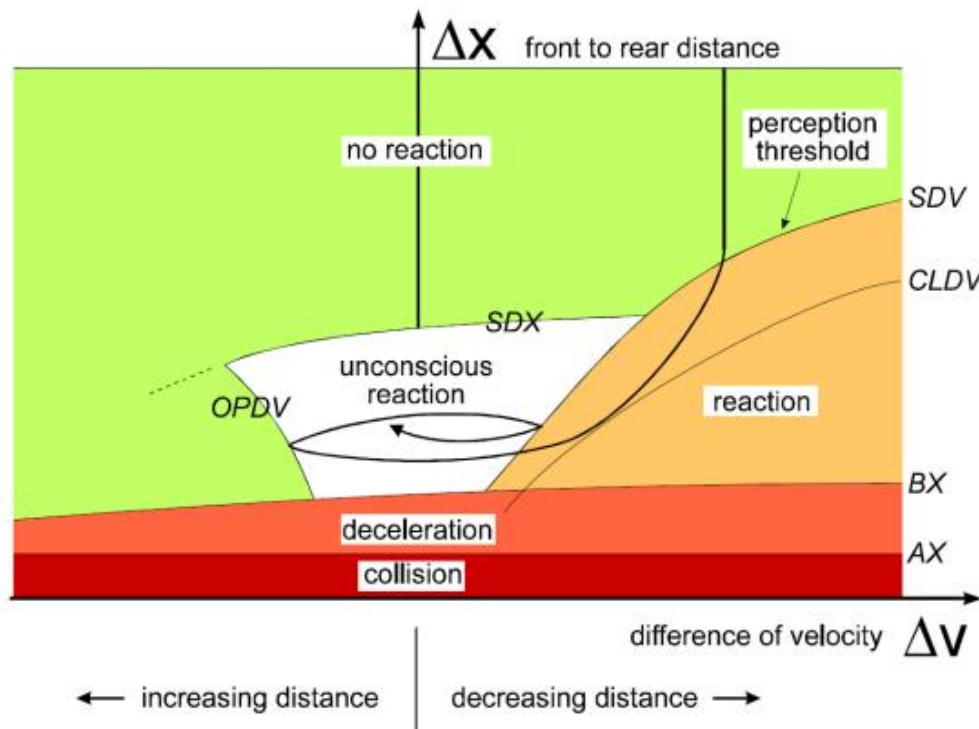


Figure 14: States of PTV Vissim model source: PTV Vissim 9 manual [33]

Driving behaviour is described in detail using Wiedemann model parameters: Wiedemann 74, such as safety distances, lack of attention duration or lack of attention probability and Wiedemann 99: time distribution of the speed-dependent part of the desired safety distance, time of deceleration before reaching safe distance, influence of distance on speed oscillation, and desired acceleration when starting from standstill.

Acceleration is explained for each of the four driving states as a function of current speed, speed difference, distance to the previous vehicle, and individual driver and vehicle attributes.

Drivers change states when they approach a specific threshold, which can be defined as a function of speed difference and distance. Small differences in speed, for example, can only be perceived over short distances. Whereas large speed differences already force drivers to react over long distances.

The perception of speed variations, as well as the desired speed and safety distance maintained, varies among drivers.

Because the model takes into account both psychological and physiological limitations in drivers' perception, it is known as Acceleration is explained for each of the four driving states as a function of current

speed, speed difference, distance to the previous vehicle, and individual driver and vehicle attributes.

Drivers change states when they approach a specific threshold, which can be defined as a function of speed difference and distance. Small differences in speed, for example, can only be perceived over short distances. Whereas large speed differences already force drivers to react over long distances.

The perception of speed variations, as well as the desired speed and safety distance maintained, varies among drivers.

Because the model takes into account both psychological and physiological limitations in drivers' perception, it is known as psycho-physical car-following model. The basic concept of this model is that the driver of a faster moving vehicle starts to decelerate as he reaches his individual perception threshold to a slower moving vehicle. Since he cannot exactly determine the speed of that vehicle, his speed will fall below that vehicle's speed until he starts to slightly accelerate again after reaching another perception threshold. There is a slight and steady acceleration and deceleration. The different driver behaviour is taken into consideration with distribution functions of the speed and distance behaviour [33].

Vissim calculates the acceleration of a vehicle during free traffic flow, below the desired speed, based on the following:

- If the desired safety distance is set to 100 percent, the vehicle drives at the same speed as its preceding vehicle.
- If the desired safety distance is set to between 100 and 110 percent, the speed is interpolated between the vehicle's desired speed and the speed of its preceding vehicle.
- If the desired safety distance is set to greater than or equal to 110 percent, the vehicle accelerates at its desired speed [33].

2.5.1. Microsimulation model calibration

As mentioned above, the transportation microsimulation model consists of various parameters, which need to be estimated in order to present results compliant with the actual state of traffic flow. In the calibration process, those parameters are adjusted in order to make a model more similar to observed data [34].

The transportation microsimulation model consists of different kinds of parameters, depending on their complexity, adherence to physical

(infrastructural) or behavioural characteristics, or specific kinds of users (vehicle categories).

Calibration methods are also based on these characteristics along with the amount of measurements taken, depending on whether they present data only from one point [35, 36], specific points in several locations [37], various locations [38, 39], or the full, continuous trajectory, for the whole modelled network, for one vehicle or for all of them.

Calibration is the optimisation problem, that aims to minimise (or maximise) fit quality parameters. To reach this aim, the most common methods are manual or automated calibration [40, 41], based on the genetic algorithms [36, 42, 43] or the simplex method [35]. Manual methods are used in the literature example [39, 44-46], yet due to its difficulty in estimating parameters, it is not recommended on the bigger models [34]. Automated methods allow us to calibrate parameters for the greater area or to calibrate multiple parameters simultaneously.

Measures indicating a goodness of fit are usually based on comparing each single pair of modelled and observed result. An example of such measures are error measures, including: percent error [44-45], squared error [38, 47], mean error [48], mean normalised error [38, 47, 48], mean absolute error [40], mean absolute normalised error [35, 40, 42, 44], exponential mean absolute normalized error [36], root mean squared error [37, 48], and root mean squared normalized error [40, 41, 46, 48]. Other examples include GEH statistic [38, 39, 49], correlation coefficient [46], Theil's bias proportion [46, 49, 50], Theil's variance proportion [46, 49, 50], Theil's covariance proportion [46, 49], Theil's inequality coefficient [40, 46, 48-50], the Kolmogorov-Smirnov test, Moses's test and the Wilcoxon test [42].

2.6. Vehicle movement surveying

To reproduce driver behaviour to a high level of precision, it was necessary to have precise vehicle motion recorded including data relating to speed, acceleration and braking. Moreover, for further investigation of the problem, it was important to note interactions between vehicles; these interactions include the distances between successive vehicles, braking forces when noticing approach to the car in front, and speed and distance fluctuations when following. These parameters can be adopted in the Wiedemann model, used in PTV Vissim software.

None of the aforementioned speed measurements can deliver full, continuous movement information. For full vehicle movement data, one must study the entire vehicle trajectory along the set route.

Speed measurement types can be divided into two categories of measuring technique: inside and outside the vehicle.

2.6.1. Measurements inside the vehicle

Measurements taken from inside the vehicle usually involve measuring devices used inside a test vehicle, to measure velocity, acceleration and braking.

The first method, also known as floating car, involves a measurement car equipped with a movement tracking device, such as a car computer, that records the distance travelled by, and speed of, the car, or additional values such as acceleration and braking pedal pressure. Another solution for floating car motion recording is the use of GPS devices, which record not only the speeds of the vehicle, but also its trajectory; this means that in every time stamp (for example 1 second), the position of the vehicle is recorded. When using this method, it should be noted that GPS has an accuracy of 2-5 meters [51], which can have a negative influence on the results. Floating car can also be used to measure the parameters of different vehicles – in this case, apart from the floating car's measuring devices, there are also devices installed that measure vehicle movement relative to the floating car – such as differences in velocity, etc.

The second method involves using vehicles equipped with a GPS device that collects time-space data. This is usually achieved via mobile device applications, e.g. for navigation or taxi/rideshare services. This solution allows us to collect a greater amount of data, however it raises privacy concerns, thus there are limited permissions for using this kind of data.

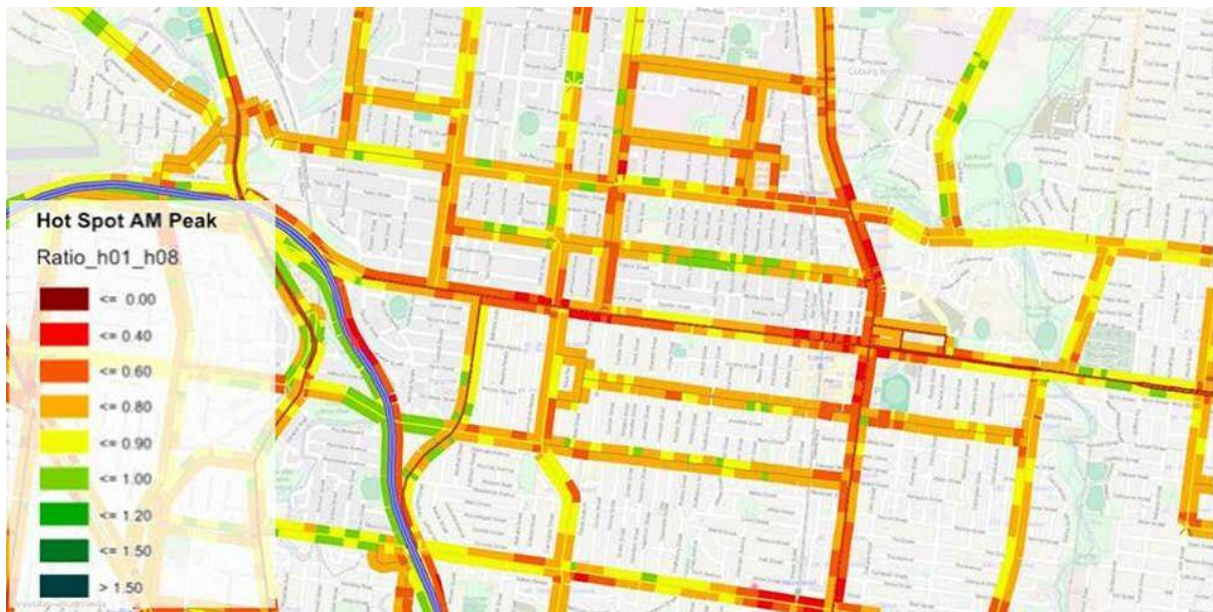


Figure 15: Floating car data presented as a heatmap of the link speed. Source: PTV Visum software

2.6.2. Measurements outside the vehicle

Measurements taken from outside the vehicle, unlike the above methods, are able to record the behaviour of more than one vehicle.

Speed measurements taken from outside the vehicle can be classified into four groups depending of several characteristics [52].

- Spot (instantaneous) speed – the speed of a vehicle at a given point on the road, measured the moment a vehicle passes a measuring point. A measuring field can consist of more than one measuring point.
- Journey speed - speed measured as a travel time between two points and delivering data about the average velocity on the link between those two points.
- Space mean speed – instantaneous speed of all vehicles on the road being measured.
- Running speed – average speed of a trip, excluding stops.

These methods involve the following measurement tools:

- Radar meters – measure the individual speeds of the vehicle using radio waves reflected off the vehicle. This is a simple and portable solution, however, in case of two vehicles driving next to each other,

Parametrizing macroscopic road network model of traffic-calmed zones.

it is uncertain which vehicle speed will be measured. Also, data may be biased if the observer is visible [53].

- Enoscope – measures speed over a short distance. It consists of two mirrors that enable us to shift the line of sight by 90 degrees along the tripod that separates them. The observer measures the time during which a vehicle is visible in one mirror and then the other using a stopwatch [54]. This solution is sensitive to human error as the observer is responsible for relating the sampled vehicle at both moments and to measure the time [55].

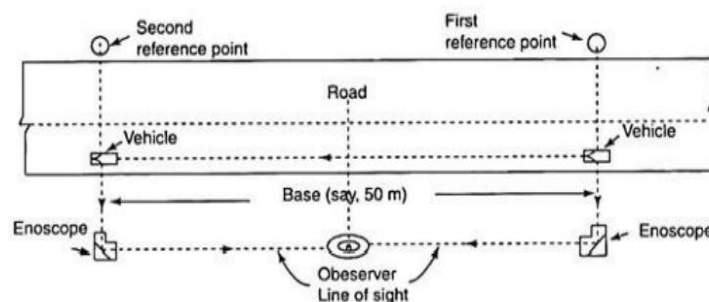


Figure 16: Enoscope working scheme, source: [54]

- Vehicle detectors – a pair of detectors placed next to each other, measuring speed by comparing the time taken to detect the vehicle. These detectors can be divided into those that detect a single axle and those that detect the whole vehicle. Among the axle detectors there are:
 - Pneumatic tubes, which detect the change of air pressure in the tube caused by the car's tyre
 - Treadle detectors, which detect the electric current generated by the car tyre forcing contact between two copper elements.
 - "Jarvis brick" optical infrared detectors, which detect the vehicle's tyre when it interrupts a light ray between a light source and receiver
 - Triboelectric cables, consisting of a coaxial cable and a central conductor, which detect cable compression and cause electric charge to accumulate

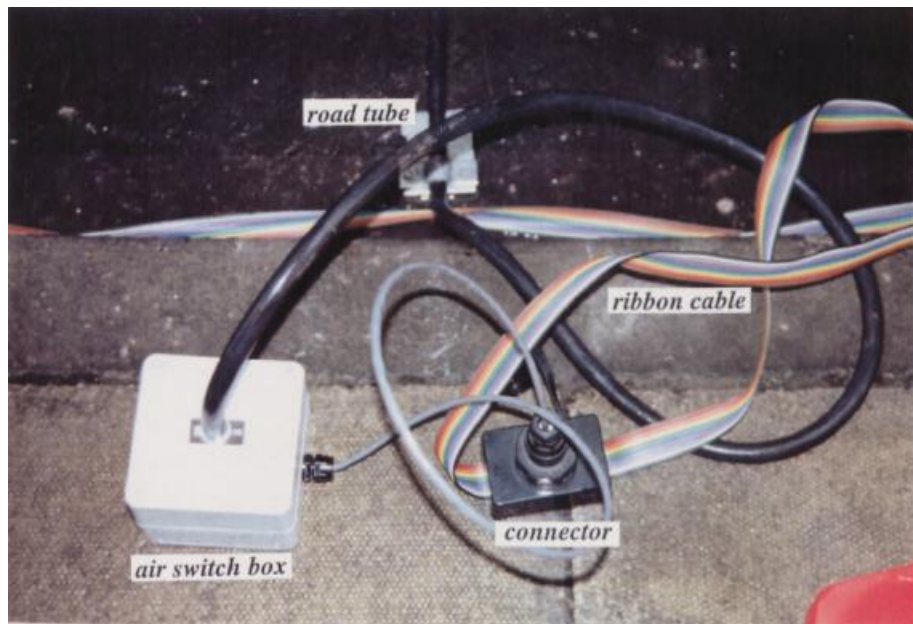


Figure 17: Pneumatic tube device setup. Source: [57]

Among vehicle presence detectors there are:

- Inductive loop – a coil installed onto a paved road. The car above the loop changes its inductance and the vehicle is detected. This solution can be widely seen on accommodative signalised intersections to detect traffic flow and adjust traffic signals. A pair of such loops is able to detect vehicle velocity.
- Video detectors, which use cameras to detect vehicles and other users, also used on accommodative signalised intersections. Cameras can be installed on the existing or temporary infrastructure. Alternatively, cameras can be placed airborne, on the unmanned aircrafts. Deeper review of this topic is placed in a chapter 2.6.4
- Microwave sensors using the Doppler effect [56].

These methods involve strategies like pneumatic tubes for speed measurement or radar control [57], and can be connected to speed control, photographing or video recording facilities. Unfortunately, most of these methods only work in one specific point of the measured road or area; therefore, one needs to provide measurements in other points as well. However, gaps between measurement points still exist.

2.6.3. Video detection – vision-based vehicle speed estimation

The development of digital imaging and traffic cameras has led to them being used for various tasks in the ITS, including video-detection. This allows for simple speed estimation without the use of expensive, dedicated speed detection sensors [58]. However, this kind of velocity measurement requires a series of conditions in order to estimate speed accurately. For vision-based vehicle speed estimation, we can include video cameras, which record continuous video material, and speed cameras, which use sensors (radar, laser or vision) to measure speed together with a camera that takes a photograph of the vehicle. In this section, video cameras will be discussed in view of the possibility for continuous speed monitoring.

Beyond video-detection itself, using video-detection for speed estimation presents various challenges, including those related to optical or geometrical aspects.

The first of these aspects is camera settings. According to the camera's resolution, focal length, location and angle to the road, one needs to determine what portion of the road is represented by one particular pixel of the video recording. This parameter, known as meter-to-pixel ratio, is one of the most important variables to estimate when applying video footage to real conditions [59-68]. In order to properly estimate this parameter, camera calibration is needed to account for camera optical system imprecisions, geometrical issues, etc. This includes soft calibration (including camera placement and framing on the road) [69-78], and hard calibration (for preinstalled cameras) [79-81]. Calibration can be manual or automatic. A few limited sources also indicate negligence of camera calibration [82-84].

The next challenge is finding a vehicle detection method. In this section, we cite three principal methods. The first of these consists of subtracting the background. The only moving object on the recording should be a vehicle, therefore the part of the image that remains unchanged is the background [59, 60, 69, 70, 73, 74, 76, 80, 82, 85-102]. The second methods consists of detecting a license plate [103-107] or any other, easily distinguishable vehicle feature [61, 65, 77, 81, 101, 104, 108-112]. In the last method, machine-learning algorithms detect vehicles in every single frame of a piece of video footage. Due to increasing learning possibilities and the existence of algorithms already capable of detecting classes of objects, use of this

Parametrizing macroscopic road network model of traffic-calmed zones.

method has been growing recently [66, 67, 72, 78, 83, 97, 110, 111, 113, 114].

After detecting a vehicle, the next step is to track it in the subsequent frames of the video. It is important that the tracking point belong to the same fragment of the vehicle in every frame of the video. This allows for precise movement tracking. In principle, there are three main categories of tracking methods. The first is based on tracking the set of vehicle features [62, 64, 72, 73, 75, 79, 80, 81, 90, 92, 94, 98, 108, 110]. The second consists of finding a middle point, a centroid of the vehicle, and to track it [59, 63, 67, 86, 87, 95, 100, 102, 115, 116]. Finally, the third method consists of tracking the vehicle as a whole [61, 66, 71, 74, 76, 82, 83, 88, 91, 97, 99, 110, 111, 117, 118] or selecting one specific part of it [64, 105, 107, 119] (e.g. license plate).

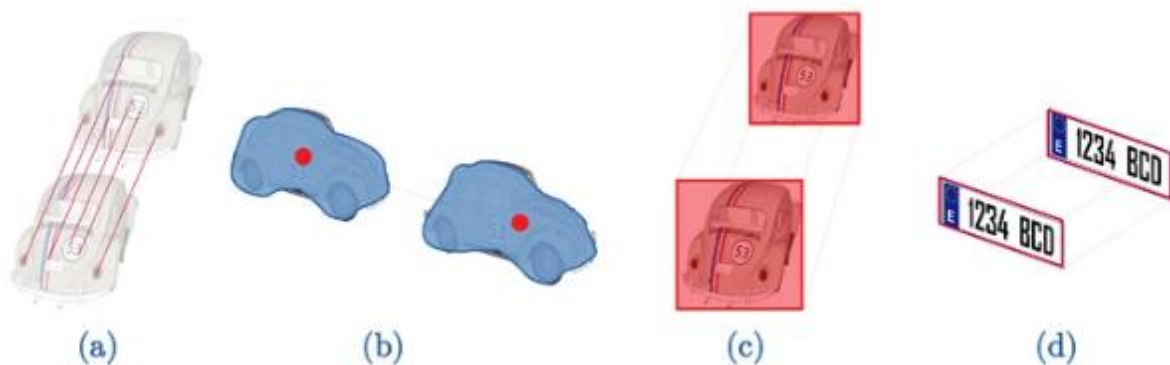


Figure 18: Methods of vehicle tracking, source: [58]

After a vehicle has been detected, placement of the vehicle in the road space is needed for proper speed measurement. This can be achieved by calculating the distance between the vehicle and the camera [71, 73, 80, 86, 92, 107, 111] or by introducing the coordinate system for the image [85, 87, 120]. Both solutions are leading to come down to calculating the angles from the central point of the camera.

Finally, the vehicle's speed needs to be estimated. Depending on the purpose of speed estimation, there are several methods available. The first of these consists of measuring velocity at a given point (a gate), for example by comparing the vehicle's distance in the gate and its distance one frame before or after it. One could measure multiple gates or only one, depending if a speed estimation is only needed punctually or if the speed chart is needed [85, 87, 120]. Second is the velocity estimation between two points (gates) on the road – this is done by calculating/measuring the time taken

for the car to pass between these two points/gates [59, 61, 63, 65-67, 121]. Finally, velocity can be estimated continuously, frame by frame in the video footage. This last solution offers a variety of possibilities for tracking the vehicle's movement, much broader than the sensor measurement methods [103, 104].

Aside from vision-based vehicle estimation methods, the camera's field of view plays a significant role in the spatial range of speed survey. By enlarging the observable area of the road, the number of obstacles grows. To avoid this, it is necessary to place the camera higher above the street. This is feasible when there are tall buildings surrounding the area, but such approaches are usually limited. Alternately, recordings can be made from the air. In that case, it is suitable to use the unmanned aerial vehicles, popularly named as drones.

2.6.4. Unmanned aircraft

To provide coverage of a large area with only low buildings, an unmanned quadcopter was used to hover 80 meters above ground level and record traffic along an approximate length of 110 meters of road. The quadcopter is able to fly for around 25 minutes, which, taking into account a safe reserve of battery time, take-off, positioning above the street and landing, leaves around 15-20 minutes of traffic recording at any one time. Recordings were made at a high definition of 1920*1080 pixels resolution and 40 frames per second.

An unmanned aerial vehicle (UAV) is an aircraft with no humans aboard. This type of aircraft is operated by automatizing various elements of flight operation. In most cases, UAV is operated, with a lower or higher level of autonomy, by a human operator. In that case, it is called a remotely-piloted aircraft (RPA) [122, 123].

In terms of their flying capabilities, UAVs can be classified as follows. Their first classification is based on their maximal attitude: HAP (High Altitude Platforms) [124-126] are able to operate within an altitude higher than 10 km above ground (in the higher layers of the stratosphere), contrary to LAP (Low Altitude Platforms) [127-129] which operate within an altitude lower than 10 kilometres above ground. The other classification differentiates UAVs by their flying method. According to this classification, there are vertical take-off and landing (VTOL) vehicles [130], aircraft [131-133] and balloons [134, 135]. Typically, various types of helicopters, including multirotors (quadcopters, hexacopters, etc.), are classed under VTOL. The biggest advantage of this kind of UAV is its ability to hover in one position. This enables it to record video footage for one place, without moving the frame. Additionally, this type of UAV is able to take off and land vertically, thus requiring only a small space [130]. The next category comprises aircraft that are standard constructions, able to fly when moving horizontally at a certain velocity. Unlike VTOLs, they are unable to hover in one place, and need a larger space to take off and land. However, they require less energy to fly. They can be used for long distance missions [131-133]. The third and final category is balloons. They have the advantage of very low energy consumption, enabling them to stay airborne practically without limits. However, they have the disadvantage of low velocity and manoeuvrability. Balloons can be free-flying or fixed to the ground. The second option, a balloon tied to the ground enables to stay at high altitudes in the same location for a longer time. This enables them to monitor the area using sensors or a camera for a longer time [134, 135].



Figure 19: Balloon used for the video detection of the vehicles. Source: [237]

Due to their technical development and increasing affordability, UAVs' field of application is expanding. For the longest time, various UAVs were only used by the military, especially for combat and surveillance. They are typically known as drones. Outside of military usage, UAVs are also used as search and rescue devices, in the form of aerial and naval (overwater and underwater vehicles). Their advantage in this field is the increase of the operator safety, as the operator can be kept away from danger. Their subsequent application is related to industry. UAVs can be used for construction and infrastructure inspections. It is useful in places that are difficult to access, for example at high altitudes. Such inspections can be done visually or with the use of various sensors. Beyond industrial inspections, UAVs can also be used for agriculture. As seen in the previous case, they can be used for inspection, but agricultural UAVs are also replacing agricultural aeroplanes because of their lower operation costs and easier handling and maintenance. Added to this, UAVs also have a commercial usage. They were primarily developed as the goods delivery system, where they replace overground logistics, especially in the cities. Furthermore, UAVs also provide wireless coverage. Finally, UAVs can be

Parametrizing macroscopic road network model of traffic-calmed zones.

applied to surveillance jobs. Placing the camera on the UAV above the ground provides greater optical coverage of the area. Moreover, UAVs can be used for road traffic monitoring [136].



Figure 20: The example of the VTOL UAV available on market: DJI Phantom IV. Source: Manufacturer's materials

The key advantage of UAVs in traffic monitoring is their large visual coverage [109]. This, along with the replacement of video cameras with sensors, enables them to monitor numerous vehicles over large continuous road segments [137]. This can be done by detecting vehicles frame-by-frame, collecting such data as: speed, driver behaviour, registration plates, etc. [109, 138].

The main applications of UAVs in traffic monitoring are as follows. First we have accident monitoring. UAVs can quickly localise traffic accident sites before the arrival of rescue teams. Fast aerial localisation is important for such situations because it avoids congestion, which typically builds up after an accident [139] (139). UAVs can also detect traffic violations on the road, such as illegal stopping or parking, overtaking, speeding or other dangerous manoeuvres [139, 140]. This can be done by identifying registration plates, using either UAVs or road cameras.

A second traffic monitoring application is pedestrian traffic monitoring. Pedestrian detection allows one to estimate Origin-Destination flows, crowding areas or other pedestrian behaviour in crowded areas, such as public transport changing hubs, pedestrian zones, crowded intersections or events [141].

Finally, traffic monitoring makes it possible to gather large amounts of vehicle movement data. It starts by measuring traffic volume, thus removing the need to install sensors, then proceeds to origin-destination estimation for intersections or small areas, before finally tracking vehicles' movements and trajectories [142].

Vehicle movement data makes it possible to collect data that is essential for the construction and calibration of the microscopic model. Through video-detection it is possible to record the total movement data of a vehicle – continuous, instantaneous velocity and simultaneous position of multiple vehicles. This not only enables speed modelling, but also, thanks to vehicle interaction data, estimation and calibration of car-following model parameters [121, 143-145].

As mentioned before, VTOLs and aircraft are the most popular UAVs because of their various practical applications. However, its main practical challenge is battery flight time. For the most popular VTOLs, standard flying time is about 30 minutes. This requires frequent landings in order to replace the battery, which causes interruptions to a UAV's mission and increases the number of maintenance activities. Increasing its battery capacity is not an efficient solution, as this also increases its mass, and with it, its battery consumption, while also reducing flying time [146-152]. The simplest solution for achieving an uninterrupted UAV mission is to replace it with another, charged UAV during the mission for the time of battery replacement, however, this requires twice as much equipment and operating two UAVs at the same time. Another solution, when operating in one location is required, is to connect a UAV to the ground via a power line. This is only possible if the UAV hovers in one place [153].

Another challenge for UAVs is their legal requirements, especially regarding their access to airspace. In urban areas, where traffic monitoring is often used, typically, due to airport proximity, the airspace is controlled. This, depending on the type of airspace control or the country, has a close connection to UAV usage limitation or the requirement for special permissions. For example, in Poland, in the CTR controlled airspace, maximal flying altitude is 100 meters above ground level. Altitude limitation can limit the visual range of observation for the UAV's camera. However, for locations 6 km or closer to the airport, special permissions are required and constant connection with the control tower is needed to take off and fly, which can be interrupted at any time [154].

3. Traffic calming

3.1. Traffic calming definition and level of influence

According to a definition by the Institute of Transportation Engineers [155], traffic calming is a set of measures, the purposes of which are to reduce the negative effects of motor vehicle use, alter driver behaviour and improve conditions for non-motorised street users. This includes reducing traffic volume, and with it noise and air pollution, thus improving road safety and quality of life. Traffic calming began in the 1960s and 1970s in Great Britain, Germany, Netherlands and Denmark, and was connected with pedestrianisation – the policy of prioritising walking by closing streets or slowing car speed down to walking pace [57].

Traffic calming can be divided into three levels according to scale of influence [156]:

Level I – actions restricted to a local, residential level with low traffic volumes and capacities to restrain traffic speeds and reduce traffic impacts

Level II – actions extended to a corridor, which have an influence on traffic along that corridor, but not across the network

Level III – actions at macro-level, introduced across a greater area and having an influence on the traffic network

The aims of the traffic calming can be achieved by two main factors: reducing the velocity or the traffic volume. By the reduction of the traffic volume, a negative factors of the car traffic dependent on the traffic volume can be reduced. Those are pollution, noise and safety.

The increasing velocity is also strictly connected with the road accidents, fuel consumption and pollution. The social costs of those factors are shown in Figure 11.

Parametrizing macroscopic road network model of traffic-calmed zones.

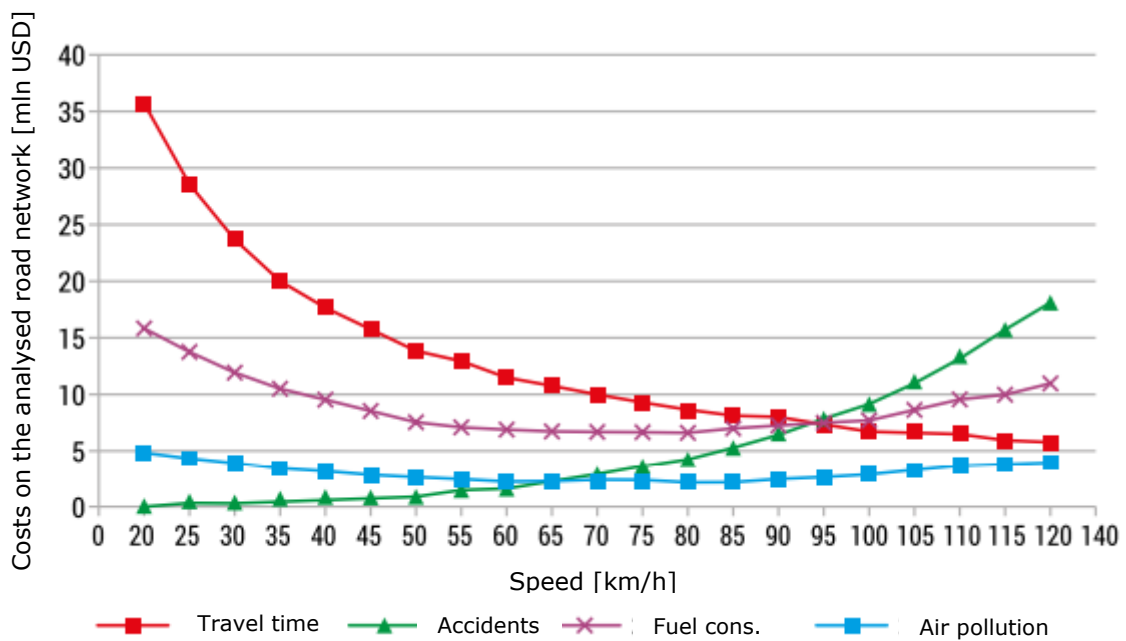


Figure 21: Social costs of the travel time, source: [157, 158]

Numerous research proves the low level of acceptance of the speed limits, especially the low speed limits on the local roads, where enforcing low speeds is crucial due to proximity to the residential areas. Thus it is important to find the measures forcing the drivers to maintain a limited speeds.

Considering the previously mentioned purposes of the traffic calming measures, they can be classified in four groups [159]:

- Velocity control measures: which include link and node related measures, such as: vertical and horizontal deflections
- Access control measures: street closure or one-way streets
- Traffic control measures: introducing street parking, on-street bus stops, islands, etc.
- Pedestrian and cyclist infrastructure: walking or cycling lanes, crossings, etc.

3.1.1. Link related measures

The first category of infrastructural traffic calming measures, are those installed along the street. These measures come in two main sub-categories: vertical and horizontal deflections. Horizontal deflections can be further divided into road narrowing and central islands.

Vertical deflections are measures that aim to reduce vehicle speeds at a single point. These measures force speed reduction by raising the road surface – otherwise the car can be damaged. This category includes: road humps, plateaus, speed cushions and uneven road surfaces. A road hump [160] is a short raised area that is either flat-topped or round [161]. A plateau raises the road level across a longer distance [162]. A speed cushion can come in the form of a hump or plateau, but is not extended over the full width of the lane, allowing heavy vehicles, buses and cyclists to pass unhindered [163]. An uneven road surface reduces vehicle speed by increasing noise and vibration, and with it the discomfort of driving [164].



Figure 22: Examples of the vertical deflections: speed hump (left) and speed cushion (right), source: [157]

Horizontal deflections enforce a vehicle's speed reduction by making it change its trajectory and take a sharp turn [165]. The standard example of the horizontal deflection is a chicane – on a straight street there is a narrowing on one side of the street and then on the other, forcing the vehicle to turn sharply. This solution however is not suitable for roads used by buses or heavy vehicles, as their length prevents them from crossing the chicane. In such cases one must reduce the sharpness of the turn, however, this is less effective for speed reduction [166]. A related measure in this category is that of road narrowing. This kind of traffic calming measure can be used in two ways. The first is lane narrowing – limiting the space on the sides of the vehicle to make it drive slower and more carefully [167]. In

such cases it is still possible for vehicles moving in the opposite direction to pass [167]. The final measure of this category is that of central islands. Their role is to narrow the lane by putting an object in the middle of the street. Moreover, they can serve as a pedestrian crossing refuge.

All the aforementioned measures, vertical or horizontal, can also be combined. For example, chicane or road narrowing can be combined with speed bumps, cushions or plateaus.

3.1.2. Intersection related measures

When it comes to traffic calming devices installed at intersections, their main aim is to increase the safety (of the drivers and pedestrians) in this area. As with link-related measures, vertical deflections are also present in this category. They can be applied as a traffic plateau or by elevating the whole intersection. This enforces speed reduction, while intersection elevation increases pedestrian comfort when crossing the street.

Horizontal deflections at intersections involve changes in intersection alignment, whereby speed is reduced because there is no straight line to cross the intersection. A similar effect can be achieved by reducing the junction area – in that case, the smaller area contains sharper turns. Finally, a central island or a roundabout can also be a traffic calming solution, as it prevents crossing the intersection in a straight line.



Figure 23: Example of the intersection related measure: mini roundabout. Source: [157]

Another traffic calming measure is that of gateways at the entrance to intersections. These can involve various traffic calming measures, such as plateaus, humps, narrowing or islands.

3.1.3. Traffic calming on main roads

The traffic calming measures mentioned above are mostly used on secondary roads. However, traffic calming introduction is also possible on main roads. The primary aim of this kind of traffic calming is to increase safety and reduce traffic noise. It usually involves enforcing a 50 km/h speed limit on these kinds of streets – with higher speeds, noise levels increase dramatically.

Typically no humps or chicanes are used for this kind of traffic calming. Main roads need to be able to move heavy traffic at large capacity, so this kind of traffic calming would be harmful. Instead, road narrowing of various kinds can be used. This solution encourages drivers to reduce their speed while at the same time creating space for pedestrians and/or cyclists. Apart of road narrowing, islands can also be installed. Their aim is to narrow a lane into a single point and to create safer pedestrian crossing by adding a refuge between the lanes.

Another traffic calming solution for main roads involves traffic light settings. Signalled intersections along one and the same route can be coordinated to provide a “green wave”. The pace of this coordination can be set at a specific speed, for example 50 km/h. In this case, any driver travelling at a higher speed would encounter a red light. Such a measure has the effect of shaping behaviour among road users, because respecting the speed limit is made more individually beneficial than speeding [168, 169].

3.1.4. Area traffic calming

Area traffic calming is a set of measures applied to an area of a city in order to minimize its influence on motor traffic in the wider area [162]. Typically, its aim is to reduce transit traffic through secondary roads and to direct it onto main roads. This can be achieved by all of the aforementioned traffic calming measures, applied both to links and intersections. Moreover, this kind of traffic calming can be supported by the traffic organisation. The organisation can indeed introduce limited access streets, e.g. for inhabitants only, or for any other selected groups of vehicles. Also, one-way streets can be used for traffic calming. The first advantage of this solution is that it reduce the number of lanes to one, thereby freeing up space in the road cross-section, e.g. for on-street parking, or more pedestrian or cyclist space. Additionally, one-way streets can be set up in such a manner, that it is impossible to use them for transit traffic – in that case, they are set up to only allow traffic in or out of the zone, not through it.

3.1.5. Impact on the pollution

The general aim of the traffic calming is to provide a safety for the road users, especially for the pedestrians and cyclists through, in general, limiting the vehicles speed. Nevertheless, the important aim is also to reduce the emission and noise, connected with the driving. Typical driving characteristic consists of the driving with the stated velocity, braking, accelerating and driving in neutral.

In theory, by reducing vehicles' velocities, traffic calming should also be able to reduce their emissions. However, some traffic calming measures force drivers to reduce their speed only at a single point. This causes braking followed acceleration, which potentially increases overall energy consumption and emission.

The proportions between this activities depends on the drivers' driving style, road type and traffic conditions. It is essential in the topic of the vehicle emissions. Traffic calming measures requires a significant velocity reduction. As a consequence, the velocity varies on the traffic calming measure and between them. The growth of the traffic dynamics, especially acceleration is a reason of the higher emission [170-174].

Parametrizing macroscopic road network model of traffic-calmed zones.

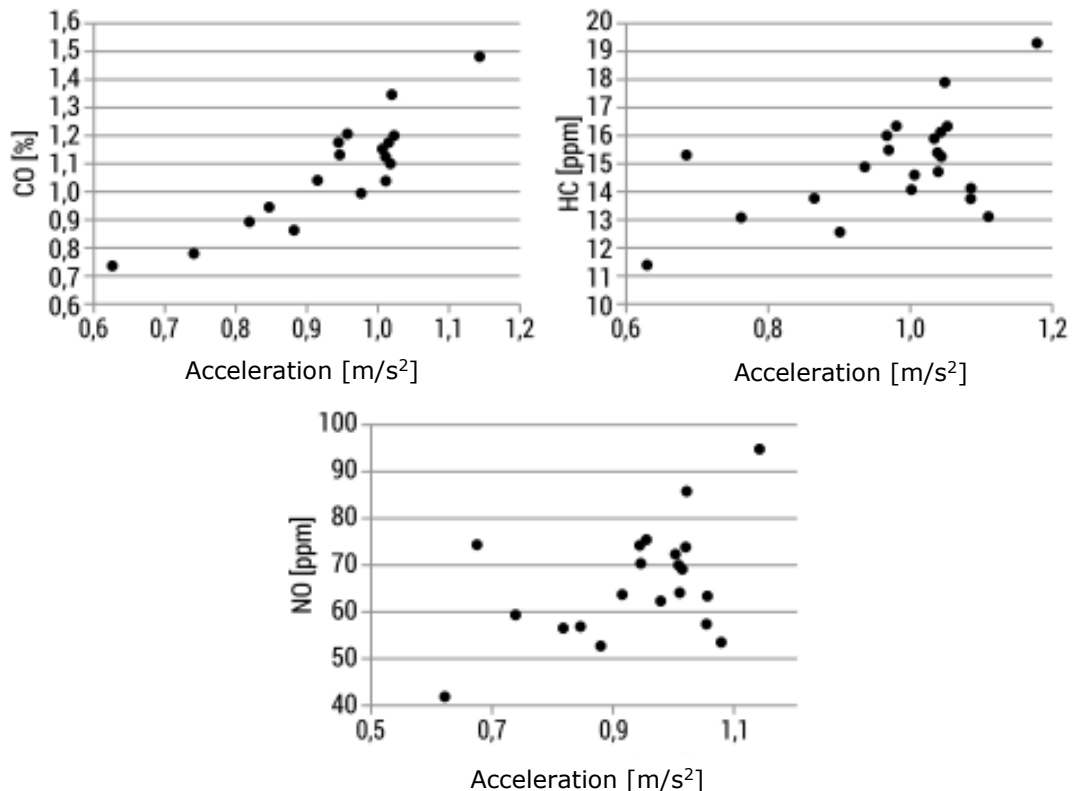


Figure 24: The influence of the acceleration on the emission (170)

According to the research results, the biggest influence on the emission has a driving style. Fuel consumption as well as the emission are the biggest during the braking and acceleration. Vlioger [174] et al proved, that a more dynamic driving behaviour results in a triple growth of CO, HC and NOx and 30-40% fuel consumption growth in the same travel time. Unal et al [175] researched, that emission is influenced by the higher amount of factors, where among of others, a speed and acceleration plays a significant role. However, they didn't confirmed the role of the braking in the emission growth. Similar results have been researched by Bokare et al [176]. In addition, Wang et al proved, in the statistical models reproducing the emission, that the greatest role in the emission plays the acceleration dynamic in the low velocities.

Below, some experiments have been reviewed individually

The first mentioned experiment took place in Germany. In part of the town of Buxtheude (approx. 30 000 inh.), an area traffic calming measure, in the form of a 30 km/h speed zone, was introduced. Seven floating cars travelled around the area, before and after introducing the traffic calming measure. Driving parameters, speed, gear selection and fuel consumption were recorded and later reproduced on the dynamometer to measure their

emissions. The result was a measured decrease of NO_x by 30%, CO by 20% and HC by 10%. However, the registered fuel consumption increased by 5% [177, 178].

Going further, the next two studies are on the topic of speed humps. The first study was conducted in Sweden. It includes modelling and calculations of the other traffic calming scenarios with a different number of speed humps. The assumption was that both deceleration before and acceleration after the speed humps would amount to 1,5 m/s². CO₂ and NO_x emissions were simulated using a Nordic Calculation Model for Vehicle Exhaust Pollution. For the link with one hump, it was simulated that emissions would rise by 20% and fuel consumption by 5%. In the case of 10 bumps, emissions were expected to rise three times higher, and fuel consumption to increase by 40-50%. Assuming that drivers would not accelerate after each hump, a smaller increase was predicted [179, 180].

The second experiment was undertaken in Austria. The floating car was used to test by introducing traffic calming with 6 humps stretched over 1,5 km of street. In the first phase of the experiment, the vehicle slowed down to 15 km/h before each hump, whereas on the second phase the vehicle stopped completely before each hump. Both situations were then compared to a third scenario where the vehicle moved with the constant speed of 30 km/h. For phase one, NO_x came out eight times higher and for phase two, ten times. Carbon oxide emission increased threefold in both phases. CO₂ emission and fuel consumption increased by 25% in both phases [181].

The final experiment that we will discuss took place in Sweden. The goal was to test the influence of mini-roundabouts on emissions. A floating vehicle collected data on 21 roundabouts in the city of Växjö. The data was in the form of speed profiles, comprising acceleration, braking and speed. Later, the data was used for emission simulation modelling. The result was an increase of CO emission by 5,6% and NO_x emission by 4% [182].

3.1.6. Impact on the noise

Excessive noise from the traffic has a negative influence on the life quality of those living in the neighbouring areas of the of the vehicle routes. It is estimated, that, according to the research [251], for the distance of 30 m

negative effects on health and irritability of people may occur along 21-22 % of the suburban sections of the road network of Mazowieckie voivodship. The biggest noise generators in vehicles are the engine and the powertrain [183], tyre-road surface contact, noises connected with the aerodynamics, and the noise from the moving of the cargo and other elements, especially in the heavy vehicles. The factors of the biggest noise generation are [184]:

- Traffic volume
- Velocity
- Share of the noisy vehicles in the traffic volume, such as heavy vehicles or motorcycles

The most significant influence on the traffic noise has a velocity. Activities connected with the application of the traffic calming measures can also influence the traffic noise. Those factors are:

- Velocity
- Homogeneity and fluency of the velocity
- Traffic volume and the traffic composition

In general, the vehicle noise increases together with the velocity. This relation is strongly noticeable considering the lower speeds and is stronger for the cars rather than heavy vehicles, where the noise is mostly generated by the engine and powertrain [185-187]. In the research, it was proved, that installing the speed humps resulted in the significant reduction of the maximal vehicle noise. Thanks to a significant speed reduction. Together with that, vertical deflections have caused the noise increase of the heavy vehicles, even besides the reduction of the velocity. Campoletti [187] proved, that a positive influence on the noise reduction can have a replacement of the signalised intersections by the roundabouts. In a work, it was proved, that a complex, area traffic calming can reduce a noise level. A successful limitation of the heavy vehicles connected with the reduction and unification of the average velocities can lead to reduction of the noise. It have to be emphasised however, that drivers after passing the speed hump starts to accelerate, which leads to the increased noise level. Abbott [184] was researching the influence of the specific kinds of the speed humps on the noise. He proved, that the noise reduction depends on the distance between humps and the vehicle category. For the cars, reduction fluctuated between 6,6 and 8,7 dB(A) to 10 dB(A). In case of buses, speed humps have reduced the noise level of the buses by 4 dB(A) and it didn't decreased the comfort of the passengers. For the vans, speed cushions increased the noise level by 2-7 dB(A), speed humps by 6 dB(A) and flat speed humps caused a reduction by 2 dB(A).

In conclusion, velocity and its fluency are the main parameters shaping the noise level. In the condition of the fluent traffic and with the relatively low speed, the noise level reduction can be significant. According to the research, the lowest noise emission is for vehicles with the constant speed between 30 and 50 km/h [188].

3.1.7. Impact on the driving behaviour and speed

Driver behaviour can be defined as the way the driver operates the vehicle [235]. The most prominent behaviour parameter is chosen speed in a given situation – e.g. link, speed limit, intersection or traffic calming device. Furthermore, in terms of speed, traffic behaviour can also be defined as acceleration and braking. Behaviour can alternately be described as the distances from, and reactions to, other objects, such as other vehicles, cyclists and pedestrians. In this review, the focus will be on vehicle velocity reduction.

Vertical deflections have a great influence on driving behaviour, especially speed on the link. Speed reduction varies according to the type and size of the deflections. Speed humps have a great influence on speed, forcing drivers to reduce their speeds to 20-30 km/h [189, 190]. In case of higher, round-top speed bumps (e.g. 100mm high), speed is reduced to around 20 km/h, whereas lower speed bumps (e.g. 75mm high) reduce speed down to 30 km/h. Low speed bumps (50 mm high) reduce speed to around 45 km/h [162, 163, 191]. Speed cushions work similarly to speed bumps for smaller vehicles, yet because of their design, they do not reduce the speed of the wider vehicles. Uneven road surfaces reduce vehicle speed by the smallest amount, around 4-5 km/h [192].

The effectiveness of horizontal deflections in speed reduction depends on the intensity of lateral direction shift and available space [193]. Furthermore, the effectiveness of a road narrowing to one lane depends on the traffic volume in both directions – with low traffic volume there is barely any need to stop and give way to the opposite direction [194, 195]. Chicanes can reduce speed to around 30-40 km/h because of the need for direction shift [196]. As for road narrowing, its influence on speed is not as significant. There are examples of speed reduction from 33 km/h to 30 km/h for a narrowed link. Central islands, for their part, have not been shown to reduce speed unless they are combined with other measures.

Regarding the intersection-related measures, roundabouts have been found to reduce speed. Typically, this kind of traffic calming measure reduces the average speed to 30 km/h, even if the initial speed was around 50 km/h [182]. Gateways at intersections can reduce speed to around 10-15 km/h and are compatible with 30 km/h speed limit [197, 198].

Traffic calming on main roads enforces speed limits for higher class roads, with high design parameters, which encourage drivers to travel at higher speeds. As mentioned above, for this road class, it is virtually impossible to install any kind of deflection. Thus, speed can be enforced by traffic light coordination, for example. Another positive effect of speed reduction is easier merging of buses departing from bus stops, or easier and safer pedestrian crossing without traffic signals.

Area traffic calming can reduce traffic volumes on traffic-calmed areas by assigning them to transit roads. With the reduction of traffic volume, however, it is crucial not to enable/encourage drivers to drive at higher speeds using measures initially meant to reduce speed.

Speed humps have been first used in 1970s in the Netherlands [199, 200]. Speed research of its presents have proved a high efficiency in the reduction of the velocity statistic parameters (average speed, speed quantile). On the other hand, vertical deflections influenced on the great heterogeneity and dispersion of the instantaneous speeds in the traffic calming location. V_{85} quantile of the speeds ranged from 18 to 50,9 km/h [201, 202], which is explained as the usage of the specific measure (speed humps, speed cushion) and its geometrical characteristics (height, shape, inclination). Geometrical characteristics of the vertical deflections have been researched multiple times [203-207]. Analysis of the deflection height (3-10 cm) influence on the velocity have shown, that the increase of the height is causing a speed reduction. Based on the research undertaken in Denmark [199], it was shown, that raising the deflection height by 1 cm, will reduce the velocity by 1 km/h. Shaping a less steep ramp connected with the lower height of the deflection favours driving with the higher velocities and exceeding the speed limits 30 meters before and after crossing the vertical deflection [203]. Moreover, dependency analysis between a deflection geometry and velocity have proven, that among the basic geometrical parameters, the biggest influence has its height and the ramp profile [208-214]. Effectiveness of the deflections and low installation costs made them to be used widely in multiple countries. Researchers have worked an optimisation models of the shape and height of the deflections [204, 210, 215]. In the field research of the influence of the traffic calming measures on the change of the drivers' behaviour in the topic of the velocity [216-218], it is becoming popular to use the driving simulators and computer

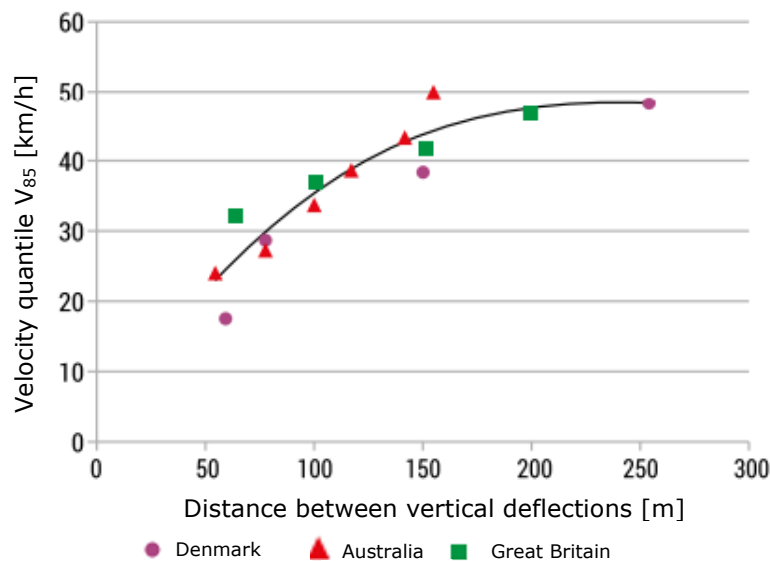
programs to analyse various solutions [219-222]. Results of the research have shown, that the most efficient speed reduction measures are various vertical deflections, as speed humps, elevated pedestrian crossings or intersections and speed cushions.

Traffic calming measures are often installed singly instead of the complex, area-based solution. This is caused by the easiness to install and a lack of the complex guidelines. Vertical deflections have a strong influence on the speed reduction, however its influence range is small. Moreover, installing those measures singly causes traffic fluency disruptions caused by the aggressive acceleration and braking instead maintaining a constant speed [223]. Often slowing down and accelerating manoeuvres can also lead to the additional, dangerous behaviours [224, 225].

In the USA, at the beginning, the first traffic calming measures have been placed in the distance of around 150 m between each other. As a result, it was confirmed, that between the measures, the desired speed haven't been achieved. However, placing the measures too close to each other caused users' protests. The reason of the protests, could be, that the installation took place in a remote location in suburbs [226]. Kveladze and Agerholm [227] have proved, that the changing distance between the vertical deflections influence the median velocity in the intermittent points, however did not formulated any specific function relations. Yeo et al. (228) have analysed the influence of the vertical deflections on the V_{85} speed quantile, and have indicated, that maintaining the constant velocity of 30 km/h is possible when the measures are placed between 20 and 70 meters between each other. Vatikus et al. [229] recommended the gap 150-200m, 100m, and 75m to achieve a desired speed of 50, 40 and 30 km/h respectively. US research have indicated, that for every 100 feet (30,5m) the speed increases between 0,8-1,6 km/h when the deflections are installed in the distance of 1000 feet (305m).

Parametrizing macroscopic road network model of traffic-calmed zones.

Figure 25: Speed in a function of the distance between the vertical deflections (230)



The influence of the vertical deflection on the traffic conditions have also been researched. Garcia et al [221] have simulated the speed humps influence on the traffic conditions depending on the distance between them. As a result, they have researched the worsen of the traffic conditions with the traffic volume higher than 900-1200 veh/h with the humps placed 25 and 50 meters from each other. The Swedish guidelines indicates, that vertical deflections shouldn't be used when the average day traffic volume exceeds 5000 veh/24h. French and American requirements in this case states a limit of 10 000 veh/24h [231, 232].

Summing up, the results of the influence of the traffic calming measures introduction is not clear. In most of the literature, it was stated, that the introduction of the traffic calming influences influenced on the reduction of the traffic volume, and the observed reduction was between 1% and 64% [233, 234]. However, in the research of Evans in Oxfordshire [235], there was observed a slight (2%) increase in the traffic volume. Analysis undertaken in the USA [236], have confirmed a significant changes in the capacity depending on the kind and distance between speed humps and speed cushions – the installation of the cushions every 320 meters have decreased the capacity by 23% and every 106m by 32%. In the research of the speed hump, there was no linear relation between the distance and the capacity reduction.

3.2. Conclusions from the literature review

The literature review presented in this thesis included the topics connected with the micro- and macroscopic traffic modelling, with the emphasis on the traffic assignment in the four-step model. In the review, the whole process of the macroscopic modelling, volume-delay functions and its estimation method have been reviewed. Next, the microscopic modelling have been shown together with the methods of calibration and trajectory researching.

For the part of the trajectory research, it was reviewed, that the new methods of the vehicle detection emerged, such as machine-learning video detection. This gives the possibilities of the new methods of the trajectory research, thus the calibration of the microscopic model.

During the review, it was shown, that the capacity and the volume-delay functions plays a significant role in the transportation network modelling. As a result, the capacity and volume-delay functions alters the traffic assignment results, which is a basic result of the macroscopic traffic modelling. In the review, also the traffic assignment methods have been showed.

In the review of the volume-delay function estimation, it was discovered, that macroscopic models are lacking in estimating the VDFs, assuming values existing earlier in the literature instead. Moreover, it was reviewed, that there is a lack in the methods of the VDF estimation, especially for the links, where the speed is varying along them.

As the example of the link with the varying velocity, the traffic calmed streets have been stated. During the literature review, it was discovered, that the traffic calming measures alters the vehicles speed, depending on their characteristics and density. Together with the research on the velocity, the literature review have shown the research on the influence of the traffic calming on traffic conditions. However, there is no research result stating a clear and parametrised influence of the traffic calming on the traffic conditions.

Summing up, during the literature review of this thesis, it was shown, that there is a lack of the systematic research of the influence of the traffic calming on the traffic conditions, especially VDFs. At the same time it was reviewed, that methods of the VDFs estimation are lacking in the field of the links with the fluctuating speed, for example the traffic-calmed links. This with the connection to the new method of the video detection can result in the new, cheaper and more accurate methods of model development.

4. Research method

In this chapter, the algorithm of the research method (fig. 4) is explained. The more detailed description of each step can be found in the following subchapters.

The research method begins with the area video recording of the chosen link. It is done with the quadcopter hovering above the link. This can be done also by other ways placing the camera, when a good visibility and great coverage area is maintained.

The next step is the video detection of the vehicles. With the help of machine learning, vehicles and pedestrians are detected, frame by frame.

After detection, the objects are identified and tracked between frames. Each of them gets its trajectory and movement data.

Trajectories and movement data are later transformed into speed profiles and speed distributions, acceleration and braking data for each significant part of the link. Speed profiles ($V(x)$) are the reference data to check the compliance of the microscopic created afterwards.

With the speed, acceleration and braking data, microscopic model can be developed. Its speed profiles are later calibrated as a comparison with the speed profile from the measurement.

Developed microscopic model is used in this step to simulate the link in the various traffic conditions. Starting from the traffic volume close to 0 (the traffic volume, which does not affect the free flow travel time) to the maximal traffic volume able to be carried through the link, simulation is played. In the simulation, the travel time of the link is measured for every traffic condition.

Based on the data from the microsimulation model, the relation between traffic volume, density and travel time is created. Those relation are further analysed later.

From the data about the travel time, velocity and volume, the relation Time (volume) was created. However, considering fact, that this relation has two phases – critical and subcritical, it is impossible to present it as a function. As a result, the second relation was created – Time (density). This constantly growing relation (with the growth of the density, the travel time increases) can be presented as a function and is the entry point for the volume-delay function estimation.

Parametrizing macroscopic road network model of traffic-calmed zones.

Next point is the VDF estimation – the basic result of this research and the ending point of the proposed methods. In this point, the Time (density) relation is transformed into the volume-delay relation. Later, for the needs of this research, this relation is fitted to the BPR2 function form and the fitting is checked.

The next points are connected with the application of the VDFs estimated in this research. Firstly, VDFs were applied in the toy network in order to check their influence on the traffic assignment. In this experiment, the correctness of the capacity estimation was checked. Secondly, VDFs were checked at the Kraków model on the analysed link to check if their implementation improves the traffic assignment quality.

The toy network was created to research two topics. The first was to check the result of the traffic assignment algorithm in Visum and to compare it with manual calculations. After that, the influence of the VDF change on the assignment was researched – its influence was compared with the influence of the other factors, like free flow speed or capacity.

Finally, VDFs were implemented in the real network of the Kraków model. In this case the traffic assignment changes were analysed. The most important factor was control if the calibration improved after implementing the VDF.

Parametrizing macroscopic road network model of traffic-calmed zones.

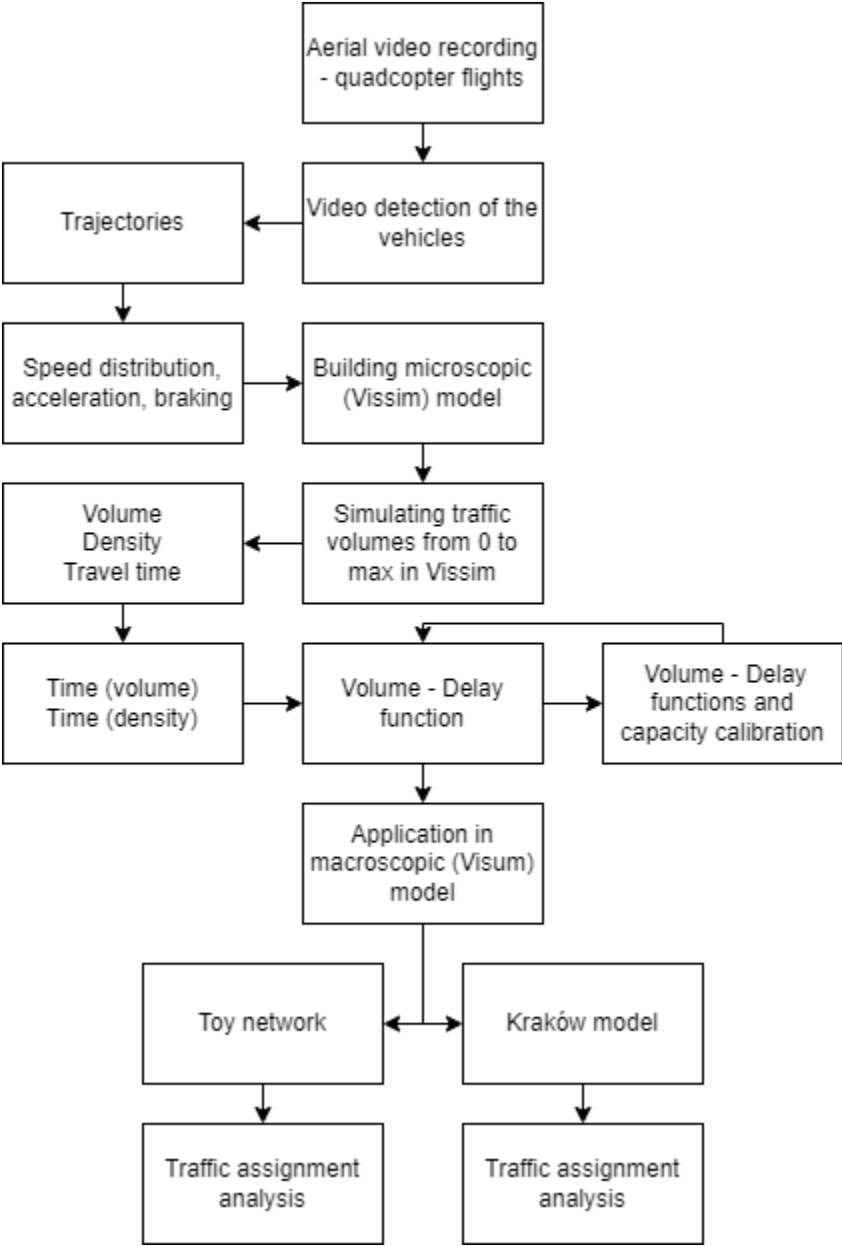


Figure 26: Algorithm of the proposed research method

4.1. Aerial video recording – quadcopter

Data collection begins with the trajectory research. In this method, a video detection is used, by using the unmanned aerial vehicle. Its placement should cover the whole analysed area, which requires an adequate altitude and camera angle. During this experiment, with the use of the quadcopter DJI Phantom IV, recording 110-130 meters of the road requires the altitude of 80-100 meters. When planning the flight, it is important to comply with the local aviation law, considering fly zones, permission only zones, no fly zones and maximal allowed altitudes for the particular zones. It is also important to record the footage in such a quality to be used in the detection. In the case of the aforementioned UAV it is 1080*1920 pixels, with 40 frames per second, Moreover, the UAV is equipped with the GPS flight stabilisation and camera stabilising gimbal to record the stable, unmoved video frame.

The next aspect is to plan an adequate amount of flights to achieve a statistically correct amount of observations. To achieve that, it is needed to perform a test recording (for example one UAV flight) to gain the data structure statistics – average and variance of the analysed velocity. This allows to calculate the sample size – the minimal amount of vehicles needed to be detected to achieve the desired error of the speed data. To calculate this, the formula (4) can be used:

Formula 4: Sample size of the measurement

$$n = \frac{u_{\alpha}^2 \cdot \sigma^2}{b_v^2} \quad (4)$$

$$b_v^2 = b \cdot \bar{x}$$

, where:

u_{α} - confidence level of the normal distribution

σ^2 - variance

b – desired error, for example 0,02 or 0,05

\bar{x} - mean value

After calculating the minimal sample size of the amount of the vehicles, the length of the recordings can be planned in order to collect desired amount of the vehicle data.

4.2. Video detection of the vehicles

The trajectories from the video have been processed by the company DatafromSky (237). The processing result was delivered in two files – one for the DatafromSky viewer software used to visualise the results, the other a csv file containing all the data, consisting of timestamp, coordinates, object ID, and object type (car, heavy vehicle, bus, bicycle, pedestrian).

An accurate video detection of the vehicles is the crucial beginning of the trajectory analysis process. Because of that, the quality control of the detection is important. There are two solutions for this. First is the detection of the floating vehicle, equipped with the GPS or board computer motion register. The quality control is based on the comparison of the trajectory from the detection and the floating vehicle. The second method is to use visualised trajectories to compare them with the video footage. This allow visual control of the quality of the detection.

The screenshot of the DatafromSky viewer software is presented in Figure 15.

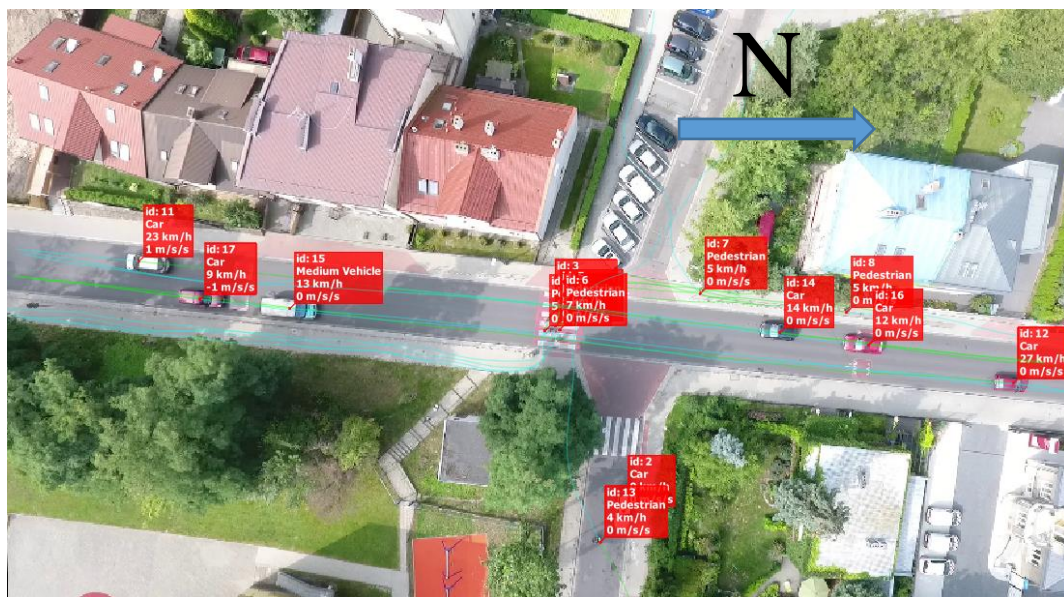


Figure 27: DatafromSky viewer software screenshot with car detection and trajectory data displayed (source: own)

4.3. Trajectories and driving behaviour characteristics

Vehicle trajectories from various traffic calming measures, such as speed cushions, speed bumps, chicanes and traffic islands, are extracted from the previously collected video recordings. With the help of video-detection systems, each vehicle position is registered on every frame of the film. The framerate used in this footage is 40 frames per second. In order to discover the vehicles' speed, vehicle coordinates are compared between frames to measure the distance travelled. Vehicles' velocities are then sorted according to their positions on the road in order to assign them to assign them a chainage distance.

Speed results are organised in this manner for two reasons. First, it makes it possible to localise traffic calming measures at a specific point of road section. This allows us to produce statistics on vehicle velocities, such as: speed distributions for every vehicle type ready to be input into the Vissim simulation. Second, it makes it possible to create a table and chart of velocities in reference to location. This allow us to assess the compatibility between measurements and model and to perform the calibration.

Processing the data acquired from the recordings was done as follows. First, the street visible in Figure 1 was divided into measurement sections of 10 cm in length. Instantaneous velocities were identified in each section for all vehicles, which were divided into vehicle classes, such as cars (standard and van), buses and heavy vehicles. These sections were then put together to create speed charts, showing the speed profiles of the analysed road and taking account of velocity changes on the speed cushions.

Speed distributions were produced according to the measured, cumulated frequencies of each vehicle type. Separate speed distributions were produced for each of the recorded speeds, for example near or far from the traffic calming measure in question. At the threshold between speed distributions, accelerations and braking were identified.

4.4. Developing the microscopic (Vissim) model

Microsimulation modelling is done using PTV Vissim software. The first step is to create a link with the same length as the measured road section. Next, a traffic calming measure needs to be input as a reduced speed area or a change of lane number in the chainage corresponding to its location on the footage. The parameters of this input consist of the speeds of each vehicle type based on speed distributions according to measured cumulated frequencies. Together with speed distributions, accelerations and decelerations were inputted, as measured. Speed distributions for the whole link were inputted in the same manner. Later, for calibration, other reduced speed areas can be added, together with speed distributions on the corresponding sections. The next step is to set vehicle compositions and traffic flow. Initially, in order to assess and calibrate the model, these parameters are set according to measurements.

After preparing the model, the simulation is run. The results of the simulation are exported and extracted as average speed profiles of all vehicles in order to compare them with the measurements, with the help of a correlation coefficient and r-square factor. To avoid inaccuracy in the model results, the links were lengthened beyond the limits of the drone camera coverage, reaching the nearest intersections. Calibration of the model requires that we use only the speed distributions of unimpeded vehicles – otherwise, the simulated speeds turn out higher than measured. The shape of the speed profile is calibrated by estimating the acceleration and braking characteristics of the vehicles. If the model still needs calibration, the link can be divided into more parts using the different speed distributions.

Parametrizing macroscopic road network model of traffic-calmed zones.

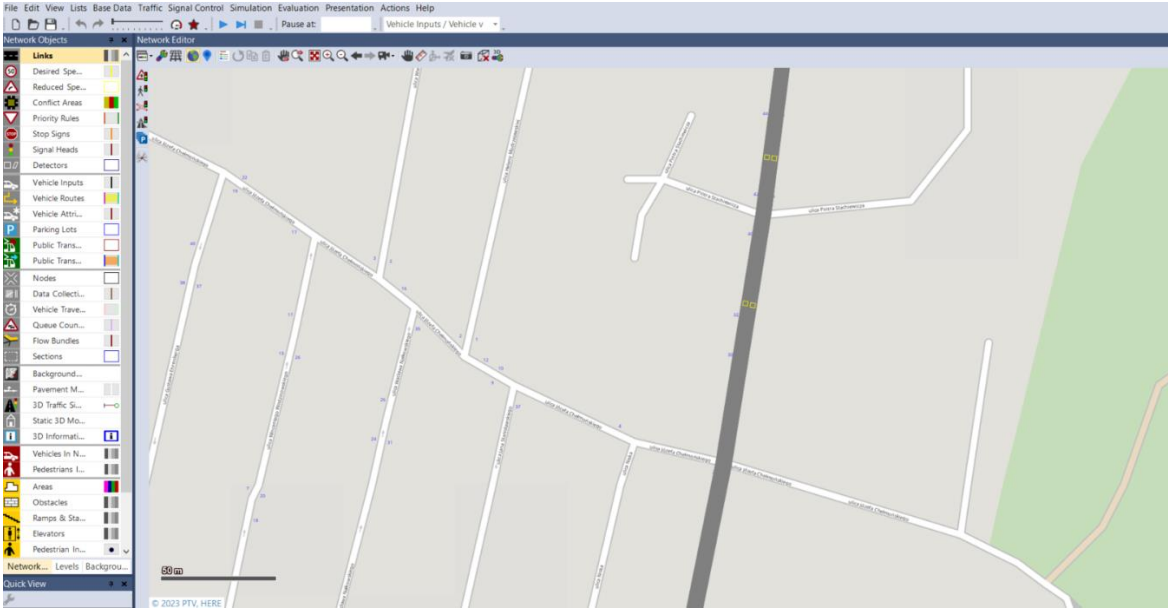


Figure 28: The view of the PTV Vissim model in the program

4.5. Simulating traffic volumes

This calibrated macrosimulation model facilitates our understanding of the relationship between traffic flow and travel time and enables us to formulate volume-delay functions for traffic calmed roads. To achieve this, various traffic flows were tested and compared for traffic-calmed and non traffic-calmed links. Traffic flow in the simulation was reduced by 10% until it reached its minimum, while travel time no longer decreased increased in free flow traffic. In tandem with this reduction, initial traffic flow also increased accordingly in order to achieve maximum capacity, signalling, via error message in Vissim, that no more vehicles could travel the road during that given time period. A section's capacity will be the first parameter that is compared in terms of the presence or absence of a traffic calming measure.

To observe travel time in traffic volumes exceeding capacity, another was added to the simulated link in order to accumulate queues. Travel time (later used to calculate velocity) is equal to the link's travel time plus extensions (and queue travel time if applicable) minus travel time on extensions in free flow. The initial result of this experiment was a relation between traffic volume [veh/h] and velocity [km/h].



Figure 29: The view of the PTV Vissim running simulation

4.5.1. Volume, density and travel time relation

The example of the volume and travel time relation is presented on fig.16

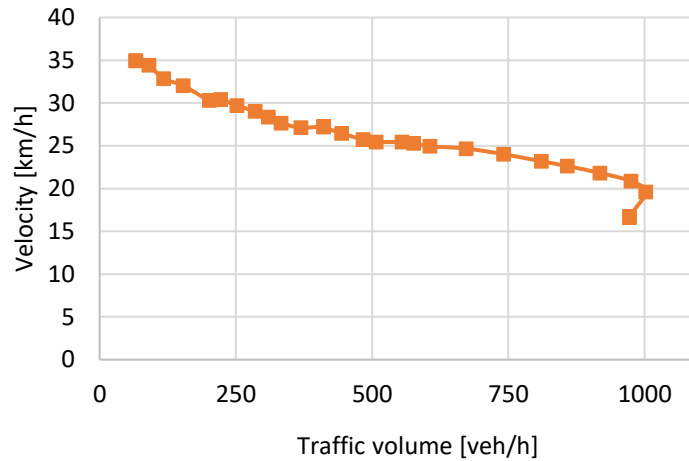


Figure 30: Traffic volume–speed relation (source: own)

On Figure 16, a reduction in speed along with traffic volume can be seen. As it reaches capacity, velocity decreases along with maximal traffic volume. This establishes a relation compliant with a fundamental diagram of traffic flow, in which there are two results for velocity with the same traffic volume, depending on whether it is above or below capacity. To express this relation as a function, traffic volume [veh/h] is replaced with traffic density [veh/km] (14) [30]. In this expression, after reaching capacity, density still increases with velocity reduction. This is presented in Figure 17.

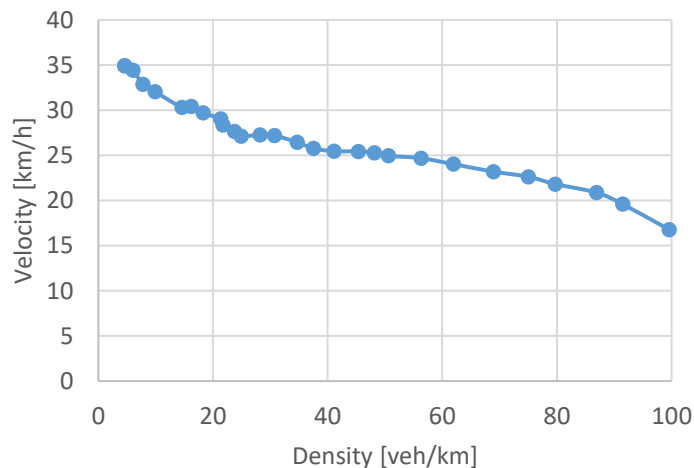


Figure 31: Traffic density–speed relation. (source: own)

4.6. Volume-delay function

To correspond with volume-delay function form they were presented as a minimal travel time (with minimal traffic flow) multiplied by a coefficient right to obtain travel time in actual traffic flow. Traffic flow was calculated as saturation grade, which is equal to traffic flow divided by capacity.

According to the literature review of the volume-delay functions, three function forms have been chosen for the testing the fitness of the function. Among the functions reviewed, the functions, which considers a queue fluctuations have been eliminated as they have no usage in the research of the VDFs for the traffic-calmed links. For the function fitness comparison, the four functions forms have been chosen: Davidson, Conical, BPR and BPR2. Below, in the Table 3, the aforementioned functions have been presented.

Table 4: Table of used VDFs formulas

No.	Name	Function formula
1	Davidson (20)	$t_{cur} = t_0 \left(1 + \frac{J \cdot sat}{1 - sat} \right)$
2	Spiess (17) (Conical)	$t_{cur} = t_0 \left(2 + \sqrt{\alpha^2 (1 - sat)^2 \cdot \beta^2 - \alpha \cdot (1 - sat) - \beta} \right)$
3	BPR (16)	$t_{cur} = t_0 (1 + a \cdot sat^b)$
4	BPR2 (16)	$t_{cur} = \begin{cases} t_0 \cdot (1 + a \cdot sat^b), & sat \leq sat_{crit} \\ t_0 \cdot (1 + a \cdot sat^{b'}), & sat > sat_{crit} \end{cases}$

Where:

t_{cur} –travel time in the following traffic flow

t_0 - free flow travel time

$J, \alpha, \beta, a, b, b'$ – shape parameters

sat – saturation grade

Parametrizing macroscopic road network model of traffic-calmed zones.

In this functions t_{cur} , t_0 and saturation grade is given. Variables prior to modelling are (depending on the function) coefficients:

- J for the Davidson function,
- α, β for Spiess (Conical) function,
- a, b for the BPR function,
- a, b, b' for the BPR2 function.

For the comparison, the dataset of the volume-delay relation have been taken. The results of the function fitness have been presented in Table 4. To fit the functions, square difference minimisation method is used.

Table 5: Correlation and r^2 coefficient of the chosen VDFs

No	Name	r^2	correlation
1	Davidson	0.27	0.52
2	Spiess	0.90	0.95
3	BPR	0.87	0.93
4	BPR2	0.99	0.99

Among the volume-delay functions available in Visum, one was chosen, which fit the best the relation researched in the simulation. The example of that function is BPR2, used in Kraków and many other Polish models.

4.7. Application in macroscopic (Visum) model

The purpose of discovering the volume-delay functions is to apply them in the macroscopic model. When doing that, VDF are applying a correct travel time, which leads to the corrected traffic assignment results. In this thesis, the influence of this kind of change have been researched as well as the scale of improvement of the traffic assignment according to the empirical traffic volume measurements.

To understand the reaction of the traffic assignment in the macroscopic model, two experiments have been made. First using a toy network, the second on the Kraków model. Those experiments are shown in chapter 6.

The toy purpose of the toy network experiment was dual. First, was to check if the results of the Visum traffic assignment calculations were the same as the manual, mathematical calculations of the user equilibrium traffic assignment. The second was to compare the amount of traffic redirected from the link with the traffic-calming VDF to the link with the VDF without the traffic calming. The results of the traffic assignment as the influence of the VDFs were also compared with the influence of the capacity or the free flow travel time adjustments.

Finally, the experiment have been checked on the Kraków model. The purpose of this experiment was to check how the new volume-delay functions, calculated capacity and the free flow velocity affects and changes the traffic volume already set in the traffic assignment.

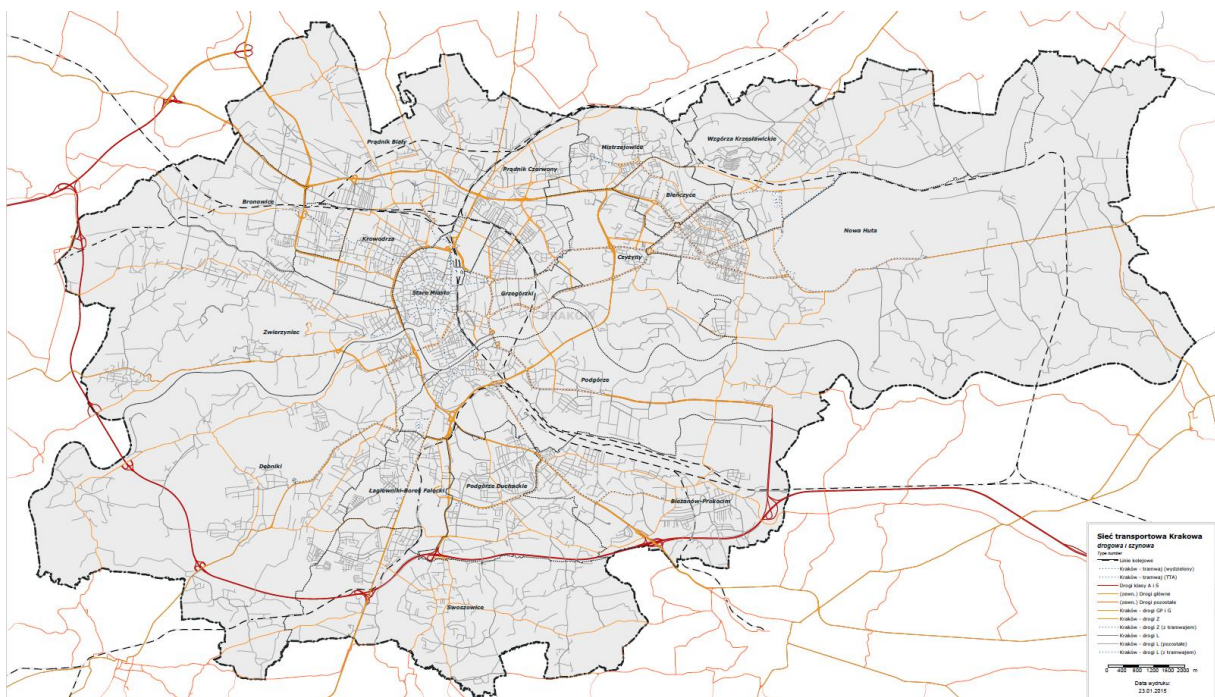


Figure 32 Kraków transportation network in model

5. Research method - example

The research method have been tested in the particular areas of the Kraków street network. Its aim was to research functioning of the method for the real data

The first, pilot experiment was carried out on Stachiewicza street in Kraków, a section of which contained pre-existing speed cushions. The experiment went through the following stages: surveying, building and calibrating a macrosimulation model, experimenting with various traffic flows, and estimating the volume-delay function. Later, the influence of the aforementioned volume-delay functions on traffic assignment were examined.

5.1.1. Video Data Collection

To provide coverage of the whole measured area, where a high point to place a camera was not present, an unmanned quadcopter (DJI Phantom IV) was used. Its coverage was 110 m of the street with an altitude of 80 m above ground level. The duration of the flight was approximately 25 min, which, after subtracting the ascend and descend, left 15–20 min of traffic recording. The video parameters were: 1920 × 1080 pixels resolution and 40 frames per second. Test flights of the Stachiewicza street took place in October 2017. During tests, the stability of the recording was checked, which was suitable for the later video detection, due to GPS and stabilising systems installed in the quadcopter, including gyroscopes and camera gimbal. The actual flights for the Stachiewicza street took place in late April 2018.

The flights for this research were undertaken firstly in October 2017. During those, the tests of the research procedure have been made. In that case, recording altitude was 80 meters above the ground level, covering 110 meters of the street. During the tests, the flight quality was checked, which proved, that the use of the quadcopter equipped with the GPS receiver to stabilise its position and the image stabilisation system is able to deliver a video footage unmoved through the whole measurement period. The test of the procedure also confirmed the usability of the video detection services provided by the DataFromSky Company. The trajectories delivered by the company complied with the video footage. The flights used for this

research have been undertaken in late April 2018. For the flights, the important factor for the battery time, footage quality, and the flight safety was weather. It is required to be no rain or snow, which might interfere with the propeller motion and increase battery usage as well as no strong wind, which also increase battery usage and can reduce a recording stability.

Firstly, a test flight and test detection were made. 30 vehicles were detected and their speed analysed. Average speed on the analysed link was 20,69 km/h and variance 32,66 km/h. Analysing Fig. 18, it can be seen that the results have a normal distribution.

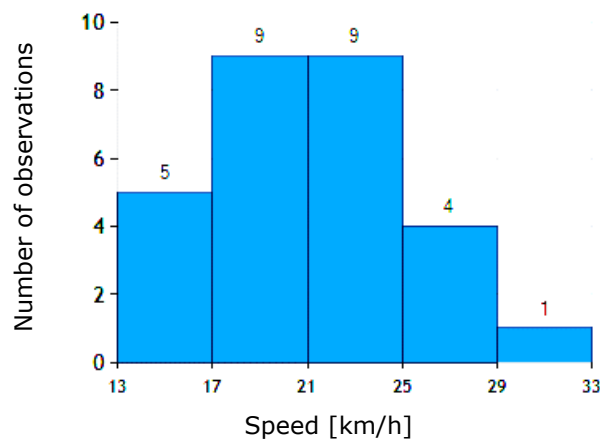


Figure 33: Distribution of the sample measurements

Therefore, the formula (4) from the chapter 4.1 can be used to estimate a minimal sample size

Assuming confidence level for $1-\alpha=0,95$ and the error equal to 0,05, calculated sample size was equal to 117 vehicles. Based on this amount, the flight was planned to collect enough of the vehicles data.

5.1.2. Trajectory Analysis

For this measurement, 20 min of the recording was used, containing 192 vehicles: 165 cars, 18 vans, 3 heavy vehicles, and 6 buses. There were also 90 pedestrians detected, although they were not used in this study. Charts of speed profiles are presented below in Figures 19 and 20.

Parametrizing macroscopic road network model of traffic-calmed zones.

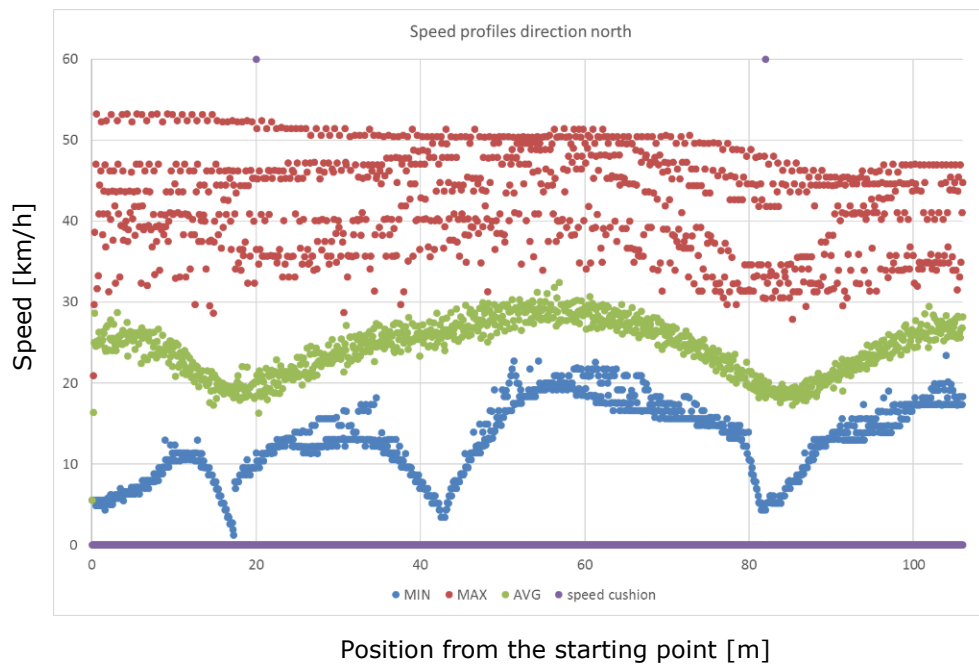


Figure 34: Speed profile for Stachiewicza street, northbound (source: own).

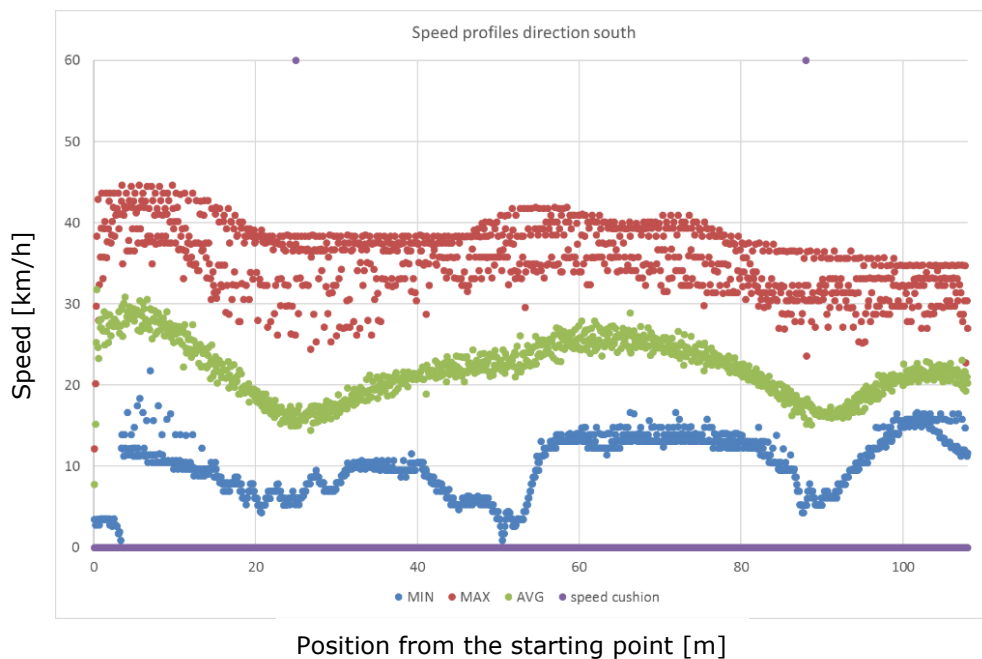


Figure 35: Speed profile for Stachiewicza street, southbound (source: own).

The charts show speed profiles for the 107m length of Stachiewicza Street under study. Speed cushions along this section are indicated by violet dots at the top of the charts, at 20m and 82m northbound, and 26m and 88m southbound. Minimum speed in each section is indicated by blue dots. Reduction of minimal velocity between the speed cushions (40m-60m) shows the cars stopping on the pedestrian crossing. Average velocity is represented by green dots—its decrease in the speed cushions area is

Parametrizing macroscopic road network model of traffic-calmed zones.

clearly visible. The red dots marking maximal speed show the presence of vehicles that did not slow down on speed cushions, especially northbound.

5.1.3. Microsimulation Model

Development of the microsimulation model began by preparing the speed distributions. In this model, there are two traffic directions, each on a separate link. There are two reduced speed areas in each link, representing speed cushions. For every direction and for every reduced speed area, a separate speed distribution was inputted. Examples of speed distributions are presented in Figure 21.

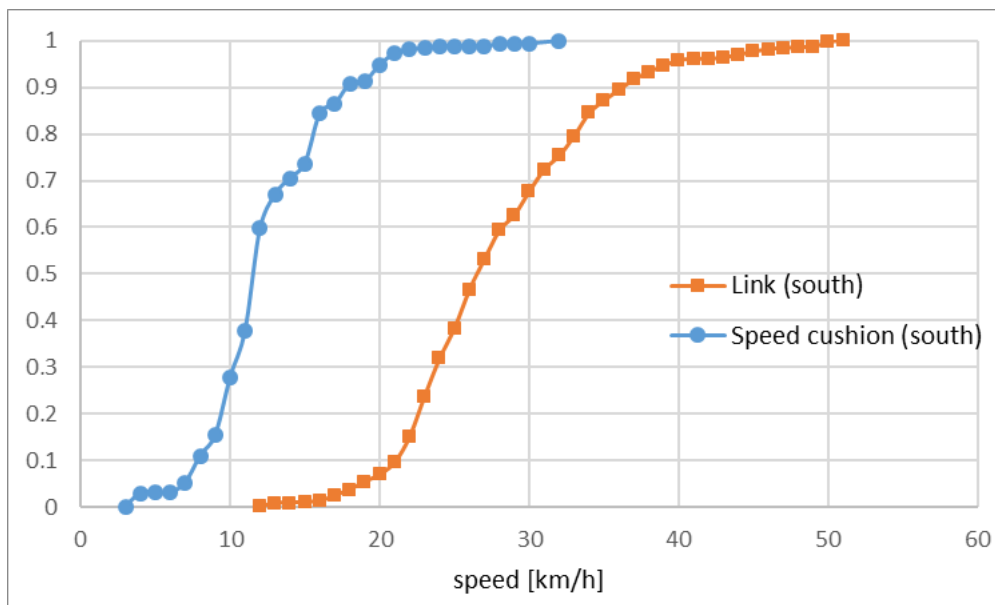


Figure 36: Car speed distributions for the link, southbound (orange) and with second speed cushion (blue), source: own.

In the Vissim microsimulation model, speed distributions, acceleration and deceleration data were inputted. Later, the simulation was run for a traffic volume equal to that during measurement, to check calibration. In order to compare the simulated trajectory data with the measured data, average speed profiles for all vehicles from the simulation were exported. Calibration was done using speed distributions where traffic volume allows unimpeded traffic to correspond with simulated velocities. Velocities in the simulation were adjusted to comply with measurements. In order to calibrate the speed profile shape, vehicles' acceleration and braking were estimated. For the first direction along Stachiewicza street (northbound), the correlation coefficient between model and measurement was equal to 0.79. The compared speed profiles are presented in Figure 22.

Parametrizing macroscopic road network model of traffic-calmed zones.

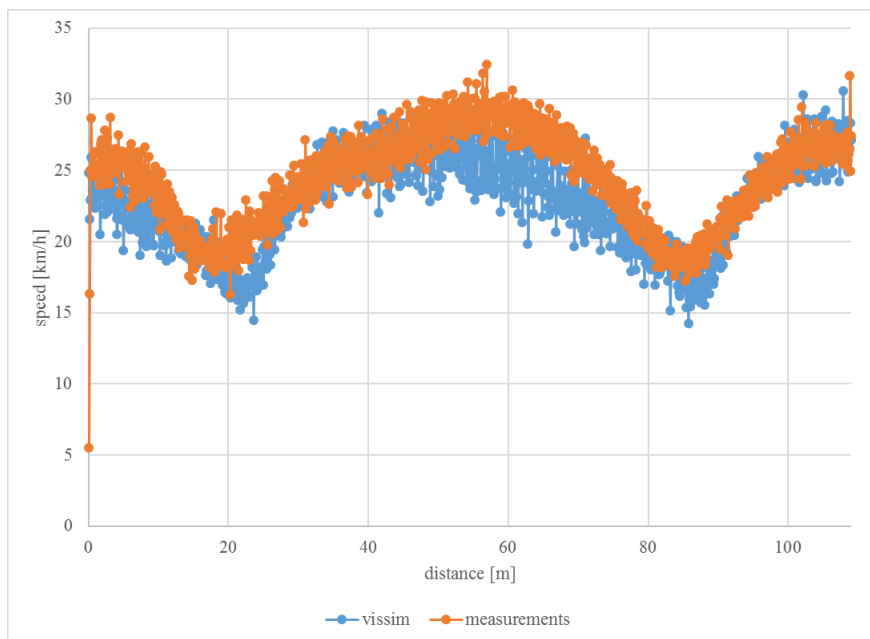


Figure 37: Comparison of speed profiles on the measured street section, northbound, source: own.

For the second direction (southbound), the correlation coefficient was 0.71. Figure 23 shows this comparison.

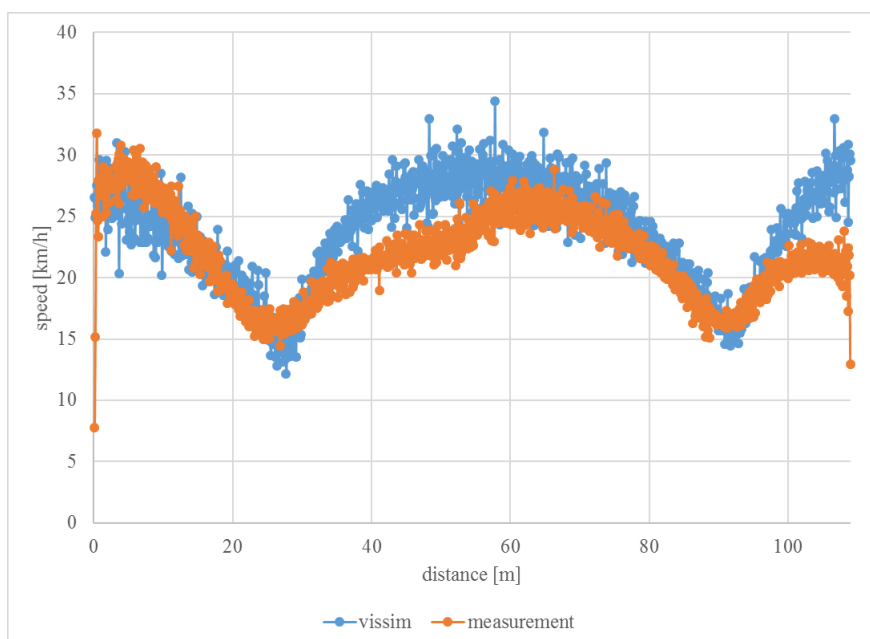


Figure 38: Comparison of speed profiles on the measured street section, southbound, source: own.

The correlation coefficient between measured and simulated speed profiles (0,71 and 0,79) was assessed as acceptable. If better correlation and further calibration are needed, the car-following model (Wiedemann) parameters can be adjusted or the link can be divided into more parts, with their own speed distributions, acceleration and breaking parameters.

Parametrizing macroscopic road network model of traffic-calmed zones.

For the volume–delay function estimation, a variety of traffic volumes were simulated for both traffic-calmed and non-traffic-calmed links.

The form of the travel times was calculated, with form corresponding to the volume–delay function presentation available in PTV Visum. This means that the relationship between saturation grade (density divided by maximum traffic volume density) and travel time is equal to t_0 (free flow travel time) multiplied by the rest of the function. In the macroscopic transport model of the city of Kraków, volume–delay functions were estimated using the BPR2 volume–delay functions shape (see formula (5)):

Formula 5: BPR volume–delay function, source: (16)

$$t_{cur}(sat) = \begin{cases} t_0 \cdot (1 + a \cdot sat^b), & 0 < sat < 1 \\ t_0 \cdot (1 + a \cdot sat^{b'}), & sat \geq 1 \end{cases} \quad (5)$$

where:

t_0 —free flow travel time (for the following speeds: with traffic calming: 28 km/h, without traffic calming: 30 km/h);

a, b, b' —parameters of the function;

sat —saturation grade (q/q_{max}).

The function parameters for the best fit were estimated using squared difference minimisation. Parameters' values are shown in Table 5.

Table 6: Function parameter values.

Coefficient	Direction 1 with Traffic Calming	Direction 2 with Traffic Calming	Direction 1 without Traffic Calming	Direction 2 without Traffic Calming
a=	0.641	0.759	0.528	0.612
b=	0.739	0.644	0.906	0.647
b'=	6.760	5.293	7.080	2.592
q_{max}	1068	1044	1308	1158

Parametrizing macroscopic road network model of traffic-calmed zones.

The function fitting had a high correlation coefficient: over 0.9 in every case. Empirical relation and function fitting are compared in Figure 24.

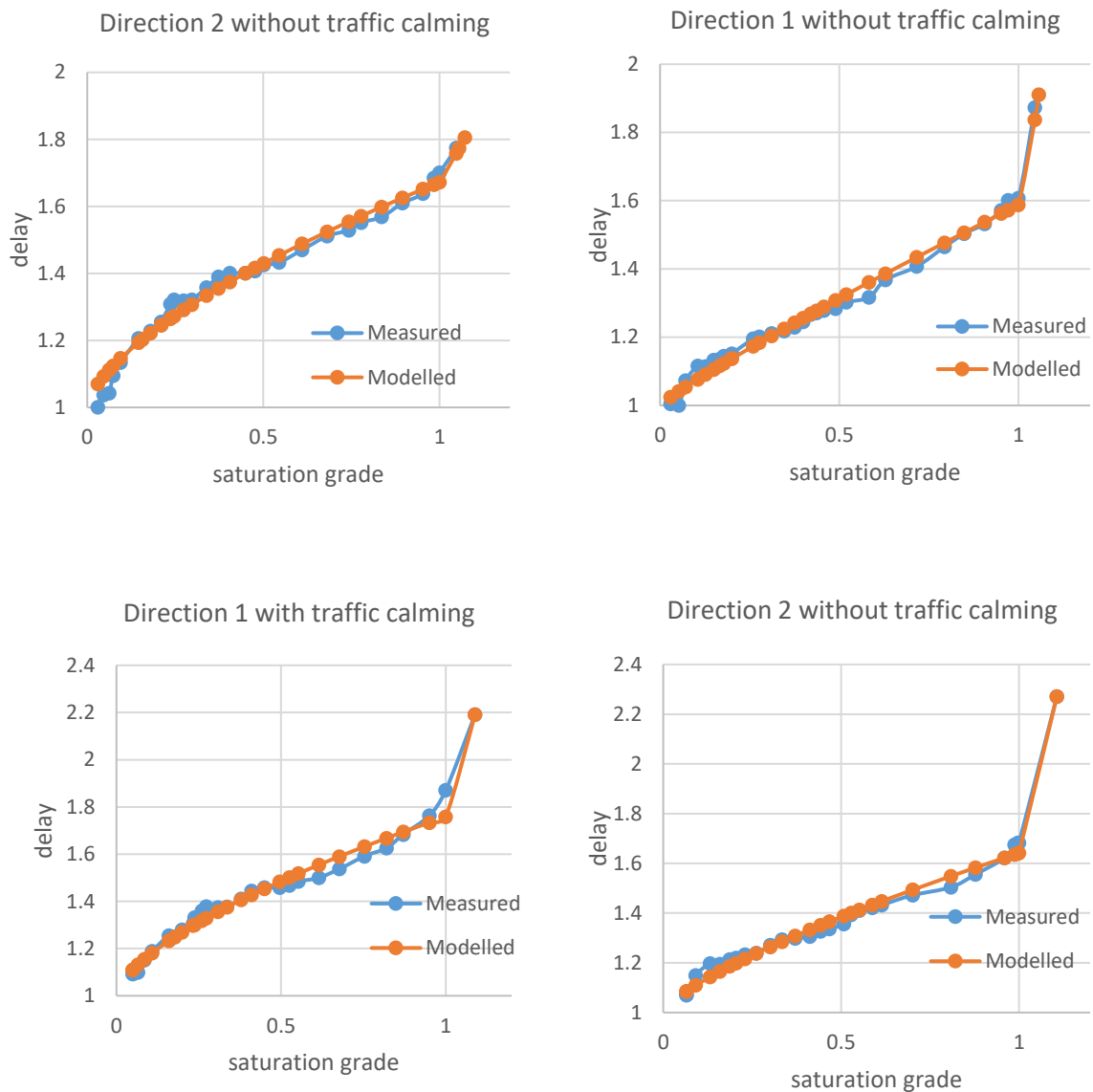


Figure 39: Fitting of the volume–delay functions (source: own).

5.2. Sensitivity analysis

Sensitivity analysis is a quantitative technique used in decision-making processes to evaluate the impact of changes in input variables on the output of a system or model. It is used to assess the significance of the parameters' uncertainties and to evaluate the robustness of the results under different circumstances. Sensitivity analysis aims to identify how changes in input

Parametrizing macroscopic road network model of traffic-calmed zones.

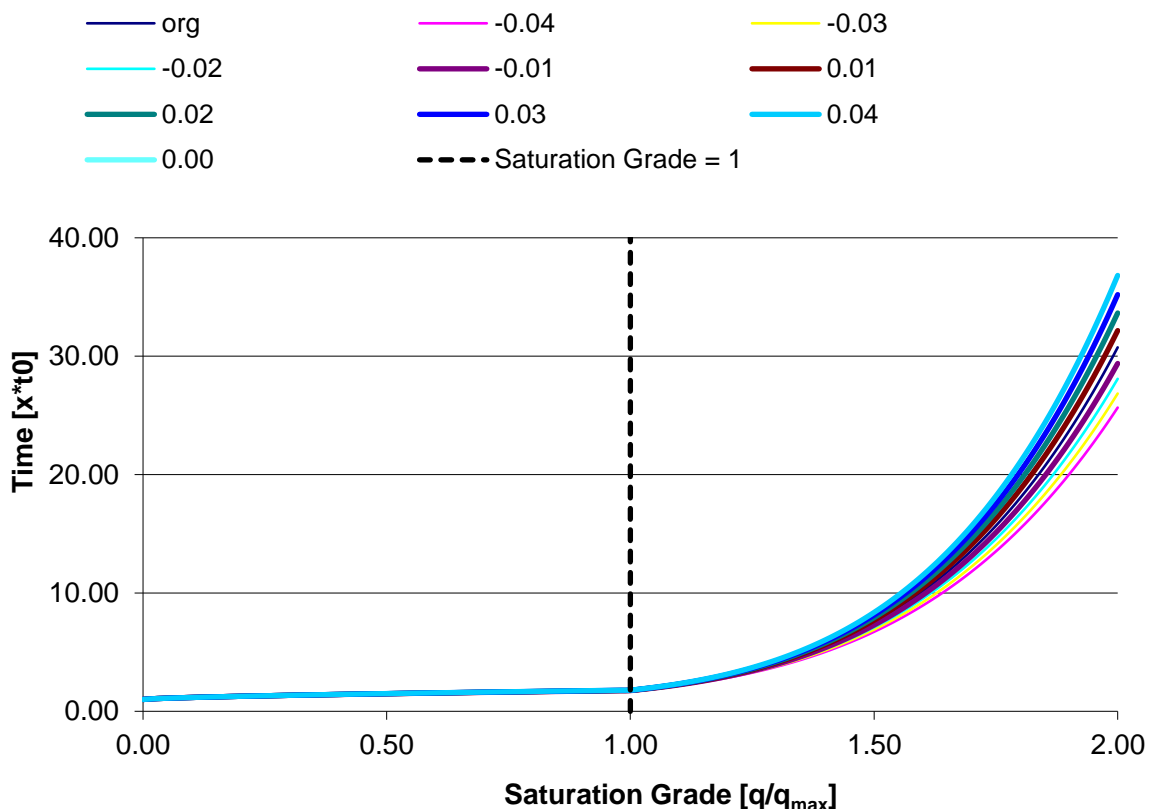
variables affect the output. This can be done by varying one or more input variables while keeping the others constant, and observing the resulting changes in the output.

The main methods of the sensitivity analysis are a one-factor-at-a-time (OFAT) and a global analysis. The OFAT method involves changing one input variable at a time while keeping all others constant. Global sensitivity analysis evaluates the sensitivity of the output to changes in all input variables simultaneously.

The aim of the sensitivity analysis in this research is to discover the impact of the eventual error in estimating the VDF parameters on the travel time. This would show the potential error in the travel time calculation as a result of the parameters estimation inaccuracy.

In this research, firstly all of the parameters have been changed simultaneously. Secondly, the parameter A and B parameters have been changed separately to discover their significance in the result calculation. The analysed error was between 96% to 104% of the original BPR function parameter values.

The shape of functions with the all parameters changed simultaneously are showed on Fig. 25



Parametrizing macroscopic road network model of traffic-calmed zones.

Figure 40: BPR function in the sensitivity analysis with the parameters a and b changed simultaneously

Next, the differences between function values have been compared. There can be shown in Fig. 26

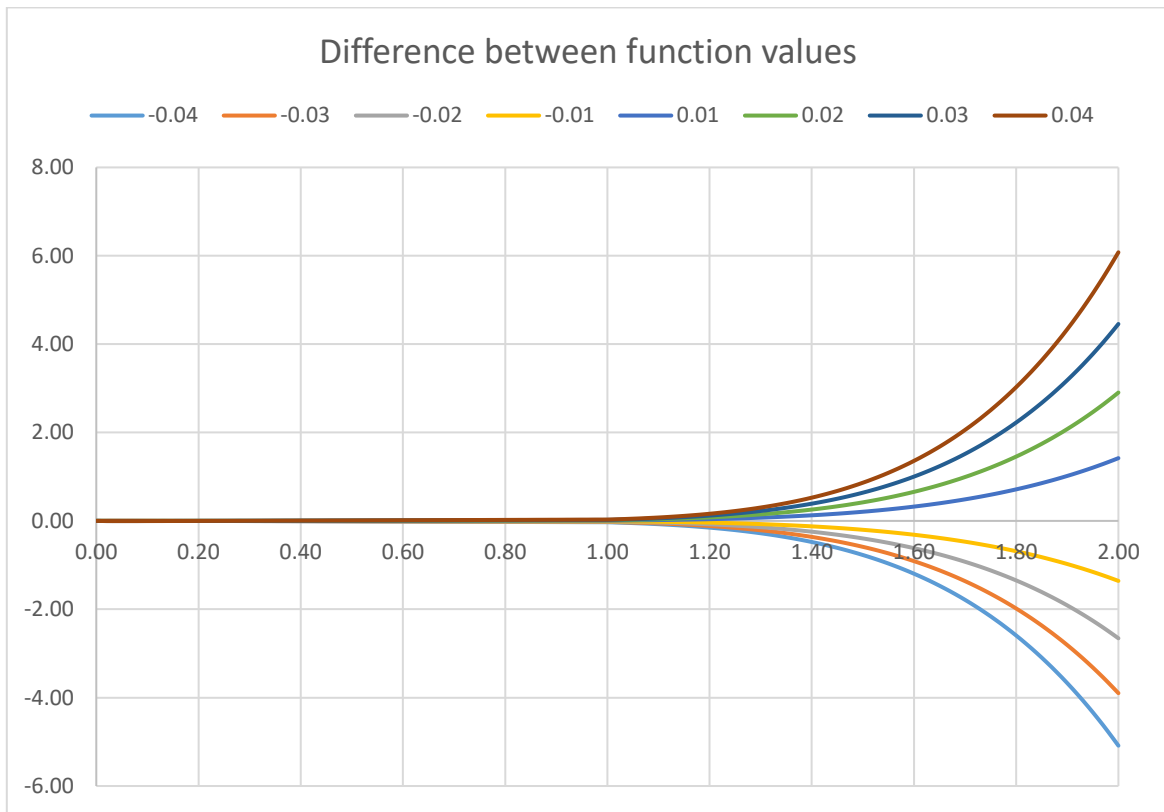


Figure 41: Difference between the BPR function values with the parameters a and b changed simultaneously

Finally, differences have been presented as a difference as a fraction of the original value. It can be shown in Fig. 27

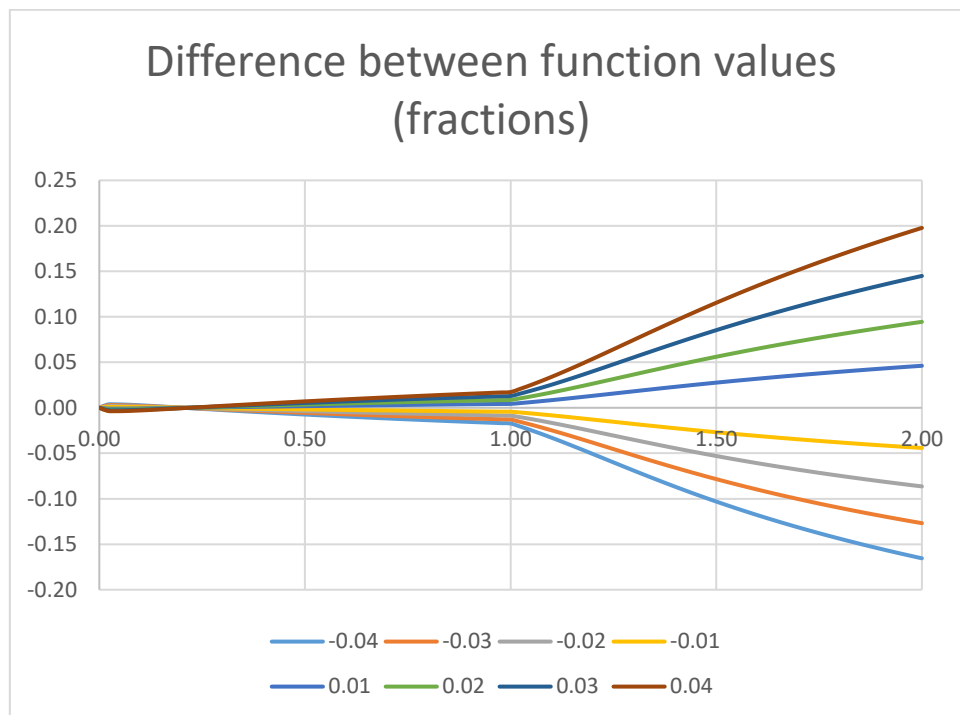


Figure 42: Difference between the BPR function values (fractions) with the parameters a and b changed simultaneously

Sensitivity analysis with the parameters a and b changed simultaneously shows a lower error influence for the results of the $q/q_{max} < 1$. It is caused by a different function form, which increase steeper when crossing 1. For this value, the maximal difference of the result is equal to 3%. For the $q/q_{max} = 1,5$, the difference is equal to 3-12%. For $q/q_{max} = 2$, the difference is equal to 5-20%.

Next analysis covered only changing the parameter a of the function. Same as previous, the analysed error was between 96% to 104% of the original BPR function parameter values. The shape of functions with the parameter a changed are showed on Fig. 28

Parametrizing macroscopic road network model of traffic-calmed zones.

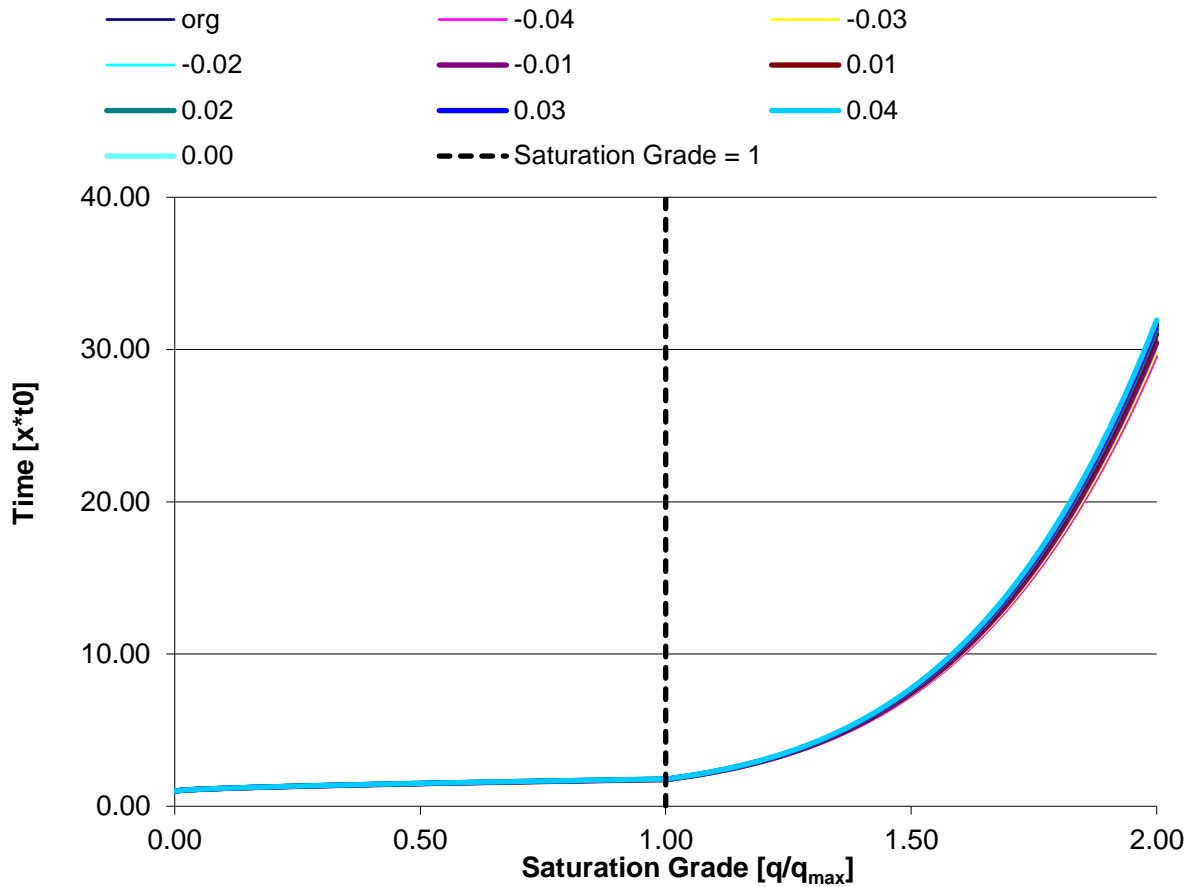


Figure 43: BPR function in the sensitivity analysis with the parameter a changed

Fig. BPR function in the sensitivity analysis with the parameter a changed

Next, the differences between function values have been compared. There can be shown in Fig. 29

Parametrizing macroscopic road network model of traffic-calmed zones.

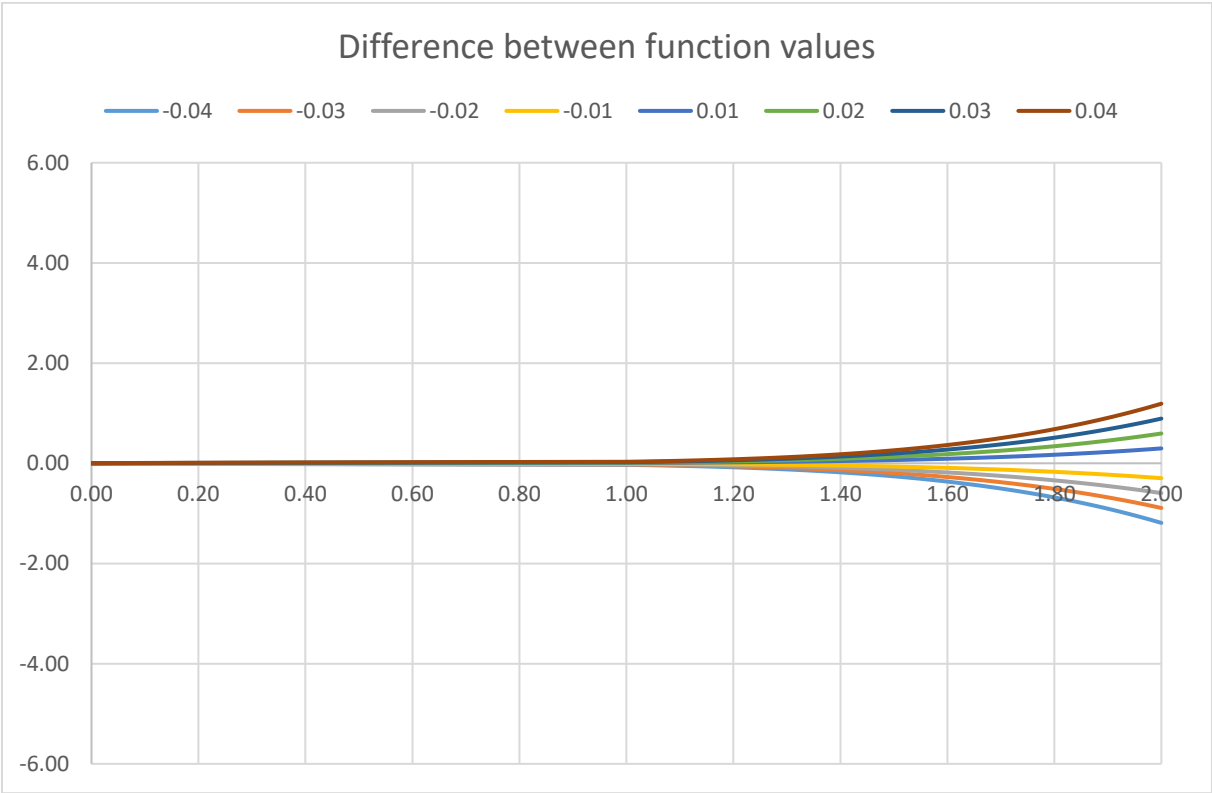


Figure 44: Difference between the BPR function values with the parameter a changed

Finally, differences have been presented as a difference as a fraction of the original value. It can be shown in Fig. 30

Parametrizing macroscopic road network model of traffic-calmed zones.

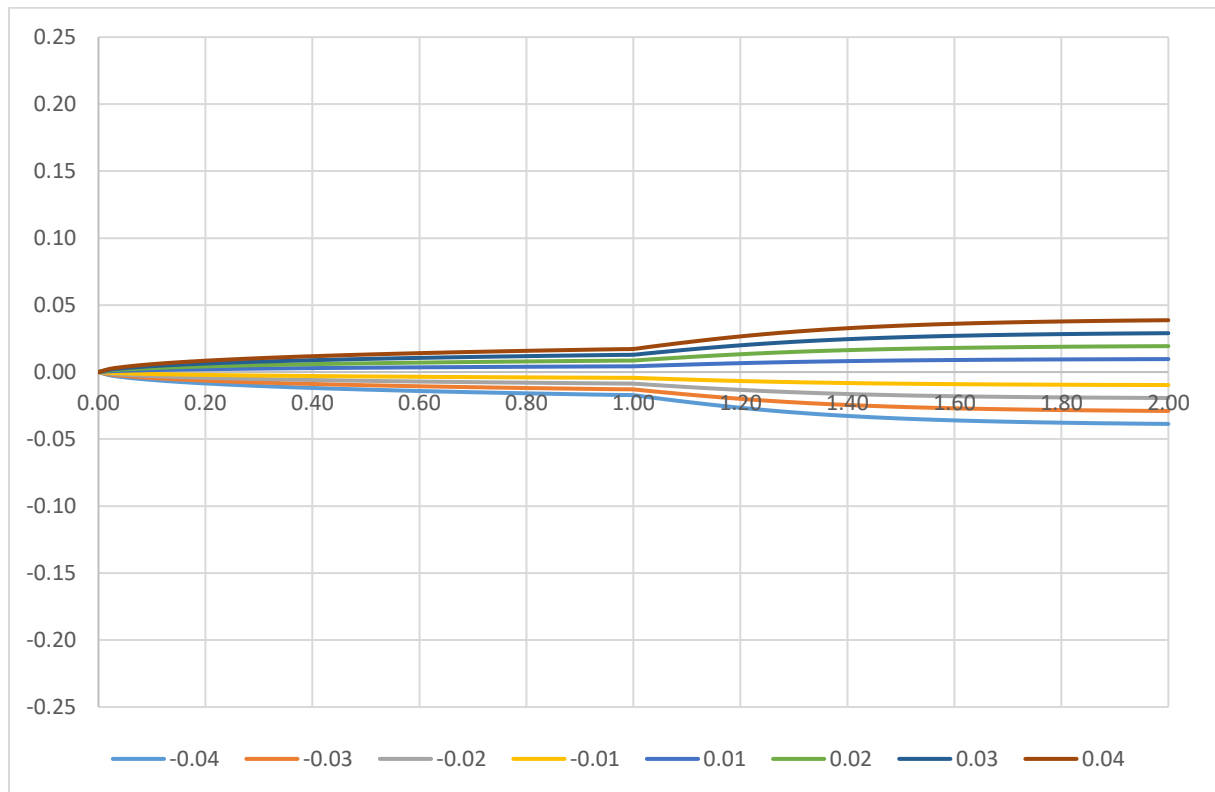


Figure 45: Difference between the BPR function values (fractions) with the parameter a changed

Sensitivity analysis with the parameters a simultaneously shows also a lower error influence for the results of the $q/q_{\max} < 1$. For the biggest change of the parameter a equal to 4%, change of the parameter a shows a insignificant change of the results, equal to 2% in $q/q_{\max}=1$ and 4% in $q/q_{\max}=2$. This analysis shows, that parameter a has a minor influence on the function results.

Final analysis covered only changing the parameter b of the function. In this case, parameter b and b' were changed simultaneously, representing the case of under- and oversaturation. The shape of functions with the parameter b changed are showed on Fig. 31

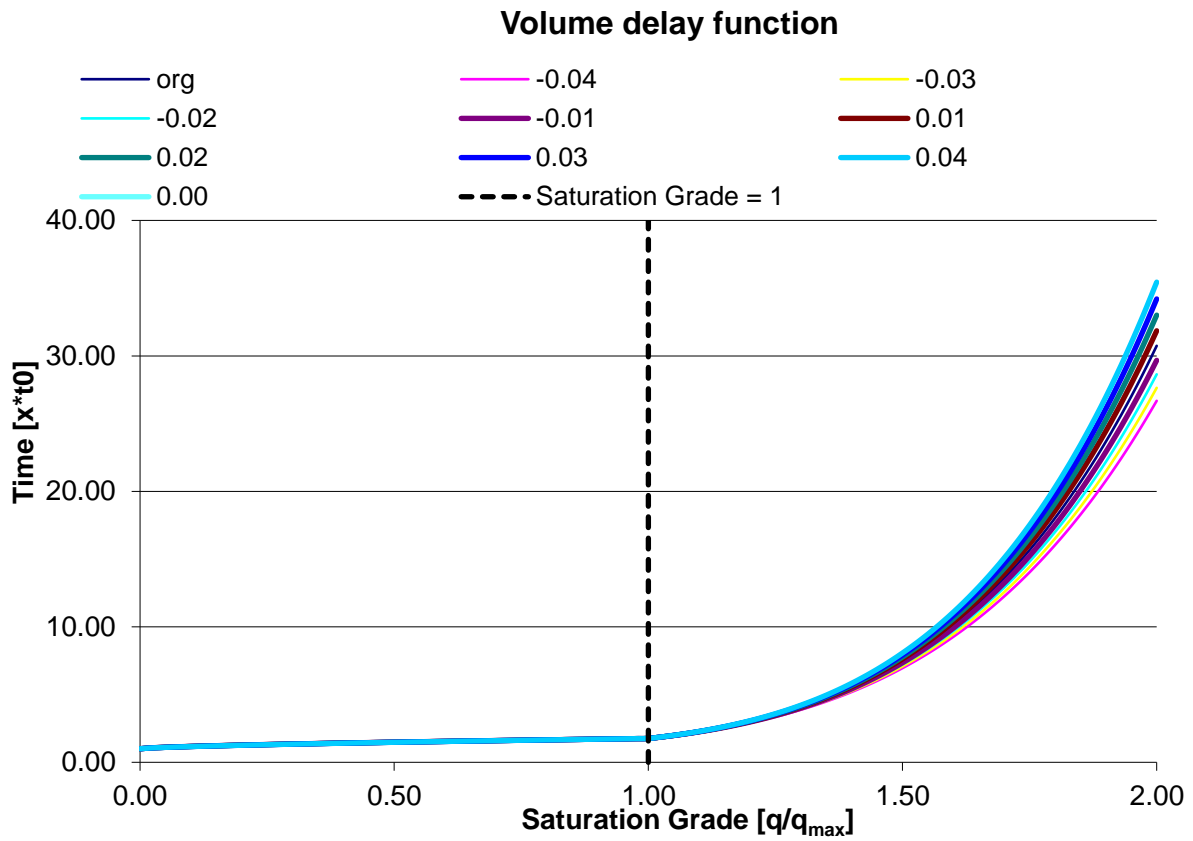


Figure 46: BPR function in the sensitivity analysis with the parameter b changed

Fig. BPR function in the sensitivity analysis with the parameter b changed

Next, same as previously, the differences between function values have been compared. There can be shown in Fig. 32

Parametrizing macroscopic road network model of traffic-calmed zones.

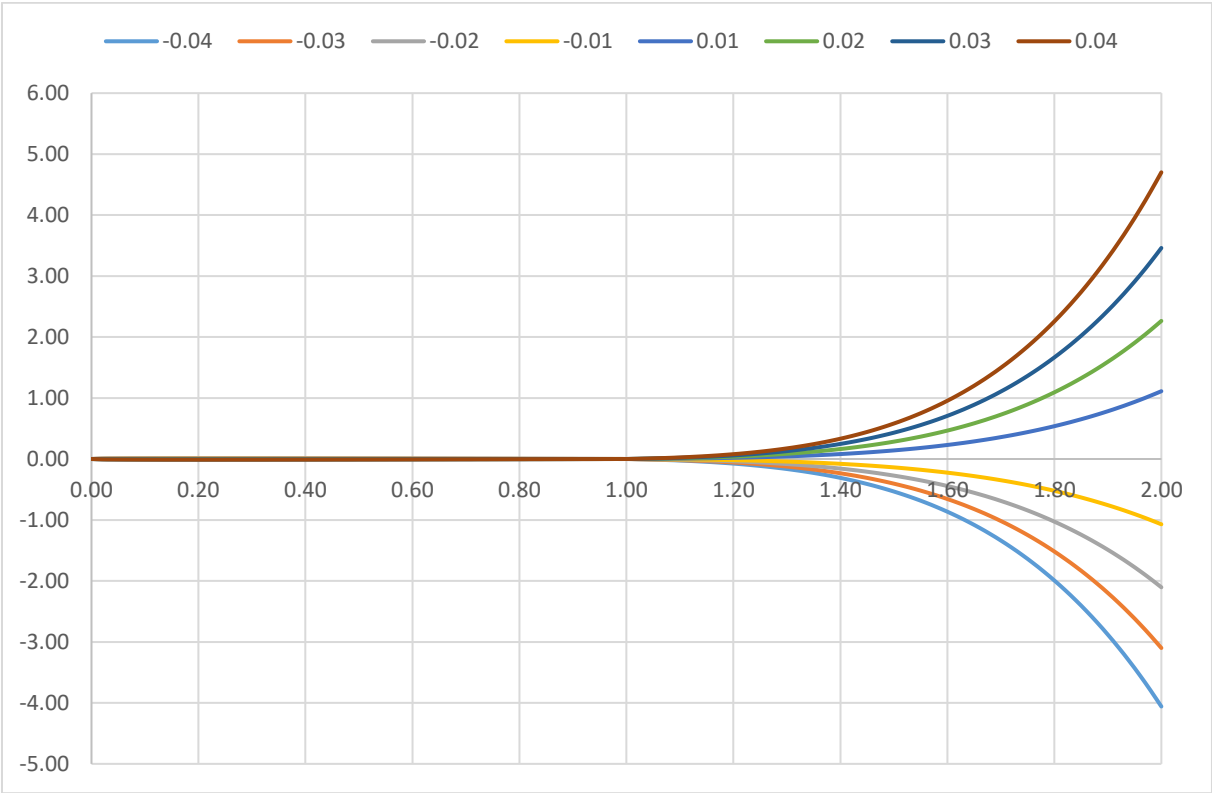


Figure 47: Difference between the BPR function values with the parameters b changed

Finally, a percent difference of the function results have been presented. It can be seen on Fig. 33

Parametrizing macroscopic road network model of traffic-calmed zones.

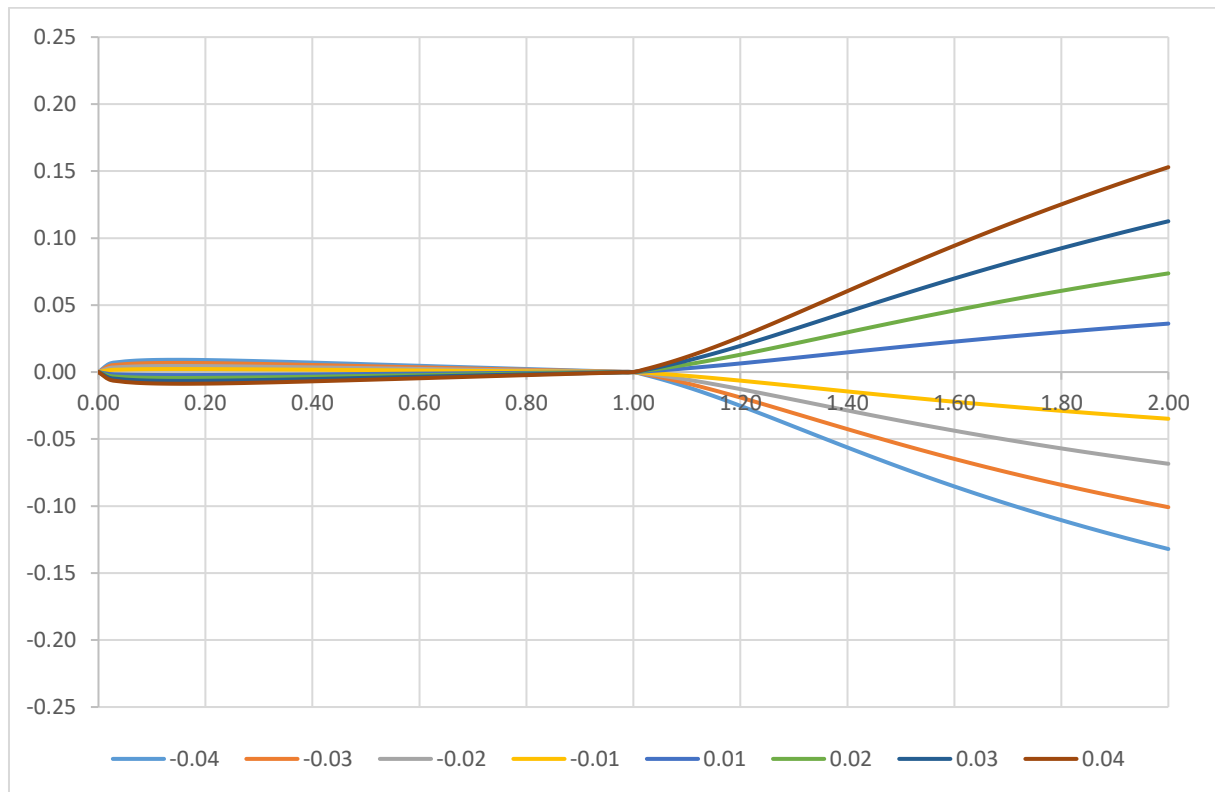


Figure 48: Difference between the BPR function values (fractions) with the parameter a changed

Analysing the sensitivity analysis of the parameters b of the function, it can be seen, that its change plays a major role in the function result. However, the change become significant after the saturation (q/q_{max}) is bigger than one.

Summing up the sensitivity analysis, it can be seen, that estimating the parameter b of the analysed BPR2 function, plays a significant role in calculating the travel time and, as a result, the traffic assignment. The sensitivity analysis shows the importance of the b parameter, especially in the case of the demand exceeding the capacity. This means, that the proper estimation plays a key role for the traffic assignment results especially in case of the saturated links.

6. Research application

6.1. Influence on traffic assignment – Toy network

6.1.1. Problem formulation

In this experiment, a “toy network” of two links of equal length was constructed, connecting a common origin and a destination. The links differed in the volume–delay function defined for them—one with, the other without traffic calming; thus, travel time is as seen in formulas (6) and (7):

Formula 6: Travel time with traffic calming.

$$t_{wtc} = t_{0(wtc)} \cdot \left(1 + a_{wtc} \cdot \left(\frac{q}{q_{max,wtc}} \right)^{b_{wtc}} \right) \quad (6)$$

Formula 7: Travel time without traffic calming

$$t_{wotc} = t_{0(wotc)} \cdot \left(1 + a_{wotc} \cdot \left(\frac{q_{tot} - q}{q_{max,wotc}} \right)^{b_{wotc}} \right) \quad (7)$$

In the experiment, we studied a situation where our toy network was in a state of equilibrium (meaning travel time is the same for every user, $t_{wtc} = t_{wotc}$). In such a case, traffic volume is different for each link, written q_{wtc} : traffic volume (for a link with traffic calming), and remaining traffic (for a link without traffic calming): $q_{tot} - q_{wtc}$ where total traffic flow is described by q_{tot} . Traffic assignment on this simple network was calculated by solving the equation given in formula (8): $t_{wtc} = t_{wotc}$.

Formula 8: The equation of the model

$$t_{wtc} = t_{wotc}$$

$$t_{0(wtc)} \cdot \left(1 + a_{wtc} \cdot \left(\frac{q}{q_{max,wtc}} \right)^{b_{wtc}} \right) = t_{0(wotc)} \cdot \left(1 + a_{wotc} \cdot \left(\frac{q_{tot} - q}{q_{max,wotc}} \right)^{b_{wotc}} \right) \quad (8)$$

Traffic assignment was calculated with the help of Microsoft Excel’s Solver together with macros to automate the process of simulating various traffic volumes, and these were then confirmed with PTV Visum software (using equilibrium traffic assignment for the aforementioned model). A graphic description of the model can be seen in Figure 15. There are two pictures, each containing a different amount of total traffic (q_{tot}): on the left: 500 veh/h, on the right: 3000 veh/h. For this model, the BPR function values of

Parametrizing macroscopic road network model of traffic-calmed zones.

Direction 2 stated in Table 1 are used—with traffic calming (*wtc*) at the top, and without traffic calming (*wotc*) at the bottom.

Figure 34 presents two chosen situations of the traffic assignment, for two traffic flows: the first of total 500 veh/h and the second 3000 veh/h. The figure shows the split of the traffic flow between the link with traffic-calming (orange) and without the traffic calming (green).

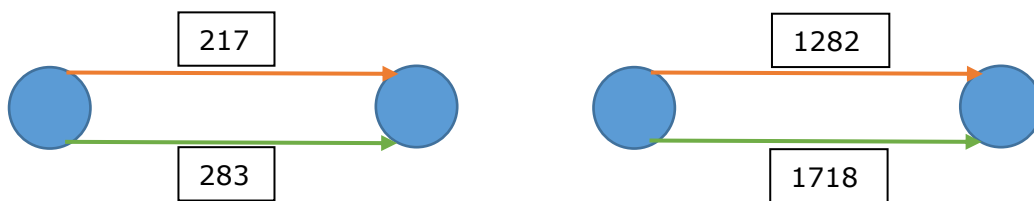


Figure 49: Example results of the traffic assignment (source: own).

6.1.2. Result

Following the experiment, a chart showing the relation between the total traffic volume (q_{tot}) and the traffic volume on each link was created. The results are shown in Figure 35.

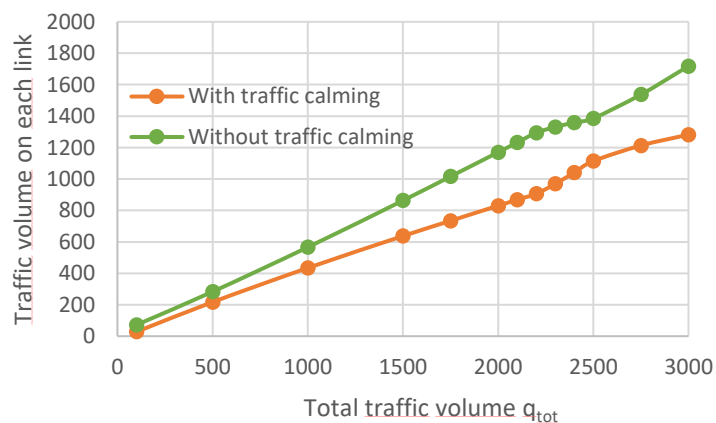


Figure 50: Traffic flow splitted on both links according to the total traffic volume (source: own)

For a better interpretation of the above chart, Figure 36 represents total traffic flow as a difference in traffic volume between each link.

Parametrizing macroscopic road network model of traffic-calmed zones.

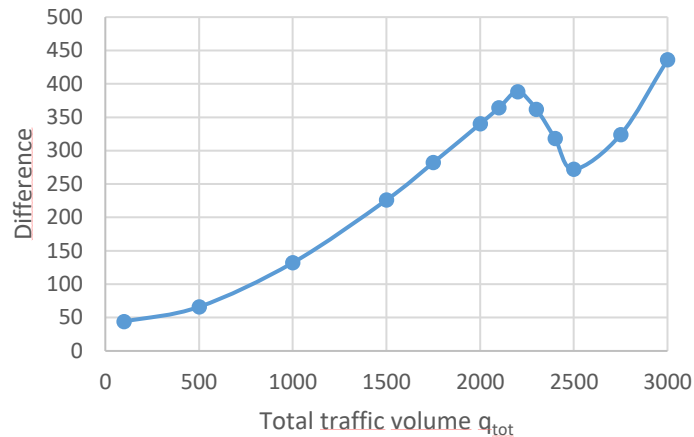


Figure 51: Difference in traffic flow on each link (source: own)

The phenomena shown in the chart can be divided into three phases, depending on the state of the network:

Both links are below capacity. If the street is empty, speed is lower on the traffic-calmed road (because of the slowdown caused by speed cushions) than on the road without traffic calming. No or a little slowdown is caused by a high traffic volume. More vehicles choose the standard road. $q_{tot} \leq 2200$ veh/h.

Because more vehicles choose the standard road, it reaches capacity earlier (despite its capacity being higher than on the other link) and causes congestion; thus, drivers choose an alternative road via a traffic-calmed one, which is still under capacity. $2200 < q_{tot} \leq 2500$ veh/h.

The traffic-calmed road exceeds capacity, along with the standard road; more vehicles choose the standard road, with higher speeds during congestion. $q_{tot} > 2500$ veh/h.

The difference in traffic volumes on links with the aforementioned volume–delay functions in relation to total traffic volume was modelled as a polynomial function shown in formula (9). Function parameters are presented in Table 6.

Formula 9: Estimation function formula

$$diff(q_{tot}) = c \cdot q_{tot}^a + b \quad (9)$$

Where:

diff: Difference between the traffic volumes

q_{tot} : Total traffic flow
 a, b, c: Function coefficients

Table 7: Function parameters

	a	b	c
1. $q_{tot} \leq 2200$ veh/h	1.751	44.7741	0.001
2. $2200 < q_{tot} \leq 2500$ veh/h	1.061	1203.815	-0.231
3. $q_{tot} > 2500$ veh/h	2.939	0	0

Results of the function fitting are shown in Figure 18.

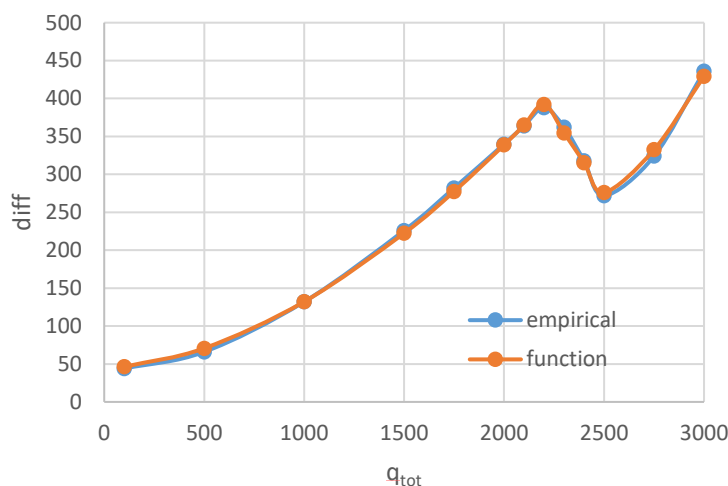


Figure 52: Fitting of the function (source: own)

6.1.3. Comparison with the Results of the current solutions

Currently, in existing macroscopic urban models, in most of the cases, there is no modelling of the volume–delay functions for traffic-calmed roads. Either for roads with small traffic (where traffic-calmed ones often belong) are no volume–delay functions defined (meaning that the travel time is not dependent on the traffic volume) or a volume–delay function is standard for the whole link type. It is considered that the traffic on the toy network of two links would be simulated as the same for both types of links unless there is no differentiation in the free flow velocity. However, when that v_0 velocity is different, in the case of a constant volume–delay function,

Parametrizing macroscopic road network model of traffic-calmed zones.

there will be no traffic on the traffic-calmed road, because it is always slower than the other one. In the case of using the same volume–delay function, together with a different v_0 velocity, which is a proper solution in existing models, the result will be as in the Figure 38.

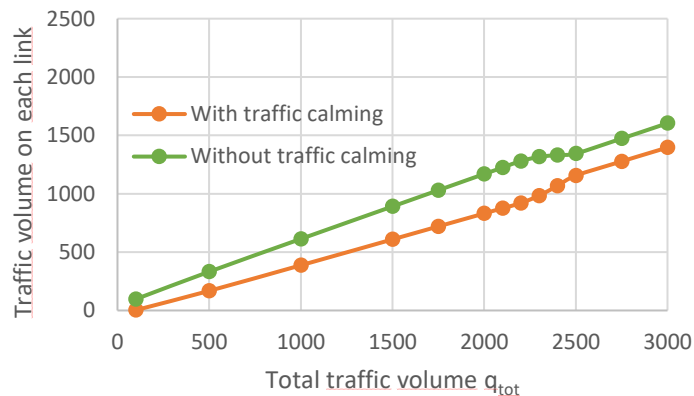


Figure 53: Traffic flow on both roads with the same volume–delay function and different v_0 velocities (source: own).

The difference between traffic volumes is shown on Figure 39.

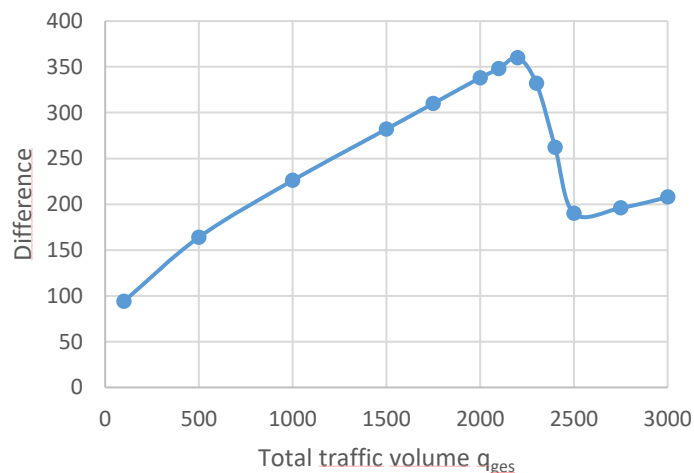


Figure 54: Difference in traffic volume between links with the same volume–delay function and different v_0 velocities (source: own)

Comparing the last two charts with Figures 19 and 20, we can see similarities such as the aforementioned three stages of traffic and similar values below capacity. This is the result of a similarity in shape between volume–delay functions for a standard and traffic-calmed road below capacity. However, the difference in shape of the volume–delay functions above capacity corresponds to different traffic assignment behaviour. When

Parametrizing macroscopic road network model of traffic-calmed zones.

we have different VDFs, the difference grows exponentially; otherwise, it grows linearly.

The described behaviour should occur in this specific case, but it is also the universal reaction of the macroscopic model for a change in volume–delay functions. The experiment and comparison with the other possible methods show that applying volume–delay functions dedicated for traffic-calmed areas produces other, possibly more precise traffic assignment results.

The result of this experiment shows the significance of modelling volume–delay functions for traffic-calmed areas: it reproduces traffic assignment despite the limitations associated with traffic-calmed areas.

6.2. Implementation of the model in real conditions – Krakow case

6.2.1. Introduction

Another traffic calming measure that we analysed was traffic bollards between the lanes of two roadways, or two-lane roads, on Armii Krajowej street in Kraków, Poland, located in the Bronowice area, in the north-western part of the city. It is a two-roadway street with two lanes on each roadway. The street is a collector street connecting Rondo Ofiar Katynia (the main node of outlet routes in north-western Kraków) and main north-south transit route (Aleja Trzech Wieszczów). Armii Krajowej street is part of the corridor connecting the Bronowice residence area and the AGH University of Science and Technology campus and students' dormitory. Six public transport bus lines operate on this street for various destinations throughout the city.

Due to numerous accidents involving pedestrians and vehicles that led to deaths and injuries, a traffic calming measure was installed across pedestrian crossings on this street. It is a set of flexible traffic bollards between the lanes, in conjunction with a narrowing of the lane width, before each pedestrian crossing – as seen in Fig. 40. Its aim is to reduce the number of accidents involving pedestrians caused by overtaking, exceeding the speed limit, and not giving way to them on pedestrian crossings.

Parametrizing macroscopic road network model of traffic-calmed zones.



Figure 55: Traffic calming measure on the analysed area. Source: [238]

The pedestrian crossing under analysis is placed near multi-storey buildings with various functions: offices, hotels and apartments. The office buildings generate great pedestrian traffic to public transport stops, which involves crossing the street.

6.2.2. Measurement

Flights of the Armii Krajowej street took place in May 2018 before the installation of the traffic calming measure and in early July 2018 after the installation.

Traffic flow data derived from the city's continuous count stations was collected and used to determine traffic volume and variability on Armii Krajowej street. The annual average daily traffic on the testing site is around 25 000 vehicles daily in both directions. During peak hours the highest traffic volumes reach about 1 200 vehicles per hour in one direction. The capacity of the street is limited by adjacent signalized intersections on both ends of the examined section.

Analysis before and after implementation was set during periods of similar traffic flow, in the afternoon peak hour around 3 PM. Traffic volumes, expressed in vehicles per hour and pedestrians crossing the street per hour, are shown in Tab. 7.

Table 8: Pedestrian and vehicle flow per hour during the analysed period –measurement before and after the change.

		Before	After
Vehicles [veh/hour]	Eastbound	1182	1040
	Westbound	1095	1120
Pedestrians [pedestrians/hour]	Southbound	359	343
	Northbound	36	4

6.2.3. Speed profiles calibration

Speed profiles for the analysed part of the road before the introduction of the bollards are shown. For the direction 1 (westbound), the correlation coefficient is equal to 0,98. The fitting of the model is shown on Fig. 41

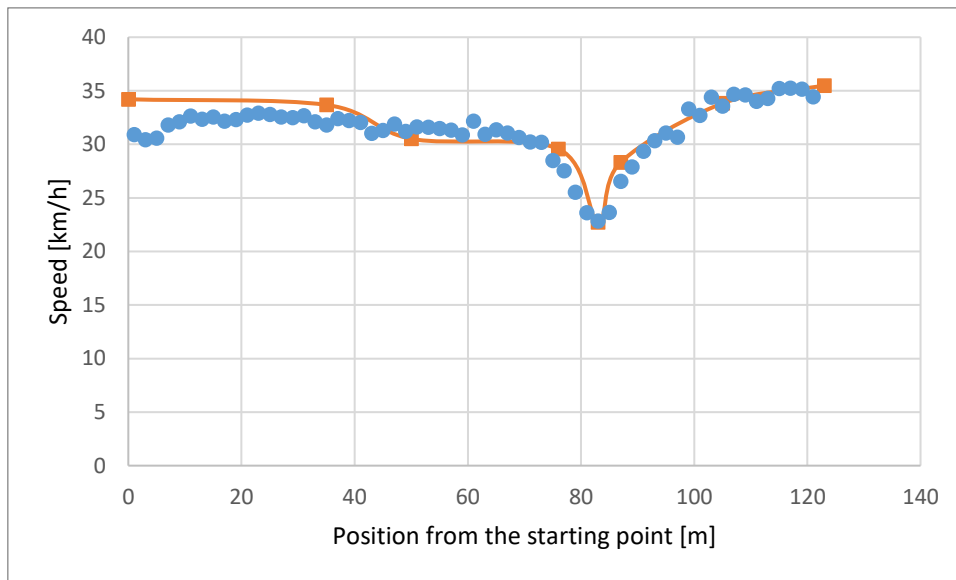


Figure 56: Fitting westbound

For direction 2 (eastbound) of the analysed road, the correlation between the measurements and the model is 0,99. The fitting of the model is shown on Fig. 42

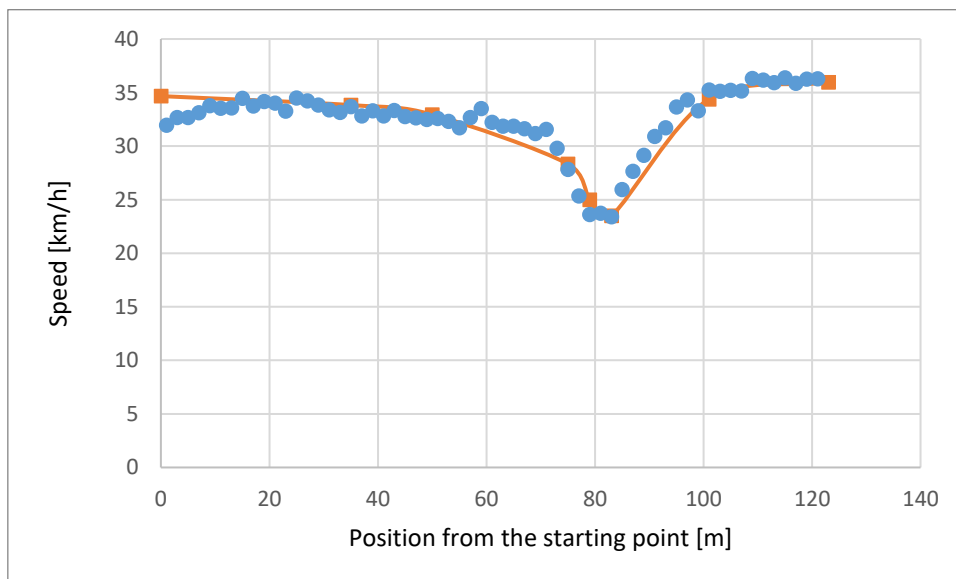


Figure 57: Fitting eastbound

We can see a decrease in the average velocity at around the 80th meter, which lasts for around 3 meters – this represents the pedestrian crossing.

Parametrizing macroscopic road network model of traffic-calmed zones.

This is where speed distributions contained velocities upward from 0 km/h, i.e. where vehicles stopped to give way to pedestrians. However, the need for a full stop was rare; in most cases a slowdown was sufficient to let the pedestrians cross the road. After passing the pedestrian crossing, vehicles accelerated to their previous velocity (average 35 km/h).

The speed profiles of the road after the installation of the traffic bollard are shown next.

For direction 1 (westbound), the correlation coefficient is equal to 0,93. The fitting of the model is shown on Fig. 43

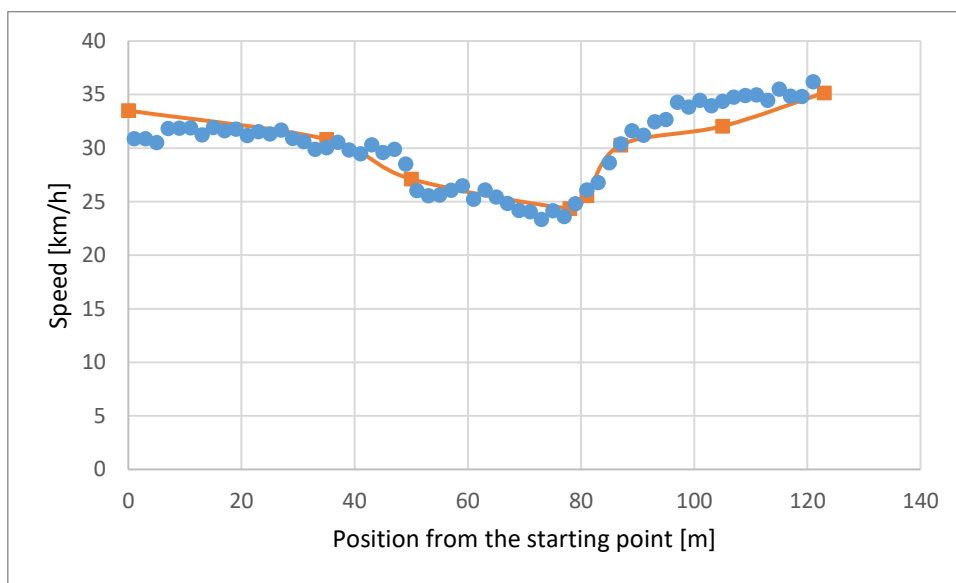


Figure 58: Fitting westbound, traffic calmed

For direction 2 (eastbound) of the analysed road, the correlation between the measurements and the model is 0,92. The fitting of the model is shown on Fig. 44

Parametrizing macroscopic road network model of traffic-calmed zones.

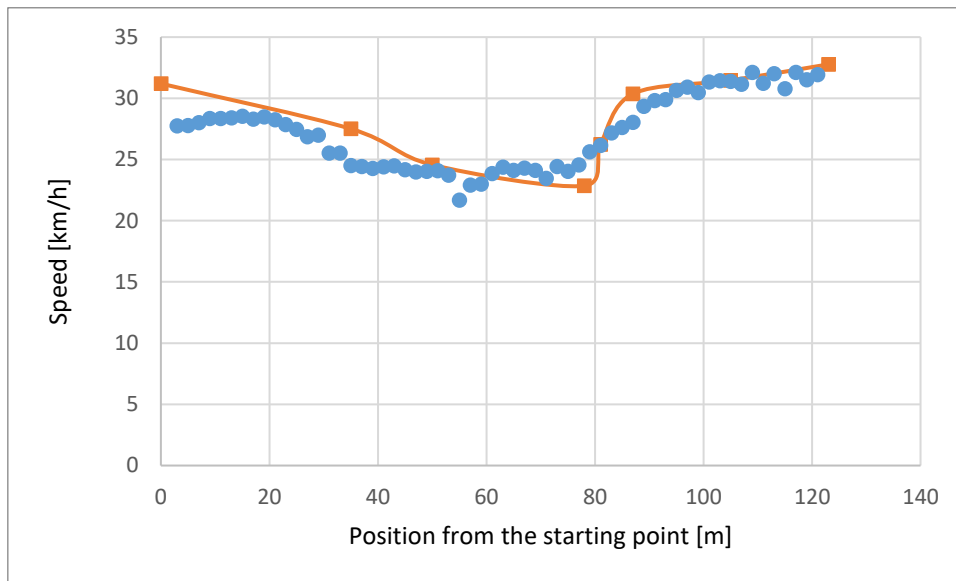


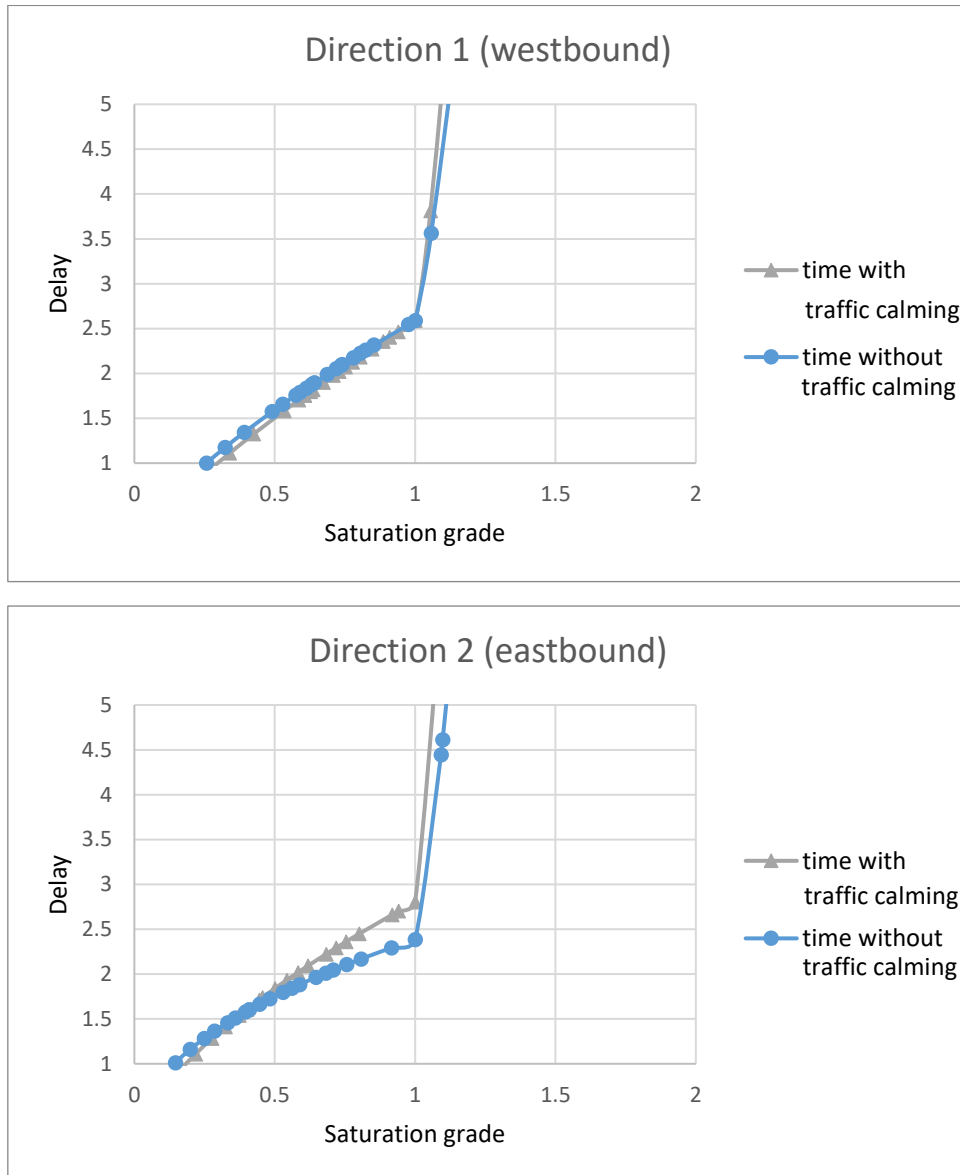
Figure 59: Fitting eastbound, traffic-calmed

In this situation, we can see that the vehicles are slowing down are slowing down farther ahead of the pedestrian crossing the pedestrian crossing, at the point where the bollards start, meaning they are approaching the pedestrian crossing at a lower speed.

6.2.4. Volume-delay functions

The range of the traffic volumes were analysed in the model, producing density-time relation and, as a result, a volume-delay function for the road before and after installing a traffic calming measure. The charts representing the volume-delay BPR function for this link are shown on Fig. 45

Figure 60: Volume-delay functions for the link



Parametrizing macroscopic road network model of traffic-calmed zones.

For both cases, we can see an increased steepness of the function after saturation reaches 1 for the traffic-calmed link. BPR function parameters are shown in Tab. 8

Table 9: BPR function parameters

	Direction 1 (westbound)			Direction 2 (eastbound)		
	a	b	b'	a	b	b'
Without traffic calming	2.588	0.699	5.717	2.385	0.446	7.05
With traffic calming	2.588	0.782	7.266	2.803	0.608	8.887

6.2.5. Impact on the Kraków model

Volume-delay functions estimated for this link were implemented in the Kraków model where the traffic calming measure in question was located. The purpose of this experiment was to check the change in the traffic assignment result, precisely, how the traffic volume have changed on the analysed link. Together with the traffic assignment recalculation, the assignment analysis have been calculated. In this case, the change of the R^2 parameter have been checked to observe if the compliance of the model have improved.

Fig. 46 shows the traffic assignment results on the analysed link with the original parameters. Westbound traffic volume is 980 E/h, eastbound 1050 E/h. In this situation, the original capacity 1900 E/h is maintained.

Figure 61: Traffic assignment results with the original volume-delay function.



Parametrizing macroscopic road network model of traffic-calmed zones.

The second traffic assignment result seen on fig. shows the volume-delay functions but with unchanged capacity. Westbound traffic volume on the link is 1050 E/h, eastbound 1100 E/h. In this case, both volume-delay functions (with and without traffic calming) produced the same result, due to their similarity for traffic volumes significantly lower than capacity.



Figure 62: Traffic assignment results with the changed volume-delay function and without the change of the capacity.

Parametrizing macroscopic road network model of traffic-calmed zones.

In the third scenario, volume-delay functions and capacity reveal the studied situation before traffic calming. The studied capacity in this case is equal to 1486 E/h. There is a significant decrease in traffic volume observed on the analyzed link – 640 E/h westbound and 650 E/h eastbound.

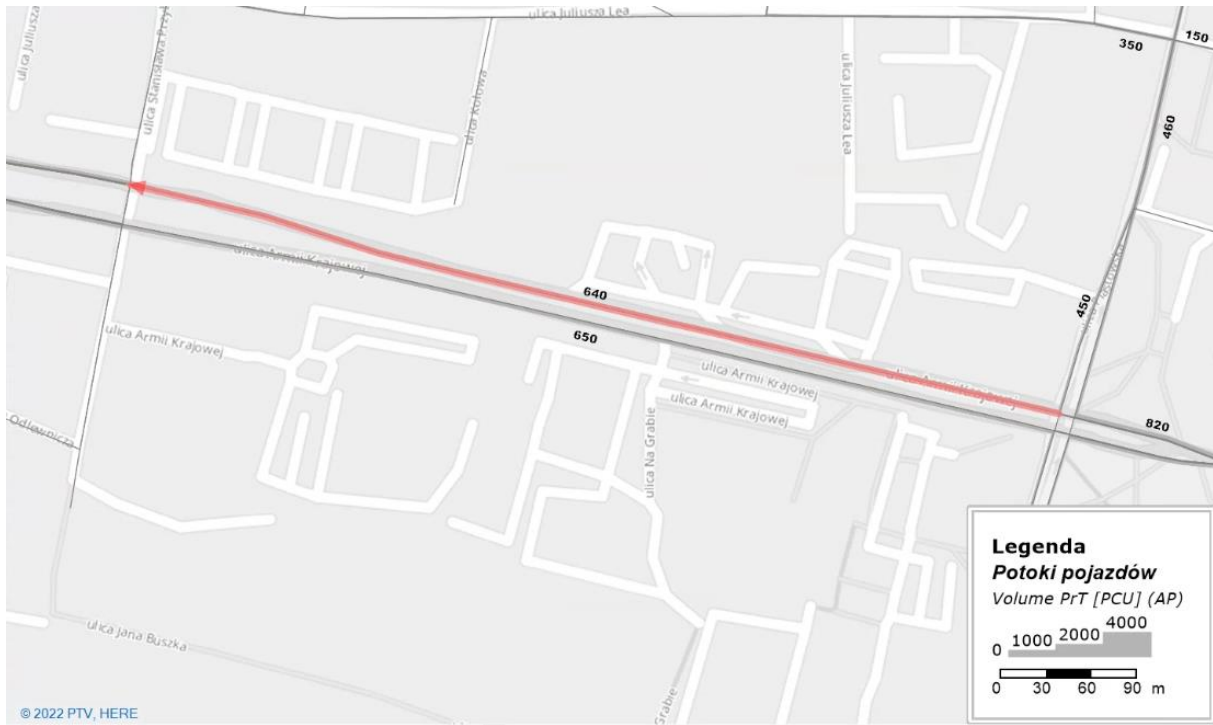


Figure 63: Traffic assignment results for the capacity and VDFs changed for the situation before the traffic calming

The R^2 fitness parameter of the whole network after changing the capacity and the VDFs for those two the non-traffic calmed links have increased by 0.000194 comparing with the original parameters.

Parametrizing macroscopic road network model of traffic-calmed zones.

In the final, fourth case, capacity and volume-delay functions are implemented for traffic calming – here the studied capacity is 1296 E/h. Only a slight decrease compared to the previous case is visible. Westbound traffic volume is 630 E/h, eastbound 620 E/h.



Figure 64: Traffic assignment results for the capacity and VDFs changed for the situation after the traffic calming

The R^2 fitness parameter of the whole network after changing the capacity and the VDFs for those two the traffic calmed links have increased by 0.000276 comparing with the original parameters.

7. Summary and conclusions

7.1. Research summary

The aim of this thesis was to create a method of volume-delay functions estimation. The primary use of the method was to estimate VDFs for the traffic-calmed streets. This required a different approach for the drivers' behaviour research. Unlike the most of the methods, in this case it was needed to record the trajectory together with the speed profiles of the vehicles, because of velocity fluctuations on the street caused by the traffic calming measures. At the same time, machine learning of the vehicle detection as well as UAV videography have developed and become reliable, accurate and available.

With the use of this technology, the created method not only have made it easier to research the links with the changing velocity, but also have made it independent from the specialist measuring equipment, such as vehicle detectors, speed radar or floating vehicle. Instead, the method made it possible to feed with data two kind of models: microscopic and macroscopic. For the microscopic model, it delivers the database of velocities and the trajectory base for the calibration purposes. For macroscopic, using the whole method delivers the volume-delay functions of any measured link types.

The experiments undertaken in this thesis confirmed, that traffic calming measures are changing the capacity and the volume-delay relation of the link. Tandemously, those characteristics have been proven to change the traffic assignment results, especially in the situation of a high saturation grades.

This thesis showed the complexity of the volume-delay characteristics for the traffic-calmed streets. Only a fraction of the possible traffic-calmed measures and only a fraction of the links of each type have been researched in this thesis. However, this thesis shows a framework and a proper methodology for the extensive research covering a numerous amount of links for a various amount of traffic-calming measures and other link types. Finally, this can lead to the volume-delay function standardisation for the particular types of links. This can make the supply modelling faster and more accurate.

Showing the method application on the Kraków model, it was shown, that adjusting the parameters of the traffic-calmed links can improve the fitness

of the macroscopic model, meaning, using this method can help to develop better calibrated models.

Summing up, the aim of the thesis was to create a method to estimate the volume-delay functions for the traffic-calmed links. This needed to be achieved by researching the fluctuating speed of the vehicles, which interfered with the capacity and the volume-delay characteristics. This have been achieved by continuous speed research of the link users' vehicles. In this method, thanks to the use of unmanned aerial vehicles and, recently developed for the practical usage, video detection, the measurements can be independent from the infrastructural measurement devices and additionally supplies the data for the microscopic model. The creation of the method have been successful, which is proven by the results obtained in this thesis. That means, the aim of the thesis have been fulfilled. Additionally, the research explaining the influence characteristics of the volume-delay functions on the traffic assignment have been made.

7.2. General conclusions

1. Traffic assignment is a key result of the transportation modelling process and strictly depends on the network model, including volume-delay functions.
2. Estimation methods and the shape of the volume-delay functions for the traffic-calmed links differ from the links without the traffic calming. The main reason causing it is the fluctuating speed on the link forced by the traffic calming measures.
3. In literature, there is a lacking in methods of the VDFs estimation for the traffic-calmed links.
4. To reproduce the driving behaviour on the traffic calmed links, it is essential to gather the trajectory and speed data for the researched link.
5. Due to the technical development in the field of the video-detection and aerial recording, the use of unmanned aircrafts is the efficient method for the trajectory and speed research. However, in literature there is still a few application examples of this method.
6. Driving behaviour can be reproduced in the microscopic model. The example of this model can be Wiedemann model used in PTV Vissim software.
7. Calibrated microscopic model allows to estimate VDFs by simulating the scope of the traffic volumes on the link.
8. Implementing the Volume-delay functions for the traffic-calmed links, alters the traffic assignment results

Parametrizing macroscopic road network model of traffic-calmed zones.

9. It was observed in this research, that implementing the VDFs for the traffic-calmed links can improve the quality of models by improving the model fitting.

7.3. Further research

During the research process, the three main fields of the further developments in this topic can be specified.

First is connected with the trajectory research. In this case, the development in the field of the video detection and unmanned aircrafts can be further applied in the traffic modelling.

Secondly, using the method of this thesis, a complex and statistically significant research of the Volume-delay function shapes can be undertaken.

Finally, provided the sufficient amount of measurements, the universal formulas modifying the current VDFs can be estimated to simplify the network development process in the macroscopic model.

More detailed insight on those topics were presented in the following subchapters.

7.3.1. Applying unmanned aircrafts and video detection in transport modelling

Unmanned aircrafts provide a vast opportunities of the traffic and driving behaviour observation. Its main advantage is an unobstructed view of the great area of the transportation network. However, most of the UAVs have a very limited flying time, which isn't suitable for long lasting traffic observations.

The solution for the first case can be using an UAV, which has a constant energy supply or requires less energy to maintain the altitude. The solution for the constant power supply can be a wire connecting the UAV with the ground power supply. The solution for the second case can be using the balloon for maintain the altitude. However, currently both solutions are either not popular in a mass production and/or expensive.

Video detection, the use of the machine learning and artificial intelligence can allow to automatize the development process of the microscopic model. Using traffic flows, trajectories, speed and acceleration as the reference data would allow to compare and calibrate those models, possibly with a high level of automation.

7.3.2. Volume-delay function database for the link types

The method shown in this thesis allows to a step by step volume-delay function estimation starting from the movement record of the single vehicle to the final function forms. Using this method would allow, assuming the sufficient sample size of the measurements, to create a database of the VDFs for the various link types. This would facilitate a better macroscopic model quality by better reproduction of the volume-delay phenomena and more accurate traffic assignment results.

7.3.3. Volume – delay functions comparison – finding the VDF modification for traffic-calmed roads

The final research field includes a comparison of the volume-delay functions and between a traffic calmed and standard link. The aim of this study is to test whether there was a universal coefficient differentiating a standard and traffic-calmed function. Below, an attempt on this research have been shown.

The parameters of the volume-delay function were compared by dividing a value (a, b or b') of the traffic-calmed road with the corresponding value in the non-traffic calmed road. The results are shown in Tab. 9

Table 10: Comparison of the BPR function parameters for Armii Krajowej street.

	Direction 1 (westbound)			Direction 2 (eastbound)		
	a	b	b'	a	b	b'
Without traffic calming	2.588	0.699	5.717	2.385	0.446	7.050
With traffic calming	2.588	0.782	7.266	2.803	0.608	8.886
Difference	1.000	1.119	1.271	1.175	1.365	1.260

For direction westbound, coefficient a for the before and after situation is very similar; only a coefficient b and b' shows substantial difference. This is clearly seen on the fig, where only values for the bigger arguments are higher for the traffic calmed situation. For direction 2 however, the differences are visible. Coefficients a differ for the before and after situation. Coefficients b are lower, but b' are higher. There are however similar differences (expressed as multiplication) for the b' coefficient. As shown, coefficients for both directions are not identical. This can be caused by a different traffic situation or situation on the pedestrian crossing. To clearly determine that matter one way or the other, a broad study needs to be undertaken.

The results have been compared with the study from chapter 4.1. The parameters can be seen in Tab. 10

Parametrizing macroscopic road network model of traffic-calmed zones.

Table 11: Comparison of the BPR function parameters for Stachiewicza street

	Direction 1 (westbound)			Direction 2 (eastbound)		
	a	b	b'	a	b	b'
Without traffic calming	0.527	0.905	7.0802	0.612	0.647	2.592
With traffic calming	0.641	0.739	6.760	0.759	0.644	5.293
Difference	1.215	0.816	0.955	1.240	0.996	2.042

For Stachiewicza street, direction 1 does not show differences between the traffic-calmed and standard street. This could be linked to the signalized intersection, which alters traffic. For direction 2, we can see similar differences in the function shape and parameters to those in Armii Krajowej street – coefficients a and b are similar regardless of traffic calming whereas coefficient b' is higher for the traffic calmed road.

The results of the VDFs comparison indicates a need to undertake a complex volume-delay function estimation for various links and link types. This can be achieved by using the researched method for the higher number of links. In the further research this can lead to two significant research results. First of them is the database of VDF parameters of the various link types. This can be expanded for the second research result, which would contain a formula adjusting a standard VDF to the traffic calming (or other) link characteristics.

8. Literature

1. Birr Krystian. *Modelowanie podziału zadań przewozowych w obszarach zurbanizowanych - Praca doktorska*. Kraków : Politechnika Krakowska, 2018.
2. *Intermodalny Krajowy Model Ruchu*. Brzeziński Andrzej. Warszawa, 2019. Materiały konferencyjne Konferencji Naukowo-technicznej "Innowacyjne metody prognozowania ruchu Krajowego-Regionalnego-Lokalnego".
3. Jacyna M. *Wybrane zagadnienia modelowania systemów transportowych*. Warszawa : Oficyna Wydawnicza Politechniki Warszawskiej, 2009.
4. Hensher David and Button Kenneth. *Handbook of Transport Modelling*. 2008.
5. Marcotte Patrice and Nguyen Sang. *Equilibrium and advanced transport modelling*. brak miejsca : Springer, 1998.
6. Small K A. The incidence of congestion tolls on urban highways. *Journal of Urban Economics*. 1983.
7. Wardrop John Glen. Some theoretical aspects of road traffic research. *Proc Inst Civ Eng Part II*. 1952.
8. Prashker Joseph and Bekhor Shlomo. Some observations on stochastic user equilibrium and system optimum of traffic assignment. *Transportation Research Part B* . 2000, 34.
9. Smith M J. The existence, uniqueness and stability of traffic equilibria. *Transportation Research 13B*. 1979, 4.
10. Daganzo C F and Sheffi Y. On stochastic models of traffic assignment. *Transportation Science*. 1977, 11.
11. *Linear User Cost Equilibrium: the new algorithm for traffic assignment in VISUM*. Gentile Guido and Noekel Klaus. Noordwijkerhout, 2009. Proceedings of the European Transport Conference.
12. Greenshields B.D. *A Study of Traffic Capacity*. 1935.
13. Petrik Olga, Filipe Moura and de Abreu e Silva Joao. The Influence of the Volume-Delay Function on Uncertainty Assessment for a Four-Step Model. *Advances in Intelligent Systems and Computing*. 2014.

Parametrizing macroscopic road network model of traffic-calmed zones.

14. Kucharski Rafał, Drabicki Arkadiusz. Estimating Macroscopic Volume Delay Functions with the Traffic Density Derived from Measured Speeds and Flows. *Journal of Advanced Transportation*. 2017.
15. Kucharski Rafał. MAKROSKOPOWY MODEL PRZEPLYWU RUCHU W SIECI DRUGIEGO RZĘDU – ALTERNATYWNY OPIS STANU SIECI. 2013.
16. Bureau of Public Roads. *Traffic Assignment Manual*. Washington, DC : Department of Commerce, Urban Planning Division, 1964.
17. Spiess H. Technical note—conical volume-delay functions. *Transportation Science*. 1990.
18. Moses R et al. *Development of speed models for improving travel forecasting and highway performance evaluation*. Florida : Department of Transportation, 2031.
19. Lazar D A, Coogan S and Pedarsani R. Routing for traffic networks with mixed autonomy. *IEEE Transactions on Automatic Control*. 2020.
20. Davidson K B. A flow travel time relationship for use in transportation planning. *Australian Road Research Board Conference*. 1966.
21. Huntsinger L F and Roupail N M. Bottleneck and queuing analysis: calibrating volume-delay functions of travel demand models. *Transportation Research Record*. 2011.
22. Akçelik R. A new look at Davidson's travel time function. *Traffic Engineering & Control*. 1978.
23. Time-dependent expressions for delay, stop rate and queue length at traffic signals. *Australian Road Research Board*. 1980.
24. The highway capacity manual delay formula for signalized intersections. *ITE Journal*. 1988.
25. Newell G F. Queues with time-dependent arrival rates I-the transition through saturation. *Journal of Applied Probability*. 1968.
26. Cheng Q et al. Estimating key traffic state parameters through parsimonious spatial queue models. *Transportation Research Part C*. 2022.
27. Zhou X S et al. A Meso-to-Macro Cross-Resolution Approach for Connecting Polynomial Arrival Queue Model to Volume-Delay Function with Inflow demand-to-Capacity Ratio. *Multimodal Transportation*. 2022.
28. Pan Y et al. A review of volume-delay functions: Connecting theoretical fundamental, practical deployment and emerging applications. *SSRN*.

29. Zawisza Marcin et al. WYBRANE PROBLEMY MODELOWANIA ROZKŁADU PRZESTRZENNEGO I CZASU PODRÓŻY NA PRZYKŁADZIE GDAŃSKA. *ZESZYTY NAUKOWO-TECHNICZNE SITK RP, ODDZIAŁ W KRAKOWIE*. 2012.
30. Oskarbski Jacek et al. ZASILANIE MODELI SYSTEMÓW TRANSPORTOWYCH DANYMI Z SYSTEMU ZARZĄDZANIA RUCHEM. *ZESZYTY NAUKOWO-TECHNICZNE SITK RP, ODDZIAŁ W KRAKOWIE*. 2014.
31. Województwo Śląskie. *Studium Transportowe Subregionu Centralnego Województwa Śląskiego wykonywanego na zlecenie Związku Gmin i Powiatów Subregionu Centralnego Województwa Śląskiego. Komputerowy modelu ruchu dla stanu istniejącego*. Sopot/Poznań/Kraków : Województwo Śląskie, 2019.
32. Brzeziński Andrzej and Waltz Andrzej. *Budowa hierarchicznych modeli ruchu w sieciach drogowych*. Warszawa : Politechnika Warszawska, 1998.
33. PTV-Ag. PTV VISSIM 9 User Manual,. Karlsruhe : PTV-Ag, 2017.
34. Hollander Yaron and Liu Ronghiu. The principles of calibrating traffic microsimulation models. *Transportation*. 2008.
35. Kim K.O., Rilett, L.R. Simplex-based calibration of traffic microsimulation models with intelligent transportation systems data. *Transport Research Record*. 2003.
36. A genetic algorithm based approach to traffic micro-simulation calibration using ITS data. *Proceedings of the 83rd TRB Annual Meeting*. 2004.
37. Dowling R., Skabardonis, A., Halkias, J., McHale, G., Zammit, G. Guidelines for calibration of microsimulation models: framework and application. *Proceedings of the 83rd TRB Annual Meeting*. 2004.
38. Chu L., Liu, H.X., Oh, J.S., Recker, W. A calibration procedure for microscopic traffic simulation. *Proceedings of the 83rd TRB Annual Meeting*. 2004.
39. Oketch T., Carrick, M. Calibration and validation of a micro-simulation model in network analysis. *Proceedings of the 84rd TRB Annual Meeting*. 2005.
40. Ma T., Abdulhai, B. Genetic algorithm-based optimization approach and generic tool for calibrating traffic microscopic simulation parameters. *Transport Research Record*. 2002.
41. Ben-Akiva M.E., Darda, D., Jha, M., Koutsopoulos, H.N., Toledo, T. Calibration of microscopic traffic simulation models with aggregate data. *Proceedings of the 83rd TRB Annual Meeting*. 2004.

Parametrizing macroscopic road network model of traffic-calmed zones.

42. Kim S. J., Kim, W., Rilett, L. R. Calibration of micro-simulation models using non-parametric statistical techniques. *Proceedings of the 84rd TRB Annual Meeting*. 2005.
43. Park B., Qi, H. Development and evaluation of simulation model calibration procedure. *Proceedings of the 84rd TRB Annual Meeting*. 2005.
44. Merritt E. Calibration and validation of CORSIM for Swedish road traffic conditions. *Proceedings of the 83rd TRB Annual Meeting*. 2004.
45. Shaaban and Radwan. A calibration and validation procedure for microscopic simulation model: a case study of sim traffic arterial streets. *Proceedings of the 84rd TRB Annual Meeting*. 2005.
46. Hourdakis J., Michalopoulos. P.G., Kottommannil, J. Practical procedure for calibrating microscopic traffic simulation models. *Transport Research Record*. 2003.
47. Toledo T., Koutsopoulos, H.N., Davol, A., Ben-Akiva, M.E., Burghout, W., Andreasson, I., Johansson, T., Lundin, C. Calibration and validation of microscopic traffic simulation tools – Stockholm case study. *Transport Research Record*. 2003.
48. Toledo T., Koutsopoulos, H.N. Statistical validation of traffic simulation models. *Proceedings of the 83rd TRB Annual Meeting*. 2004.
49. Barcelo J., Casas, J. Methodological notes on the calibration and validation of microscopic traffic simulation models. *Proceedings of the 83rd TRB Annual Meeting*. 2004.
50. Brockfeld E., Kühne, R.D., Wagner, P. Calibration and validation of microscopic traffic flow models. *Proceedings of the 84rd TRB Annual Meeting*. 2005.
51. [Online] <https://www.gps.gov/systems/gps/performance/accuracy/> (access 18.03.18).
52. TAYLOR M.A.P., YOUNG, W. *Traffic Analysis. New Technology & New Solutions*. brak miejsca : Hargreen Publising Company, 1986.
53. LABORATORY TRANSPORT RESEARCH. *Urban Road Traffic Surveys*. brak miejsca : Overseas Road Note 11, 1993.
54. HOOBS F.D. *Traffic Planning & Engineering*. brak miejsca : Pergamon Press, 1979.
55. Kennedy et. al *Fundamentals of Traffic Engineering*. brak miejsca : Institute of Transportation and Traffic Engineering, University of California, 1973.

56. BONSALL P. *Speed, Delay and Congestion Surveys*. Notes from MSc Course. Institute for Transport Studies, University of Leeds, 1992.
57. Barbosa Heloisa Maria. *Impacts of traffic calming measures on speeds on urban roads*. Leeds : University of Leeds, 1995.
58. Fernández Llorca D., Hernández Martínez, A., García Daza. Vision-based vehicle speed estimation: A survey. *IET Intell. Transp. Syst.* 15, 987– 1005. 2021.
59. Yamazaki F., et al. Vehicle extraction and speed detection from digital aerial images. *Proc. of IEEE Int. Geo. and Rem. Sen. Symp. IEEE, Piscataway*. 2008.
60. Liu W., Yamazaki, F. Speed detection of moving vehicles from one scene of QuickBird images. *Proceedings of Joint Urban Remote Sensing Event. IEEE, Piscataway*. 2009.
61. Xin Z., et al. Algorithm of vehicle speed detection in unmanned aerial vehicle videos. *Proceedings of the Transportation Research Board 93rd Annual Meeting. Transportation Research Board, Washington DC*. 2014.
62. Moranduzzo T., Melgani, F. Car speed estimation method for UAV images. . *Proceedings of IEEE Geoscience and Remote Sensing Symposium*. . 2014.
63. Salvo G., et al. Comparison between vehicle speed profiles acquired by differential GPS and UAV. . *Paper presented at the meeting of the Euro working group on transportation, Sevilla*. 2014.
64. Ke R., et al. Motion-vector clustering for traffic speed detection from UAV video. *Proceedings of IEEE International Smart Cities Conference (ISC2). IEEE, Piscataway* . 2015.
65. Long H., et al. Automatic vehicle speed estimation method for unmanned aerial vehicle images. *Journal Inf. Hid. Mult. Sig. Proc.* 9(2). 2018.
66. Li J., et al. An adaptive framework for multi-vehicle ground speed estimation in airborne videos. *Remote Sens.* 11, 1241. 2019.
67. Biswas D., et al. Speed estimation of multiple moving objects from a moving UAV platform. *ISPRS Int. J. Geo-Inf* 8, 259. 2019.
68. Vehicle speed detection and safety distance estimation using aerial images of brazilian highways. da Silva Bastos, M.E., et al. *Proc. Seminário Integrado Soft. Hard*. 2020.

69. Schoepflin T.N., Dailey, D.J. Dynamic camera calibration of roadside traffic management cameras for vehicle speed estimation. *IEEE Trans. Int. Transp. Syst.* 4(2). 2003.
70. Cathey F.W., Dailey, D.J. A novel technique to dynamically measure vehicle speed using uncalibrated roadway cameras. *IEEE Intelligent Vehicles Symposium. IEEE, Piscataway.* 2005.
71. Grammatikopoulos L., et al. Automatic estimation of vehicle speed from uncalibrated video sequences. *Proc. Int. Symp. Modern Tech., Edu. Prof. Prac. Geo. Rel. Fields.* 2005.
72. Alefs B., Schreiber, D. Accurate speed measurement from vehicle trajectories using AdaBoost detection and robust template tracking. *Proceedings of IEEE International Transportation Systems Conference (ITSC). IEEE, Piscataway.* 2007.
73. Maduro C., et al. Estimation of vehicle velocity and traffic intensity using rectified images. . *Proceedings of International Conference on Image Processing. IEEE, Piscataway.* 2008.
74. Wu J., et al. An algorithm for automatic vehicle speed detection using video camera. *International Conference on Computer Science and Education. IEEE, Piscataway.* 2009.
75. Dogan S., et al. Real time speed estimation of moving vehicles from side view images from an uncalibrated video camera. *Sensors* 10,. 2010.
76. Nguyen T.T., et al. Compensating background for noise due to camera vibration in uncalibrated-camera-based vehicle speed measurement system. *IEEE Trans. on Veh. Tech.* 60(1). 2011.
77. Czapla Z. Vehicle speed estimation with the use of gradient-based image conversion into binary form. *Proc. Sig. Proc. Alg. Arch. Arrang. Apps. (SPA).* 2017.
78. iannakeris P., et al. Speed estimation and abnormality detection from surveillance cameras. *Proc. IEEE Comp. Vis. Mach. Intell.* 2018.
79. Bauer D., et al. Embedded vehicle speed estimation system using an asynchronous temporal contrast vision sensor. *EURASIP J. Embedded Syst.* 82174. 2007.
80. Tan H., et al. Vehicle speed measurement for accident scene investigation. . *IEEE International Conference on e-Business Engineering. IEEE, Piscataway.* 2010.

81. Qimin X., et al. A methodology of vehicle speed estimation based on optical flow. . *Proc. of IEEE Int. Conf. on Serv. Op. and Log., and Inf. IEEE, Piscataway*. 2014.
82. Lee J., et al. Image-based learning to measure the space mean speed on a stretch of road without the need to tag images with labels. *Sensors 19*, 1227. 2019.
83. Kamoji S., et al. Image processing based vehicle identification and speed measurement. *Proc. of Int. Conf. on Inventive Comp. Tech. (ICICT)*. 2020.
84. Dahl M., Javadi, S. Analytical modeling for a video-based vehicle speed measurement framework. *Sensors 20*, 160 . 2020.
85. Li Y., et al. Vehicle speed measurement based on video images. . *Proc. Int. Conf. Inn. Comp. Inf. and Cont.* 2008.
86. Rahim H.A., et al. Vehicle velocity estimation for traffic surveillance system. *Int. J. Comp., Elec., Aut., Cont. Inf. Eng.* 4(9). 2010.
87. Rad A.G., et al. Vehicle speed detection in video image sequences using CVS method. *Int. Journal Phy. Sci.* 5(17). 2010.
88. Ibrahim O., et al. Speed detection camera system using image processing techniques on video streams. *Int. J. Comp. Elect. Eng.* 3(6),. 2011.
89. Shen I.Z, et al.: . Vehicle speed detection based on video at urban intersection. *Research Journal of Applied Sciences, Eng. and Tech.* 5(17). 2013.
90. Li S., et al. Video-based traffic data collection system for multiple vehicle types. *IET Intell. Transp. Sys.* 8(2). 2013.
91. Lan J., et al. Vehicle speed measurement based on gray constraint optical flow algorithm. *Optik* 125. 2014.
92. Lin L., et al. Biologically inspired composite vision system for multiple depth-of-field vehicle tracking and speed detection. *Proceedings of Asian Conference on Computer Vision (ACCV)*, pp. 473– 486. Springer, Berlin Heidelberg. 2014.
93. Rao Y.G.A., et al. Real-time speed estimation of vehicles from uncalibrated view-independent traffic cameras. . *Proceedings of IEEE Region 10 Conference (TENCON)*. IEEE, Piscataway. 2015.

94. Jalalat M., et al. Vehicle detection and speed estimation using cascade classifier and sub-pixel stereo matching. *International Conference on Signal Processing and Information Security IEEE, Piscataway*. 2016.
95. Yabo A., et al. Vehicle classification and speed estimation using Computer Vision techniques. *Proc. of AADECA. IEEE, Piscataway* . 2016.
96. Wicaksono D., Setiyono, B. Speed estimation on moving vehicle based on digital image processing. *Int. Journal of Comp. Sci. and Applied Math. 3(1)*. 2017.
97. Gerat J., et al. Vehicle speed detection from camera stream using image processing methods. *Proceedings of International Symposium. ELMAR. Croatian Society Electronics in Marine, Zadar*. 2017.
98. Kurniawan A., et al. Speed monitoring for multiple vehicle using closed circuit television (CCTV) camera. . *Proc. Int. Conf. Comp. Eng., Net. Intell. Mult. (CENIM)*. 2018.
99. Tourani A., et al. Motion-based vehicle speed measurement for intelligent transportation systems. *Int. Journal of Image, Graph. and Sig. Proc.* 2019.
100. Moazzam M., et al. Multiple objects tracking based vehicle speed analysis with Gaussian filter from drone video. *Intell. Sci. and Big Data Eng. Vis. Data Eng. (IScIDE)*. 2019.
101. Murashov I., Stroganov, Y. Method of determining vehicle speed according to video stream data. *Journal of Physics: Conf. Ser. 1419,*. 2019.
102. Cheng G., et al. Real-time detection of vehicle speed based on video image. *Proc. of Int. Conf. on Meas. Tech. and Mech. Aut.* 2020.
103. Czajewski W., Iwanowski, M. Vision-based vehicle speed measurement method. . *In: Proceedings of the International Conference on Computer Vision and Graphics,*. 2010.
104. Garg M., Goel, S. Real-time license plate recognition and speed estimation from video sequences. *TSI Trans. Electrical Electron. Eng. 1(5),*. 2013.
105. Filipiak P., et al. NSGA-II based auto-calibration of automatic number plate recognition camera for vehicle speed measurement. *Proc. European Conf.on the App. of Evolutionary Computation,*. 2016.
106. Luvizon D.C., et al. A video-based system for vehicle speed measurement in urban roadways. *EEE Trans. on Intell. Transp. Sys. 18(6)*. 2017.

107. Famouri M., et al. A novel motion plane-based approach to vehicle speed estimation. . *IEEE Trans. Intell. Transp. Sys.* 20(4),. 2018.
108. Liang W., Junfang, S. The speed detection algorithm based on video sequences. . *In: Proceedings of International Conference on Computer Science and Service System.* 2012.
109. Ke R. et al. Real-time bidirectional traffic flow parameter estimation from aerial videos. *IEEE Trans. Intell. Transp. Syst., vol. 18, no. 4.* 2017.
110. Hua S., et al. Vehicle tracking and speed estimation from traffic videos. *Proc. IEEE Comp. Vis. Patt. Rec.* . 2018.
111. Huang T. Traffic speed estimation from surveillance video data. *Proc. IEEE Comp. Vis. Patt. Rec. (CVPR),.* 2018.
112. Khan M., et al. Multiple moving vehicle speed estimation using Blob analysis. *Proc. World Conf. Inf. Sys. Tech. (WorldCIST).* 2019.
113. Bartl V., Herout, A. OptInOpt: dual optimization for automatic camera calibration by multi-target observations. *Proc. of IEEE Int. Conf. on Adv. Video and Signal Based Surv. (AVSS)* . 2019.
114. Madhan E.S., et al. A novel approach for vehicle type classification and speed prediction using deep learning. *Journal Comp. Theor. Nano.* 17(5). 2020.
115. Shukla D., Patel, E. Speed determination of moving vehicles using Lucas-Kanade algorithm. *Int. J. Comp. App. Tech. and Res.* 2(1),. 2013.
116. Gupta P., et al. Estimating speed of vehicle using centroid method in MATLAB. *Int. J. Comp. App.* 102(14). 2014.
117. Han J., et al. Vehicle distance estimation using a mono-camera for FCW/AEB systems. *Int. Journal of Automotive Tech.* 17(3). 2016.
118. Liu C., et al. A vision-based pipeline for vehicle counting, speed estimation, and classification. . *IEEE Trans. on Intell. Transp. Sys.* 2020.
119. Makarov A., et al. Real-time vehicle speed estimation based on license plate tracking in monocular video sequences. . *Sensors Transducers J.* 97(2). 2016.
120. Javadi S., et al. Vehicle speed measurement model for video-based systems. *Comp. & Elec. Eng.* 76. 2019.
121. R. Ke et al. Real-time bidirectional traffic flow parameter estimation from aerial videos. *IEEE Trans. Intell. Transp. Syst., vol. 18, no. 4.* 2017.

122. Alvarado Ed. 237 Ways Drone Applications Revolutionize Business. *Drone Industry Insights*. 2021.
123. Hu J. et al. Fault-tolerant cooperative navigation of networked UAV swarms for forest fire monitoring. *Aerospace Science and Technology*. 2022.
124. Grace T. C. Tozer and D. High-altitude platforms for wireless communications. *Electron. Commun. Eng. J.*, vol. 13, no. 3. 2001.
125. Thornton D., Grace J., Spillard, C.. Broadband communications from a high-altitude platform: The European HeliNet programme. *Electron. Commun. Eng. J.*, vol. 13, no. 3. 2001.
126. Pavlidou S. Karapantazis and F. Broadband communications via highaltitude platforms: A survey. *IEEE Commun. Surveys Tuts.*, vol. 7, no. 1. 2005.
127. Al-Hourani A. S. Kandeepan, and A. Jamalipour. Modeling air-toground path loss for low altitude platforms in urban environments. *Proc. Global Commun. Conf. (GLOBECOM)*. 2014.
128. Valcarce A. et al. Airborne base stations for emergency and temporary events. *Proc. Int. Conf. Pers. Satell. Services*. 2013.
129. Rasheed L. and Reynaud T. Deployable aerial communication networks: Challenges for futuristic applications. *n Proc. 9th ACM Symp. Perform. Eval. Wireless Ad Hoc, Sensor, Ubiquitous Netw*. 2012.
130. Airbornedrones. [Online] [Zacytowano: 21 09 2018.] <http://www.airbornedrones.co/>.
131. Sun D. W. and Matolak R. Initial results for air-ground channel measurements & modeling for unmanned aircraft systems: Over-sea. *Proc. IEEE Aerosp. Conf*. 2014.
132. Matolak R. and Sun D. W. Air-ground channel characterization for unmanned aircraft systems part II: Hilly and mountainous settings. *IEEE Trans. Veh. Technol.*, vol. 66, no. 8. 2017.
133. Sun D. W. Matolak and R. Air-ground channel characterization for unmanned aircraft systems—Part III: The suburban and near-urban environments. *IEEE Trans. Veh. Technol.*, vol. 66, no. 8. 2017.
134. Chandrasekharan S. et al. Designing and implementing future aerial communication networks. *IEEE Commun. Mag.*, vol. 54, no. 5. 2016.
135. Bucaille I. et. al. Rapidly deployable network for tactical applications: Aerial base station with opportunistic links for unattended and temporary events ABSOLUTE example. *Proc. Mil. Commun. Conf. (MILCOM)*. 2013.

136. Shakhathreh H. et al. A Survey on Civil Applications and Key Research Challenges. *IEEE Access*, vol. 7. 2019.
137. Guido G. et al. Evaluating the accuracy of vehicle tracking data obtained from unmanned aerial vehicles. *Int. J. Transp. Sci. Technol.*, vol. 5, no. 3. 2016.
138. L. Wang F. Chen, and H. Yin. Detecting and tracking vehicles in traffic by unmanned aerial vehicles. *Automat. Construct.*, vol. 72,. 2016.
139. Menouar H. et al. UAV-enabled intelligent transportation systems for the smart city: Applications and challenges. *IEEE Commun. Mag.*, vol. 55, no. 3. 2017.
140. Oh H. et al.. Behaviour recognition of ground vehicle using airborne monitoring of unmanned aerial vehicles. *Int. J. Syst. Sci.*, vol. 45, no. 12,. 2014.
141. Sutheerakul C. et al. Application of unmanned aerial vehicles to pedestrian traffic monitoring and management for shopping streets. *Transp. Res. Procedia*, vol. 25. 2017.
142. Puri A. A survey of unmanned aerial vehicles (UAV) for traffic surveillance. *Dept. Comput. Sci. Eng., Univ. South Florida, Tampa*,. 2008.
143. L. Wang F. Chen, and H. Yin. 'Detecting and tracking vehicles in traffic by unmanned aerial vehicles. *Automat. Construct.*, vol. 72,. 2016.
144. Apeltauer J. et al. Automatic vehicle trajectory extraction for traffic analysis from aerial video data. *Int. Arch. Photogram., Remote Sens. Spatial Inf. Sci.*, vol. 40, no. 3. 2015.
145. Tang T. et al. Vehicle detection in aerial images based on region convolutional neural networks and hard negative example mining. *Sensors*, vol. 17, no. 2. 2017.
146. Saha B. et al. Battery health management system for electric UAVs. *IEEE Aerosp. Conf.* 2014.
147. S. Park L. Zhang, and S. Chakraborty. Battery assignment and scheduling for drone delivery businesses. *Proc. IEEE/ACM Int. Symp. Low Power Electron. Design (ISLPED)*. 2011.
148. Swieringa K. A. et al. Autonomous battery swapping system for smallscale helicopters. *roc. IEEE Int. Conf. Robot. Automat.* 2017.
149. Michini B. et al. Automated battery swap and recharge to enable persistent UAV missions. *Proc. Infotech@Aerospace*. 2010.

Parametrizing macroscopic road network model of traffic-calmed zones.

150. K. A. O. Suzuki P. K. Filho, and J. R. Morrison. Automatic battery replacement system for UAVs: Analysis and design. *J. Intell. Robot. Syst.*, vol. 65. 2011.
151. D. Lee J. Zhou, and W. T. Lin. Autonomous battery swapping system for quadcopter. *Proc. Int. Conf. Unmanned Aircr. Syst.* 2015.
152. N. K. Ure et al. An automated battery management system to enable persistent missions with multiple aerial vehicles. *IEEE/ASME Trans. Mechatron.*, vol. 20, no. 1. 2015.
153. Walendziuk W., Słowik M. i Gulewicz M. Monitoring System Based on Unmanned Aerial Vehicle Powered from the Ground. *Environ. Sci. Proc.* 2022.
154. 2019/945 (EU) 2019/947 and. Easy Access Rules for Unmanned Aircraft Systems.
155. ITE/FHWA. *Traffic Calming: State of the Practice.* 1999.
156. Brindle R E. *Australia's Contribution to Traffic Calming.* Pearson : PTRC, 1992.
157. Ziółkowski Robert. *Zachowania kierowców pojazdów w otoczeniu środków uspokojenia ruchu w warunkach miejskich.* brak miejsca : Oficyna Wydawnicza Politechniki Białostockiej, 2022.
158. Hosseinlou M.H. Kheyraadi S.A., Zolfaghari A. Determining optimal speed limits in traffic networks. „*IATSS Research*”. 2015.
159. Biuro Ekspertyz i Projektów Budownictwa Komunikacyjnego „EKKOM” Sp. z o.o. *Zasady uspokajania ruchu na drogach za pomocą fizycznych środków technicznych.* brak miejsca : Biuro Ekspertyz i Projektów Budownictwa Komunikacyjnego „EKKOM” Sp. z o.o, 2008.
160. Devon County Council. *Traffic calming guidelines.* . brak miejsca : Engineering and Planning Department Devon County Council., 1991.
161. J Baguley C. *Speed control humps - Further public road trials.* brak miejsca : Department of Transport, TRRL Report LR1017, Transport and Road Research Laboratory, 1981.
162. C Webster D. *Road humps for controlling vehicle speeds.* 1993.
163. E Layfield R. The effectiveness of speed cushions as traffic calming devices. *Proceedings of Seminar J. 22nd PTRC European Transport Forum.* 1994.
164. HMSO, London. Highways (Traffic Calming) Regulations Statutory Instrument No. 1849. 1993.

Parametrizing macroscopic road network model of traffic-calmed zones.

165. I Hass-Klau C and Nold. Horizontal traffic calming measures-alternatives to road humps? *Environmental Transport and Planning*. 1994.
166. Driver Information and Traffic Management Division. *Horizontal deflections* : Traffic Advisory Leaflet 9/94, 1994.
167. Hass-Klau C Nold I, Bocker G and Crampton G. Civilised streets: a guide to traffic calming. *Environmental Transport and Planning*. 1992.
168. Devon County Council. *TRAFFIC CALMING GUIDELINES*. brak miejsca : Devon County Council, 1991.
169. Tolley R. *CALMING TRAFFIC IN RESIDENTIAL AREAS*. 1989 .
170. Veurman J. Gense N.L.J., Wilmink I.R., Baarbe H.I.,. Emissions at different conditions of traffic flow. *Urban Transport VIII. Urban Transport and the Environment in the 21st Century, MIT, Massachusetts* . 2002.
171. B. Owen. Air quality impacts of speed-restriction zones for road traffic. *Science of the Total Environment*. 2005.
172. Frey H.Ch. Roupail N., Unal A., Colyar J.D. Measurement of on-road tailpipe CO, NO and Hydrocarbon emissions using portable instrument. *Proceedings, Annual Meeting of the Air & Waste Management Association*. 2001.
173. Boulter P.G. Latham S., Ainge M. Driving cycles for measuring passenger car emissions on roads with traffic calming measures. *Science of the Total Environment*. 1999.
174. De Vlioger I. De Keukeleere D., Kretzschmar J.G. Environmental effects of driving behaviour and congestion related to passenger cars. *Atmospheric Environment*. 2000.
175. Unal A. Frey H.Ch., Roupail N.M.,. Quantification of highway vehicle emission hot spots based on-board measurements. *Journal of the Air and Waste Management Association*. 2004.
176. Wang M. Daamen W., Hoogendoorn S., van Arem B.,. Estimating acceleration, fuel consumption, and emissions from macroscopic traffic flow data. *Transportation Research Record. Journal of the Transportation*. 2011.
177. Holzmann E. Flächen hafte verkehrsberuhigung in Buxtehude: Auswirkungen der Massnahmen zu Tempo 30 auf die Umweltsituation (Area-wide traffic calming in Buxtehude). 4. *Kolloqium Flächenhafte Verkehrsberuhigung, am 26/27. 5.88 in Buxtehude,*. 1988.
178. German Federal Ministries of Planning, Transport and Environment. *Forschungsvorhaben, Flächenhafte verkehrsberuhigung, Folgerungen für*

die Praxis (Area-wide traffic calming: results and guidelines). brak miejsca : Bundesministerium für Raumordnung, Bauwesen und Städtebau; Bundesministerium für Verkehr; Bundesministerium für Umwelt, Naturschutz und Reaktorsicherheit,, 1992.

179. G Höglund P. Estimating traffic related exhaust emissions and immissions at road- and street intersections. *Esitelmä: KFB & VTI Research Information Days*,. 1995.

180. J Moses P. *Traffic management and safety in Europe and North America 1988 - A study tour*. 1988.

181. AIT/FIA. *Power and speed of vehicles: speed humps cause ten times more air pollution*. brak miejsca : AIT/FIA Traffic Commission meeting, 1994.

182. Hydén C Odelid K and Várhelyi A. *The effects of general speed calming in built-up areas*. brak miejsca : Results of a large scale experiment in Växjö: 1 Main report. Institutionen för Trafikteknik, Lunds Tekniska Högskola, 1995.

183. Bohatkiewicz J. Czarnecka W., Jamrozik, K. Biernacki S., Hałucha M.,. *Wpływ uspokojenia ruchu na klimat akustyczny w otoczeniu ulic. Budownictwo i Architektura*. 2014.

184. Abbott Ph. Tyler J., Layfield R.,. *Traffic calming: vehicle noise emissions alongside speed control cushions and road humps*. Report TRL 180, Crowthorne , 1995.

185. W. Gardziejczyk. *Wpływ technologii wykonania i tekstury nawierzchni drogowych na hałas pojazdów samochodowych*. Białystok : Oficyna Wydawnicza Politechniki Białostockiej, 2005.

186. Environment Agency. *Horizontal Guidance for Noise. Part 2 – Noise Assessment and Control*. 2002.

187. Campolieti D. Bertoni D. The action plan for noise reduction in Modena: methods, effects and perspectives. *Radiation Protection Dosimetry*. 2009.

188. R. Ziolkowski. Speed Profile as a Tool to Estimate Traffic Calming Measures Efficiency. *Journal of Civil Engineering and Architecture*. 2014.

189. Fwa T F Liaw C Y. Rational approach for geometric design of speed-control road humps. *Transportation Research Record*. 1992.

190. Webster D C Mackie A M. *Review of traffic calming schemes in 20 mph zones*. Department of Transport. TRL Report 215. Transport Research Laboratory, 1996.

Parametrizing macroscopic road network model of traffic-calmed zones.

191. Webster D C Layfield R. E. *Traffic calming - Road hump schemes using 75 mm high humps*. Department of Transport. TRL Report 186. Transport Research Laboratory, 1996.

192. Webster D C Layfield R E. *An assessment of rumble strips and rumble areas*. brak miejsca : Department of Transport, TRL Report 186, Transport Research Laboratory, 1993.

193. Pharoah T Russel J. Traffic calming: policy and evaluations in three European countries. *Occasional Paper 2/1989. Faculty of the Built Environment, South Bank Polytechnic*. 1989.

194. I Huttunen. *The effects of traffic calming on the dynamics of a vehicle*. brak miejsca : Helsinki University of Technology, 1995.

195. Broadbent K Salmon A M. An alternative to road humps. *Highways and Transportation*. 1993.

196. Sayer I A Parry D I. *Traffic calming - An assessment of selected on-road chicane schemes*: Project Report PR/TT/014/96, Transport Research Laboratory, 1996.

197. Wheeler A H Taylor M, Payne A. *The effectiveness of village 'gateways' in Devon and Gloucestershire*. Department of Transport. TRL Project Report 35. Transport Research Laboratory, 1993.

198. Wheeler A H Abbott P G, Godfrey N S, Lawrence D J, Phillips S M. *Traffic calming on major roads: the A49 trunk road at Craven Arms, Shropshire*. TRL Report 212. Transport Research Laboratory, 1996.

199. Engel U. Thomsen L.K. Safety Effects of Speed Reducing Measures in Danish Residential Areas. *Accident Analysis & Prevention*. 1992.

200. Layfield R.E. Parry D.I. *Traffic calming – Speed cushion schemes*. brak miejsca : TRL Report 312, 1998.

201. G.R Watts. *Road humps for the control of vehicle speed*. brak miejsca : TRRL Laboratory Report 597, 1973.

202. Pau M. Angius S. Do speed bumps really decrease traffic speed? An Italian experience. *Accident Analysis & Prevention*. 2001.

203. Antić B. Pešić D., Vujanić M., Lipovac K. The influence of speed bumps heights to the decrease of the vehicle speed – Belgrade experience. *Safety Science*. 2013.

204. Fwa T.F. Tan L.S.,. Geometric characterization of road humps for speed-control design, . *Journal of Transportation Engineering*. 1992.

205. Kiran K.R. Molugaram K., Sandeep M.,. Analysis of Speed Profiles at Speed Humps Under Various Dimensions & Simulating their LOS using VISSIM, . *Science Direct. Transportation Research Procedia*. 2020.
206. Kordani A.A. Molan A.M., Monajjem S., Sadeghvaziri E. Simulation Modeling of Dynamic Response of Vehicles to Different Types of Speed Control Humps. *Conference: Second Transportation & Development*. 2014.
207. H. Mahdy. Speed calming using vertical deflections in road alignment. *12th International Conference on Transportation Professionals*. 2012.
208. Daniel B.D. Nicholson A., Koorey G. Analysing speed profiles for the estimation of speed on traffic-calmed streets,. *Road and Transport Research: A Journal of Australian and New Zealand Research and Practice*. 2011.
209. Shwaly S.A. Zakaria M.H., Al-Ayaat A.H. Development of Ideal Hump Geometric Characteristics for Different Vehicle Types, Case Study, Urban Roads in Kafr El-Sheikh City (Egypt). *Advances in Civil Engineering*. 2018.
210. Botha T.R. Els P.S., Uys P.E., Bester R. Profile optimization of table top speed hump for speed control, w: Proceedings of the ASME 2011 . *International Design Engineering Technical Conferences & Computers and Information in Engineering Conference, Washington*. 2011.
211. Purnomo R.A.D. Handayani D., Syafi'i. Correlation analysis between speed bump dimensions and motorcycle speed in residential areas. *MATEC Web of Conferences*. 2018.
212. P.K. Sahoo. Geometric design of speed control humps in Bhubaneswar City. *International Journal of Advanced Technology in Civil Engineering*. 2009.
213. Zainuddin N.I. Adnan M.A., Md Diah J. Optimization of speed hump geometric design: case study on residential streets in Malaysia. *Journal of Transportation Engineering*. 2014.
214. Kassem E. Al-Nassar Y. Dynamic considerations of speed control humps. *Transportation Research Part B: Methodoloical*. 1982.
215. Garcia-Pozuelo D. Gauchia A., Olmeda E., Diaz V. Bump modeling and vehicle vertical dynamics prediction. *Advances in Mechanical Engineering*. 2014.
216. Lee G. Joo S., Oh Ch., Choi K. An evaluation framework for traffic calming measures in residential areas. *Transportation Research Part D: Transport and Environment*. 2013.

217. Yousif S. Alterawi M., Henson R.R. Effect of Road Narrowing on Junction Capacity Using Microsimulation. *Journal of Transportation Engineering*. 2012.
218. Bunn F. Collier T., Frost C., Ker K., Steinbach R., Roberts I., Wentz R. Area-wide traffic calming for preventing traffic related injuries. *Cochrane Database of Systematic Reviews*. 2003.
219. Ariën C. Brijs K., Brijs T., Ceulemans W., Vanroelen G., Jongen E.M.M., Daniels S., Wets G. Does the effect of traffic calming measures endure over time? – A simulator study on the influence of gates. *Transportation Research Part F: Traffic Psychology Behaviour*. 2014.
220. Ariën C. Jongen E.M.M., Brijs K., Brijs T., Daniels S., Wets G. A simulator study on the impact of traffic calming measures in urban areas on driving behavior and workload. *Accident Analysis & Prevention*. 2013.
221. García A. Torres A.J., Romero M.A., Moreno A.T. Traffic Microsimulation Study to Evaluate the Effect of Type and Spacing of Traffic Calming Devices on Capacity. *Procedia – Social and Behavioral Sciences*. 2011.
222. Abdulmawjoud A.A. Jamel M.G., Al-Taei A.A. Traffic flow parameters development modelling at traffic calming measures located on arterial roads. *Ain Shams Engineering Journal*. 2021.
223. A. Solowczuk. Effect of Traffic Calming Measures Implemented on the Approach to the Tempo-30 zone on the Degree of Speed Reduction. *IOP Conference Series: Materials Science and Engineering*. 2019.
224. M. Pau. Speed bumps may induce improper drivers' behavior: case study in Italy. *Journal of Transportation Engineering*. 2002.
225. A. Wåhlberg. Driver celeration behavior and the prediction of traffic accidents. *International Journal of Occupational Safety and Ergonomics*". 2006.
226. R.H. Ewing. *Traffic Calming: State of the Practice*. brak miejsca : (FHWA-RD-99-135), USA, 1999.
227. Kveladze I. Agerholm N. Visual analysis of speed bumps using floating car dataset. *Journal of Location Based Services*. 2018.
228. Yeo I. Baek J.G., Choi J.W., Kim Y.S. The optimal spacing of speed humps in traffic calming areas. *International Journal of Highway Engineering*. 2013.

229. Vaitkus A. Čygas D., Jasiūnienė V., Jateikienė L., Andriejauskas T., Skrodenis D., Ratkevičiūtė K. Traffic calming measures: an evaluation of the effect on driving speed. *Promet-Traffic Transportation*. 2017.
230. R.H Ewing. *Best Development Practices. Doing the Right Thing and Making Money at the Same Time*. Routledge: Taylor & Francis Group, 2017.
231. Department of Transportation, Federal Highway Administration. *Engineering countermeasures for reducing speeds: a desktop reference of potential effectiveness*. Department of Transportation, Federal Highway Administration, 2009.
232. CERTU. *Guide des coussins et plateaux*, Lyon CERTU.
233. Chadda H.S. Cross E.E. Speed (Road) Bumps: Issues and Opinions. *Journal of Transportation Engineering*. 1985.
234. B.W. Stephens. Road humps for the control of vehicular speeds and traffic flow. *Public Roads*. 1986.
235. D. Evans. Traffic calming: the first five years and the Oxfordshire experience. *Proceedings of the Institution of Civil Engineers – Municipal Engineer*. 1994.
236. Chimba D. Mbuya Ch. *Simulating the impact of traffic calming strategies, Final Report, 2019*.
237. [Online] <http://datafromsky.com/>.
238. Bochenek Adrianna. Bezpieczne zebry na Armii Krajowej. "Tego przejścia nie da się nie zauważyć". [Online] 02 06 2018. [Read: 08 05 2023.]
<https://krakow.wyborcza.pl/krakow/7,44425,23568850,bezpiecznie-zebry-na-armii-krajowej-tego-przejscia-nie-da.html>.
239. Daganzo and Geroliminis. An analytical approximation for the macroscopic fundamental diagram of urban traffic. *Transportation reseatch part B: Methodological*. 2008.
240. Helbing D. Derivation of a fundamental diagram for urban traffic flow. *THE EUROPEAN PHYSICAL JOURNAL B*. 2008.
241. Akcelik R. Travel time functions for transport planning purposes: Davidson's function, its time dependent form and alternative travel time function. *Australian Road Research*. 1991.
242. Dybicz Tomasz. Wykrywanie lokalnych ograniczeń przepustowości przy wykorzystaniu danych z systemów sondowania pojazdów. *Logistyka – nauka* . 6/2014, 2014.

243. Gaca Stanisław i Kieć Mariusz. Speed Management for Local and Regional Rural Roads. *Transportation Research Procedia*. 14, 2016.
244. Dowling R., Skabardonis, A., Halkias, J., McHale, G., Zammit, G. Guidelines for calibration of microsimulation models: framework and application. *Proceedings of the 83rd TRB Annual Meeting*. 2004.
245. Oketch T., Carrick, M. Calibration and validation of a micro-simulation model in network analysis. *Proceedings of the 84rd TRB Annual Meeting*. 2005.
246. Krystian Birr. *Modelowanie podziału zadań przewozowych w obszarach zurbanizowanych*. Kraków : Praca doktorska, 2018.
247. Jacyna Marianna. *Wybrane zagadnienia modelowania systemów transportowych*. Warszawa : Oficyna wydawnicza Politechniki Warszawskiej, 2009.
248. Cloke J. Webster D., Boulter P., Harris L., Stait R., Abbott Ph., Chinn L. *Traffic Calming: Environmental assessment of the Leigh Park Area Safety Scheme in Havant, Crowthorne, Berkshire,*. 1999.
249. Lech, J. Zintegrowany Model Ruchu, prezentacja UTK, Warszawa, 2021
250. Jacyna M. , Wasiak M. , Lewczuk K. , Chamier-Gliszczyński N. , Dąbrowski T. Decision Problems in Developing Proecological Transport System, *Rocznik Ochrona Środowiska*, 2018
251. M. Jacyna, M. Wasiak, K. Lewczuk, and G. Karoń, "Noise and environmental pollution from transport: decisive problems in developing ecologically efficient transport systems," *Journal of Vibroengineering*, Vol. 19, No. 7, pp. 5639–5655, Nov. 2017, <https://doi.org/10.21595/jve.2017.19371>

9. List of figures

Figure 1: Thesis research logic diagram	9
Figure 2: Demand – supply chart. Source: [3]	13
Figure 3: Example of trips within an activity. Source: [4]	14
Figure 4: The four-step model. Source: [3]	15
Figure 5: Trip generation (cars) – Intermodal National Traffic model. Source:[2]	17
Figure 6: Trip distribution (cars) for the May weekend peak hour – Intermodal National Traffic model Source: [2]	18
Figure 7 Traffic assignment for road transport in Poland in 2030. Source:[249]	22
Figure 8 Map of the emissions in the passenger road traffic, based on the traffic assignment. Source:[250]	23
Figure 9: Greenshield’s fundamental diagram of traffic flow, source: [12]	24
Figure 10 The example of the fundamental diagram of the Thesis research, source: own	24
Figure 11: Example of Volume-delay functions source: [15]	26
Figure 12: Graphical presentation of the VDF estimation used in Gdańsk, source: [29, 30]	32
Figure 13: Example of the function used in Katowice model: Velocity multiplier as a function of saturation grade. Source: [31]	33
Figure 14: States of PTV Vissim model source: PTV Vissim 9 manual [33]	36
Figure 15: Floating car data presented as a heatmap of the link speed. Source: PTV Visum software	40
Figure 16: Enoscope working scheme, source: [54]	41
Figure 17: Pneumatic tube device setup. Source: [57]	42
Figure 18: Methods of vehicle tracking, source: [58]	44
Figure 19: Balloon used for the video detection of the vehicles. Source: [237]	47
Figure 20: The example of the VTOL UAV available on market: DJI Phantom IV. Source: Manufacturer's materials.....	48
Figure 21: Social costs of the travel time, source: [157, 158].....	51
Figure 22: Examples of the vertical deflections: speed hump (left) and speed cushion (right), source: [157]	52
Figure 23: Example of the intersection related measure: mini roundabout. Source: [157]	53
Figure 24: The influence of the acceleration on the emission (170)	56
Figure 25: Speed in a function of the distance between the vertical deflections (230)	62

Figure 26: Algorithm of the proposed research method..... 66

Figure 27: DatafromSky viewer software screenshot with car detection and trajectory data displayed (source: own)..... 68

Figure 28: The view of the PTV Vissim model in the program..... 71

Figure 29: The view of the PTV Vissim running simulation 72

Figure 30: Traffic volume–speed relation (source: own)..... 73

Figure 31: Traffic density–speed relation. (source: own)..... 73

Figure 32 Kraków transportation network in model 76

Figure 33: Distribution of the sample measurements..... 78

Figure 34: Speed profile for Stachiewicza street, northbound (source: own).
..... 79

Figure 35: Speed profile for Stachiewicza street, southbound (source: own).
..... 79

Figure 36: Car speed distributions for the link, southbound (orange) and with second speed cushion (blue), source: own. 81

Figure 37: Comparison of speed profiles on the measured street section, northbound, source: own. 82

Figure 38: Comparison of speed profiles on the measured street section, southbound, source: own..... 82

Figure 39: Fitting of the volume–delay functions (source: own). 84

Figure 40: BPR function in the sensitivity analysis with the parameters a and b changed simultaneously 86

Figure 41: Difference between the BPR function values with the parameters a and b changed simultaneously 86

Figure 42: Difference between the BPR function values (fractions) with the parameters a and b changed simultaneously 87

Figure 43: BPR function in the sensitivity analysis with the parameter a changed 88

Figure 44: Difference between the BPR function values with the parameter a changed..... 89

Figure 45: Difference between the BPR function values (fractions) with the parameter a changed 90

Figure 46: BPR function in the sensitivity analysis with the parameter b changed 91

Figure 47: Difference between the BPR function values with the parameters b changed..... 92

Figure 48: Difference between the BPR function values (fractions) with the parameter a changed 93

Figure 49: Example results of the traffic assignment (source: own)..... 95

Figure 50: Traffic flow splitted on both links according to the total traffic volume (source: own) 95

Figure 51: Difference in traffic flow on each link (source: own)..... 96

Figure 52: Fitting of the function (source: own)..... 97

Figure 53: Traffic flow on both roads with the same volume–delay function and different v_0 velocities (source: own).....	98
Figure 54: Difference in traffic volume between links with the same volume–delay function and different v_0 velocities (source: own)	98
Figure 55: Traffic calming measure on the analysed area. Source: [238]	101
Figure 56: Fitting westbound	103
Figure 57: Fitting eastbound	103
Figure 58: Fitting westbound, traffic calmed	104
Figure 59: Fitting eastbound, traffic-calmed	105
Figure 60: Volume-delay functions for the link.....	106
Figure 61: Traffic assignment results with the original volume-delay function.....	108
Figure 62: Traffic assignment results with the changed volume-delay function and without the change of the capacity.	109
Figure 63: Traffic assignment results for the capacity and VDFs changed for the situation before the traffic calming	110
Figure 64: Traffic assignment results for the capacity and VDFs changed for the situation after the traffic calming.....	111

10. List of Tables

Table 1: Overview of the most important VDFs, source: [28]	27
Table 2: Demand definition for congested conditions in literature [28]...	30
Table 3: Comparison of VDF estimation used in Gdańsk, source: [29, 30]	32
Table 4: Table of used VDFs formulas.....	74
Table 5: Correlation and r^2 coefficient of the chosen VDFs.....	75
Table 6: Function parameter values.	83
Table 7: Function parameters.....	97
Table 8: Pedestrian and vehicle flow per hour during the analysed period – measurement before and after the change.....	102
Table 9: BPR function parameters	107
Table 10: Comparison of the BPR function parameters for Armii Krajowej street.....	115
Table 11: Comparison of the BPR function parameters for Stachiewicza street.....	116

11. List of formulas

Formula 1: Wardrop's first principle	21
Formula 2: Wardrop's second principle	22
Formula 3: BPR volume-delay function	25
Formula 4: Sample size of the measurement.....	67
Formula 5: BPR volume–delay function, source: (16)	83
Formula 6: Travel time with traffic calming.	94
Formula 7: Travel time without traffic calming.....	94
Formula 8: The equation of the model	94
Formula 9: Estimation function formula	96